

Stormwater Runoff Evaluation Report for the USEPA Office of Research and Development 'Right Sizing Project'

Submitted to

Michael Borst

USEPA Office of Research and Development

March 2015

Prepared by

James J. Houle, CPSWQ Thomas P. Ballestero, PE, PhD

Program Manager, Director,

Phone: 603-767-7091 Principal Investigator

james.houle@unh.edu Phone: 603-862-1405

tom.ballestero@unh.edu

Joel C. Ballestero, EIT

UNHSC Research Engineer Timothy A. Puls, EIT

Site Facility Manager

Lorilee Mather Phone: 603-862-4024

UNH Graduate Student <u>timothy.puls@unh.edu</u>

Table of Contents

Introduction	7
Site Descriptions	7
Tree Box Filter	7
TREEPOD Site Characteristics	7
TREEPOD Configuration and Sizing	8
TREEPOD Monitoring Instrumentation	10
Horne Street Bioretention	10
Horne Street Site Characteristics	11
Horne Street Bioretention Configuration and Sizing	12
Horne Street Monitoring Instrumentation	14
Lowell Avenue Bioretention:	14
Lowell Avenue Bioretention Monitoring Instrumentation	15
Data Synthesis	15
Tree Box Filter	16
Horne Street Bioretention	17
Analysis	17
Tree Box Filter	17
Horne Street Bioretention	41
Conclusions.	73
APPENDIX	75

Table of Figures Figure 1: UNH Storm

Figure 1: UNH Stormwater Research Facility with TREEPOD™ Installation, sampling locations, and	
drainage area defined. Blue lines are principal surface e drainage pathways	8
Figure 2: Plan view (top) and section view (bottom) of the TREEPOD™ unit at UNHSC	9
Figure 3: Picture of the TREEPOD	10
Figure 4: Horne Street neighborhood where the Bioretention System was installed with drainage	area
defined in black	11
Figure 5: Plan view (top) and section view (bottom) of the Horne Street Bioretention System insta	alled
in Dover, NH	13
Figure 6: Completed Horne Street System	14
Figure 7: TREEPOD volume reduction versus runoff depth for all individual events	18
Figure 8: TREEPOD peak inflow versus peak outflow for all individual events	18
Figure 9: TREEPOD volume reduction versus runoff depth for non-snowmelt events	19
Figure 10: TREEPOD peak inflow versus peak outflow for non-snowmelt events	19
Figure 11: TREEPOD volume reduction versus runoff depth for snowmelt events	20
Figure 12: TREEPOD peak inflow versus peak outflow for snowmelt events	20
Figure 13: TREEPOD lag time versus peak rainfall intensity	21
Figure 14: Cumulative probability distributions for TREEPOD volumetric moisture content	22
Figure 15: Cumulative probability distribution for non-zero TREEPOD inflows	23
Figure 16: Cumulative probability distribution for all TREEPOD inflows	24
Figure 17: TREEPOD inflow and outflow hydrographs for 28 August 2012 event	25
Figure 18: All TDR sensor VMC TREEPOD data for 28 August 2012 event	26
Figure 19: Selected TDR sensor VMC TREEPOD data for 28 August 2012 event	26
Figure 20: TREEPOD TDR sensor VMC data for 1 ft below the soil media surface data for 28 Augus	t
2012 event	27
Figure 21: TREEPOD temperature profile for the 28 August 2012 event.	28
Figure 22: TREEPOD well water levels for the 28 August 2012 event.	29
Figure 23: TREEPOD inflow and outflow hydrograph for the 30 May 2014 event	
Figure 24: TREEPOD VMC profile for 30 May 2014 event.	
Figure 25: TREEPOD VMC data at one foot depth into the soil media for the 30 May 2014 storm	
Figure 26: TREEPOD water level data for the 30 May 2014 event.	
Figure 27: TREEPOD temperature profile for the 30 May 2014 event.	
Figure 28: TREEPOD inflow and outflow hydrographs for 20 February 2014 event	35
Figure 29: TREEPOD VMC profile data for 20 February 2014 event	
Figure 30: TREEPOD VMC data at a depth of one foot into the soil media for 20 February 2014 even	ent.37
Figure 31: TREEPOD well water level data for 20 February 2014 event	
Figure 32: TREEPOD temperature profile for 20 February 2014 event.	
Figure 33: TREEPOD electrical conductivity profile for 20 February 2014 event	40
Figure 34: Cumulative probability distributions for Horn Street Bioretention volumetric moisture	
content through the longitudinal profile of the system at the center of the Bioretention Soil Mix ($\!\!$	BSM)
depth	42
Figure 35: Cumulative probability distributions for Horn Street Bioretention volumetric moisture	
content through the vertical cross section of the system closest to the inlet	43
Figure 36: Cumulative probability distributions for Horn Street Bioretention volumetric moisture	
content through the vertical cross section of the system closest to the outlet	
Figure 37: Locations of Sensors at the Horne Street Bioretention system	
Figure 38: All TDR Sensor VMC Bioretention System Data 50 ft from the inlet for Storms recorded	
between May 2013 and May 2014	46

Figure 39: All TDR Sensor VMC Bioretention System Data 130 ft from the inlet for Storms recorded between May 2013 and May 201446	6
Figure 40: All TDR Sensor VMC Bioretention System Data at various longitudinal locations within the system at the center of the BSM for Storms recorded between May 2013 and May 2014 4.	7
Figure 41: Cumulative probability distributions for Horn Street Bioretention temperature through the	
longitudinal profile of the system at the center of the Bioretention Soil Mix (BSM) depth 48	
Figure 42: Cumulative probability distributions for Horn Street Bioretention temperatures through the vertical cross section of the system closest to the inlet	
Figure 43: Cumulative probability distributions for Horn Street Bioretention temperatures through the vertical cross section of the system furthest from the inlet	
Figure 44: All Temperature Sensor Bioretention System Data 50 ft from the inlet for the period of recorded between May 2013 and May 2014	
Figure 45: All Temperature Sensor Bioretention System Data 50 ft from the inlet for the period of recorded between May 2013 and May 2014 with ambient air temperature data added for reference.	
Figure 46: All Temperature Sensor Bioretention System Data 130 ft from the inlet for the period of	
recorded between May 2013 and May 2014	L
recorded between May 2013 and May 2014 with ambient air temperature data added for reference.	
52	L
Figure 48: All Temperature Sensor Bioretention System Data at the center of the BSM across the longitudinal profile of the system for the period of recorded between May 2013 and May 2014 52	2
Figure 49: Cumulative probability distributions for Horne Street Bioretention conductivity through the	
longitudinal profile of the system at the center of the Bioretention Soil Mix (BSM) depth	
)
Figure 50: Cumulative probability distributions for Horne Street Bioretention conductivity levels	2
through the vertical cross section of the system closest to the inlet	5
Figure 51: Cumulative probability distributions for Horne Street Bioretention conductivity levels through the vertical cross section of the system furthest from the inlet	1
	+
Figure 52: All Conductivity Sensor Bioretention System Data 50 ft from the inlet for the period of recorded between May 2013 and May 201455	=
Figure 53: All Conductivity Sensor Bioretention System Data 130 ft from the inlet for the period of)
recorded between May 2013 and May 2014	=
Figure 54: All Conductivity Sensor Bioretention System Data at the center of the BSM across the)
	2
longitudinal profile of the system for the period of recorded between May 2013 and May 2014 56 Figure 55: VMC data for the Horne Street Bioretention system closest to the inlet for selected runoff	כ
events during the monitoring period	7
Figure 56: VMC data for the Horne Street Bioretention system furthest from the inlet for selected	′
runoff events during the monitoring period.	7
Figure 57: VMC data for the Horne Street Bioretention system at the center of the BSM across the	,
longitudinal profile of the system for selected runoff events during the monitoring period 58	0
Figure 58: Temperature data for the Horne Street Bioretention system closest to the inlet for selected	
runoff events during the monitoring period.	
Figure 59: Temperature data for the Horne Street Bioretention system furthest from the inlet for)
selected runoff events during the monitoring period59	2
Figure 60: Temperature data for the Horne Street Bioretention system at the center of the BSM across	
the longitudinal profile of the system for selected runoff events during the monitoring period 59	
Figure 61: Conductivity data for the Horne Street Bioretention system closest to the inlet for selected	,
runoff events during the monitoring period)
Ut	_

Figure 62: Conductivity data for the Horne Street Bioretention system furthest from the inlet for
selected runoff events during the monitoring period61
Figure 63: Conductivity data for the Horne Street Bioretention system at the center of the BSM across
the longitudinal profile of the system for selected runoff events during the monitoring period 61
Figure 64: Water equivalent rainfall precipitation for a selected snowfall event
Figure 65: Ambient air temperature data for a selected snowfall event
Figure 66: VMC data for the Horne Street Bioretention system closest the inlet for a selected snowfall
event
Figure 67: VMC data for the Horne Street Bioretention system furthest from the inlet for a selected
snowfall event
Figure 68: VMC data for the Horne Street Bioretention system at the center of the BSM across the
longitudinal profile of the system for a selected snowfall event
Figure 69: Temperature data for the Horne Street Bioretention system closest to the inlet for a
selected snowfall event
Figure 70: Temperature data for the Horne Street Bioretention system furthest from the inlet for a
selected snowfall event
Figure 71: Temperature data for the Horne Street Bioretention system at the center of the BSM across
the longitudinal profile of the system for a selected snowfall event
Figure 72: Conductivity data for the Horne Street Bioretention system closest to the inlet for a
selected snowfall event
Figure 73: Conductivity data for the Horne Street Bioretention system furthest from the inlet for a
selected snowfall event
Figure 74: Conductivity data for the Horne Street Bioretention system at the center of the BSM across
the longitudinal profile of the system for a selected snowfall event
Figure 75: Water equivalent rainfall precipitation for a selected snowfall event
Figure 76: Ambient air temperature data for a selected snowfall event
Figure 77: VMC data for the Horne Street Bioretention system Closest the inlet for a selected snowfall
event
Figure 78: VMC data for the Horne Street Bioretention system furthest from the inlet for a selected
snowfall event
Figure 79: VMC data for the Horne Street Bioretention system at the center of the BSM across the
longitudinal profile of the system for a selected snowfall event
Figure 80: Temperature data for the Horne Street Bioretention system closest to the inlet for a
selected snowfall event
Figure 81: Temperature data for the Horne Street Bioretention system furthest from the inlet for a
selected snowfall event
Figure 82: Conductivity data for the Horne Street Bioretention system at the center of the BSM across
the longitudinal profile of the system for a selected snowfall event71
Figure 83: Conductivity data for the Horne Street Bioretention system closest to the inlet for a selected
snowfall event
Figure 84: Conductivity data for the Horne Street Bioretention system furthest from the inlet for a
selected snowfall event
Figure 85: Conductivity data for the Horne Street Bioretention system at the center of the BSM across
the longitudinal profile of the system for a selected snowfall event

Table of Tables

Table 1: Measured probabilities when the soil median achieves saturation	23
Table 2: Measured probabilities when the soil media achieves saturation (EPA field measured	
saturation = 0.416 for biomedia, 0.4 for underlying soil, and stone layer)	44

Introduction

The University of New Hampshire Stormwater Center (UNHSC) in conjunction with the Environmental Protection Agency Office of Research and Development (EPA ORD) has completed 2 years of monitoring for the 'Right Sizing Project'. In September of 2013, a one year no-cost extension was requested and granted for the project. The new closing date for the project is 5/31/2015. This provided adequate time to collect additional data and develop the final report.

The project consisted of monitoring three stormwater treatment systems over an 18 month period with the fundamental objective of understanding system hydrology. The monitoring equipment and locations were determined by US EPA personnel and the sites for monitoring were suggested by UNHSC. The systems being studied consisted of two bioretention treatment areas in Dover, NH (Horne St. Bioretention and Lowell Ave Bioretention) and one tree filter in Durham, NH (Tree Pod).

Synthesis of continuous data and baseline analyses were performed for two of these installed filter systems; the Tree Box Filter sited at the edge of a paved parking facility in Durham NH, and a bioretention basin located in Dover NH (Horne Street Bio). The overall intent of this study was to develop a basic water balance for each system in order to understand system hydraulics and the water volume reduction each affords. All synthesis and analysis was completed using Microsoft Excel.

Site Descriptions

Tree Box Filter

The Tree Box Filter installation is a proprietary pre-manufactured system located at the northeast corner of the West Edge parking lot at the University of New Hampshire in Durham (Figure 1). The system studied was KriStar Enterprises' TREEPODTM Biofilter with pre-treatment chamber and internal bypass. The primary filter system is a pre-cast chamber with a 6-foot length by 6-foot width by 3.5-foot deep interior tree pit and an adjacent pre-treatment 2-foot length inlet/outlet sluice. The unit has an open bottom to allow infiltration and is installed on a bedding of granular fill. Inflows that enter the system at the curb inlet flow vertically through about 2.5-feet of filter media, the gravel bedding, and into the underlying native soils. Excess flows that build-up in the gravel are bypassed through a 4-inch perforated pipe installed below in the stone the media. System cross section may be viewed in Figure 2. This system was installed in 2012.

TREEPOD Site Characteristics

The TREEPOD sub-catchment area is 0.4773-acre of primarily asphalt pavement and is large enough to generate substantial runoff, which is gravity fed to the treatment structure (Figure 1). The parking lot here is curbed and entirely impervious. There is some pervious area to the west that comprises less than 0.1 acre of watershed, and upon which snow is plowed in the winter, thereby generating snowmelt runoff on the warmer winter days, even without rainfall. Parking lot vehicular activity is primarily that of UNH service vehicle parking. The runoff time of concentration for the testing area is no more than 5 minutes, with slopes ranging from 1.5-2.5%. The area is subject to frequent plowing, salting, and sanding during the winter months. Literature reviews indicate that pollutant concentrations at this site for sediment (TSS)

are above or equal to national norms for commercial parking lot runoff. The climatology of the area is characterized as a coastal, cool temperate zone. Average annual precipitation is 44 inches that is nearly uniformly distributed throughout the year, with average monthly precipitation of 3.7 inches ± 0.5 . The mean annual temperature is $48^{\circ}F$, with the average low in January at $15.8^{\circ}F$, and the average high in July at $82^{\circ}F$.

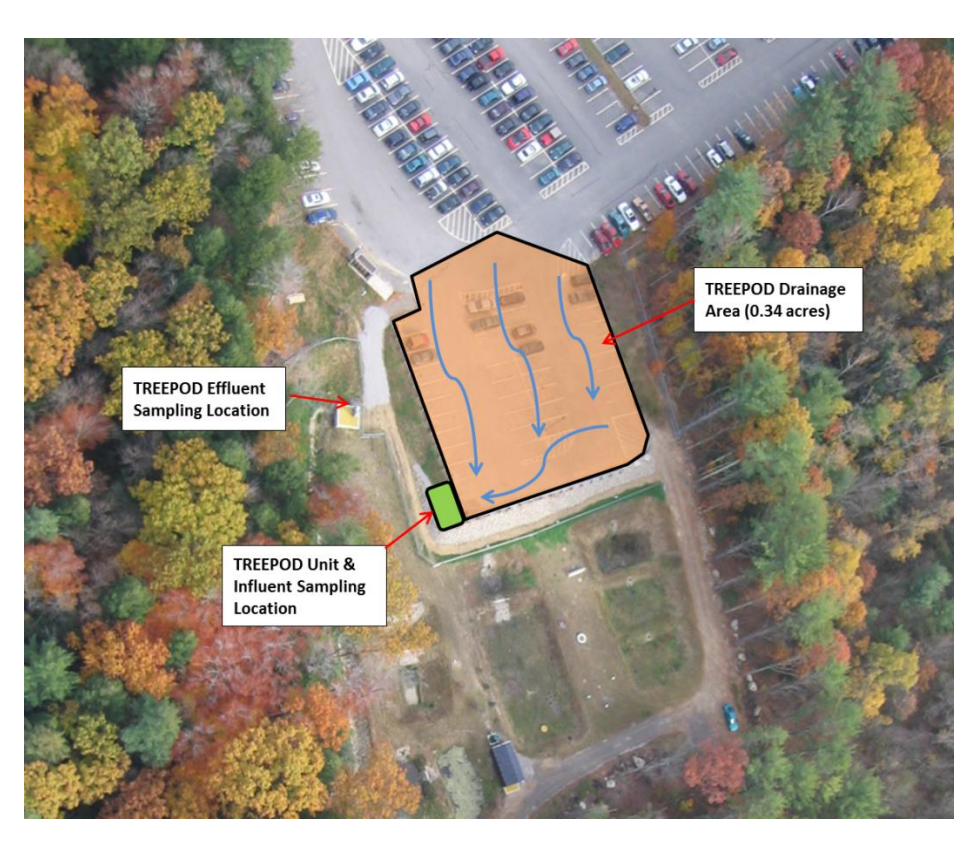


Figure 1: UNH Stormwater Research Facility with TREEPOD™ installation, sampling locations, and drainage area defined. Blue lines are principal surface e drainage pathways.

TREEPOD Configuration and Sizing

The TREEPOD system is manufactured in standard sizes and shapes and the selection is based on peak flow and directly connected impervious area (DCIA). A sizing flow used by KriStar at this site was 1 GPM/ ft²f filter area. The unit tested at the UNHSC is a single-tree system with a 6ft by 6ft internal filter chamber and 7ft by 9ft footprint area (Figure 2). The tested TREEPOD has a general rated flow capacity of 36 gallons per minute (GPM). The TREEPOD unit is equipped with a 2-ft by 6-ft pre-treatment chamber separated from the filter chamber by a coarse debris screen. The pre-treatment chamber is meant to capture gross solids and coarse sediments. An internal bypass is located downstream of the debris screen in the primary filter chamber. This location helps to prevent high flows from carrying sediments and debris over the bypass weir and out of the system.

All flow is treated initially by the debris screen. Flows less than the design flow (36 GPM) are then filtered through the media. When water level above the media exceeds the weir bypass elevation flow may bypass and in that case the bypass flow does not receive any further treatment by the TREEPOD however these flows were monitored as part of the total effluent measurement (flow from perforated underdrain and bypass). As flow infiltrates the TREEPOD media, fine sediments are deposited across the surface of the filter media as well as in the media itself.

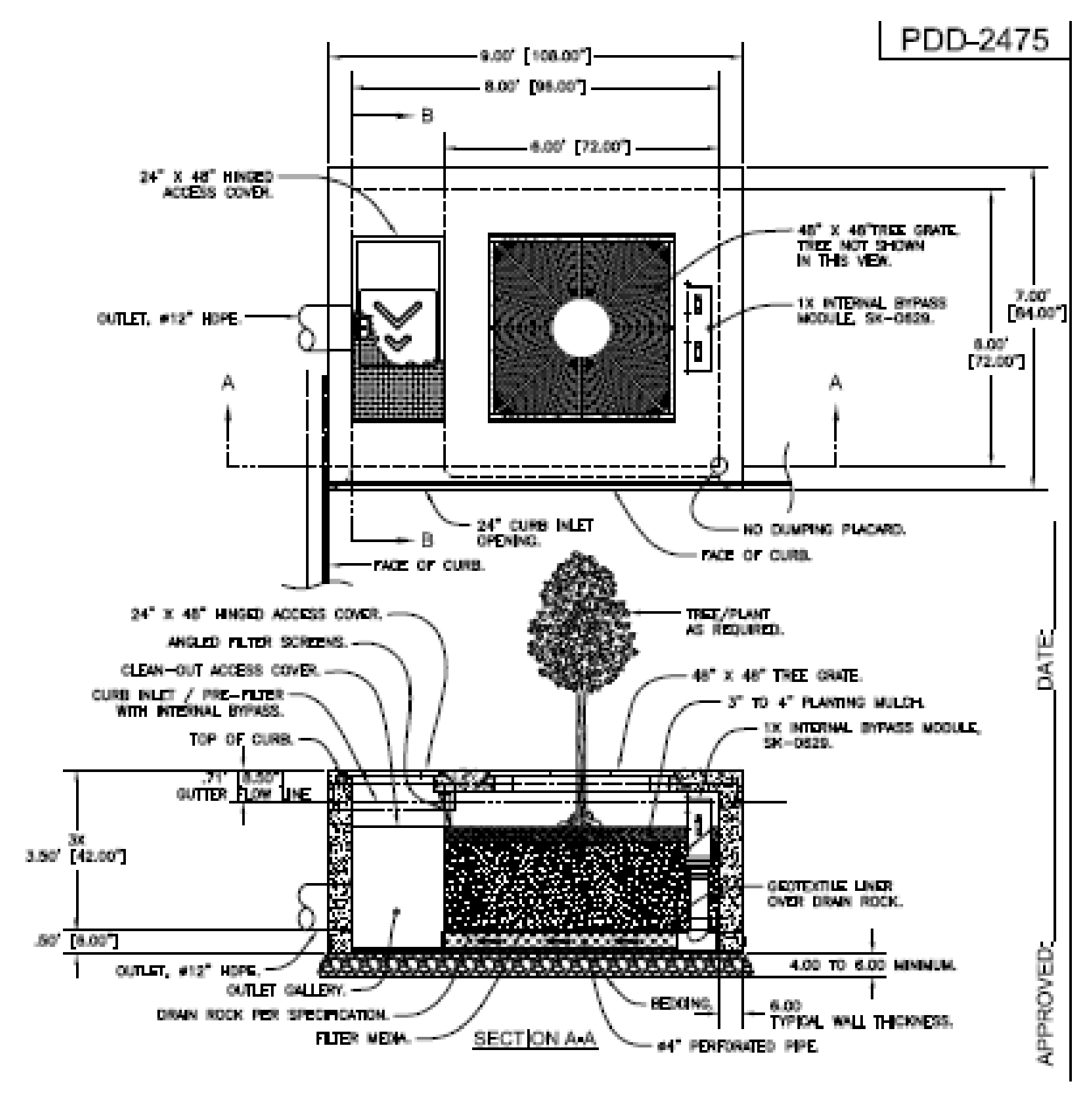


Figure 2: Plan view (top) and section view (bottom) of the TREEPOD™ unit at UNHSC.



Figure 3: Picture of the TREEPOD

TREEPOD Monitoring Instrumentation

Several monitoring instruments were installed in the system and include: time-domain-reflectometers (TDRs) to measure soil moisture, temperature and conductivity; three piezometers to measure water depth and temperature; a surface drain gage lysimeter, and inflow and outflow pressure transducers to measure influent and bypassed effluent that is not infiltrated. A rain gage is also installed at the site in an unobstructed area directly beside the system. All instrumentation is connected to site-specific data loggers. A complete description of the instrumentation of the TREEPOD system is provided in the approved Quality Assurance Project Protocol (QAPP) (attachment A).

Horne Street Bioretention

The Horne Street installation is a site-specific designed system located between Glencrest and Roosevelt Avenues, just to the north of the Horne Street School in Dover, NH (Figure 4). Running parallel along the west side of Horne Street, the system has an approximate footprint (bottom of excavation) of 140-feet in length by 15.5-feet wide and is roughly 4.5-feet deep.

Horne Street Site Characteristics

The Horne Street Bioretention watershed area is a 14.08-acre of residential land use with 27% impervious cover (Figure 4). The residential neighborhood primarily consists of 1/4 acre lots with a runoff time of concentration of 14.9 minutes as determined by the NRCS method, with slopes ranging from 1.0-3.2%. The climatology of the area is consistent with the Durham testing location and characterized as a coastal, cool temperate forest. Average annual precipitation is 44 inches that is nearly uniformly distributed throughout the year, with average monthly precipitation of 3.7 inches ± 0.5 . The mean annual temperature is 48° F, with the average low in January at 15.8° F, and the average high in July at 82° F.

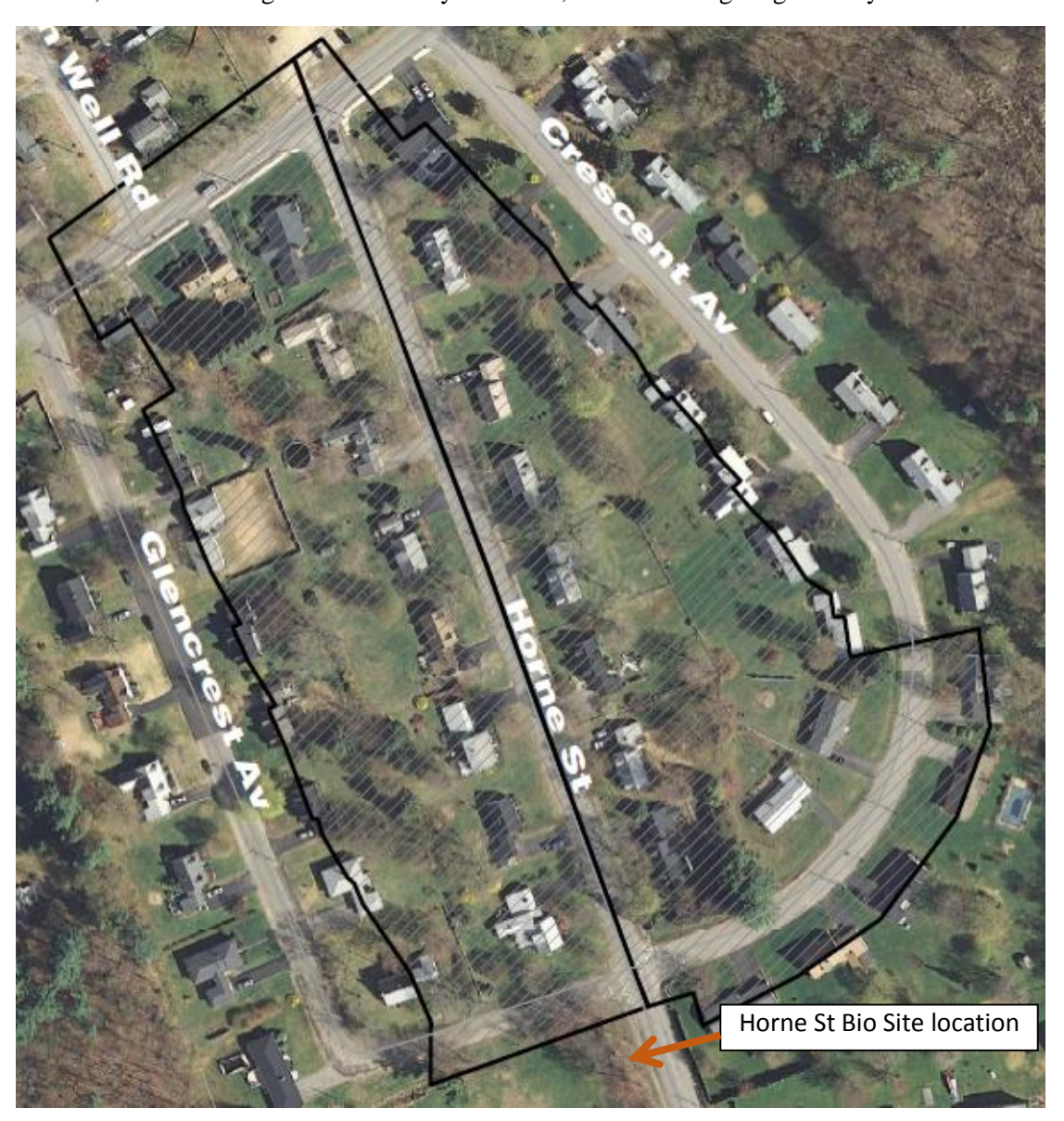


Figure 4: Horne Street neighborhood where the Bioretention System was installed with drainage area defined in black.

Horne Street Bioretention Configuration and Sizing

The Horne Street Bioretention System was designed based on the dynamic sizing equation which assumes that water continually infiltrates the bioretention soil media as the basin fills during a rain event. The bioinfiltration area (A_f) is thus sized based on principles of Darcy's Law, where:

$$A_f = Vwq * d_f/(i(h_f + d_f)t_f)$$

and:

 A_f = surface area of filter bed (square feet);

 d_f = filter bed depth (feet);

i = the infiltration capacity of the filter media divided by a safety factor (2 to 3) (feet per day);

Vwq = the water quality volume resulting from one inch of precipitation (ft³)

 h_f = average height of water above filter bed (feet); and

 $t_f = design filter bed drain time (days)$

There are different ways to size bioretention areas dictated by local stormwater management goals. Two additional methods worthy of mention are the static sizing method where the water quality volume is delivered instantaneously and stored statically within the basin geometry above the filter area and the % watershed sizing method where the filter area is required to be a certain percentage (typically 3-5%) of the contributing area. All methods have advantages and drawbacks. A plan view and system cross section of the design for the system is presented in Figure 5. Because of space limitations, the system that was designed and installed is about 18% of the full design size using the equation above. The equation estimates a bioretention surface area of almost 12,000 ft2 but the space constraints at the site limited its footprint to 2,100 ft².

Upstream stormwater runoff is collected from the street and adjacent lands into three catch basins. Bioretention system inflow enters at the finished grade level of the basin at the north end of the system via a 12-inch culvert and flows toward the south where a surface (beehive) bypass outlet is installed. Both the surface and bottom slope of the system is roughly 1% toward the south end of the basin. The surface of the basin is vegetated with a New England Erosion Control/Restoration mix, and is segmented with two small 4-inch high check dams that divide the surface of the basin into three shallow pools from the inlet pipe to the beehive bypass outlet. Stormwater collected in each pool infiltrates through 24-inches of filter media or flows along the surface. Filtered flows are either infiltrated into the native soil or transferred to the existing downstream catch basin via a 12-inch perforated underdrain installed into 24-inches of pea stone. The bioretention soil media is a mix of 60% sand, 20% wood chips, and 20% topsoil. This system was installed in September of 2012.

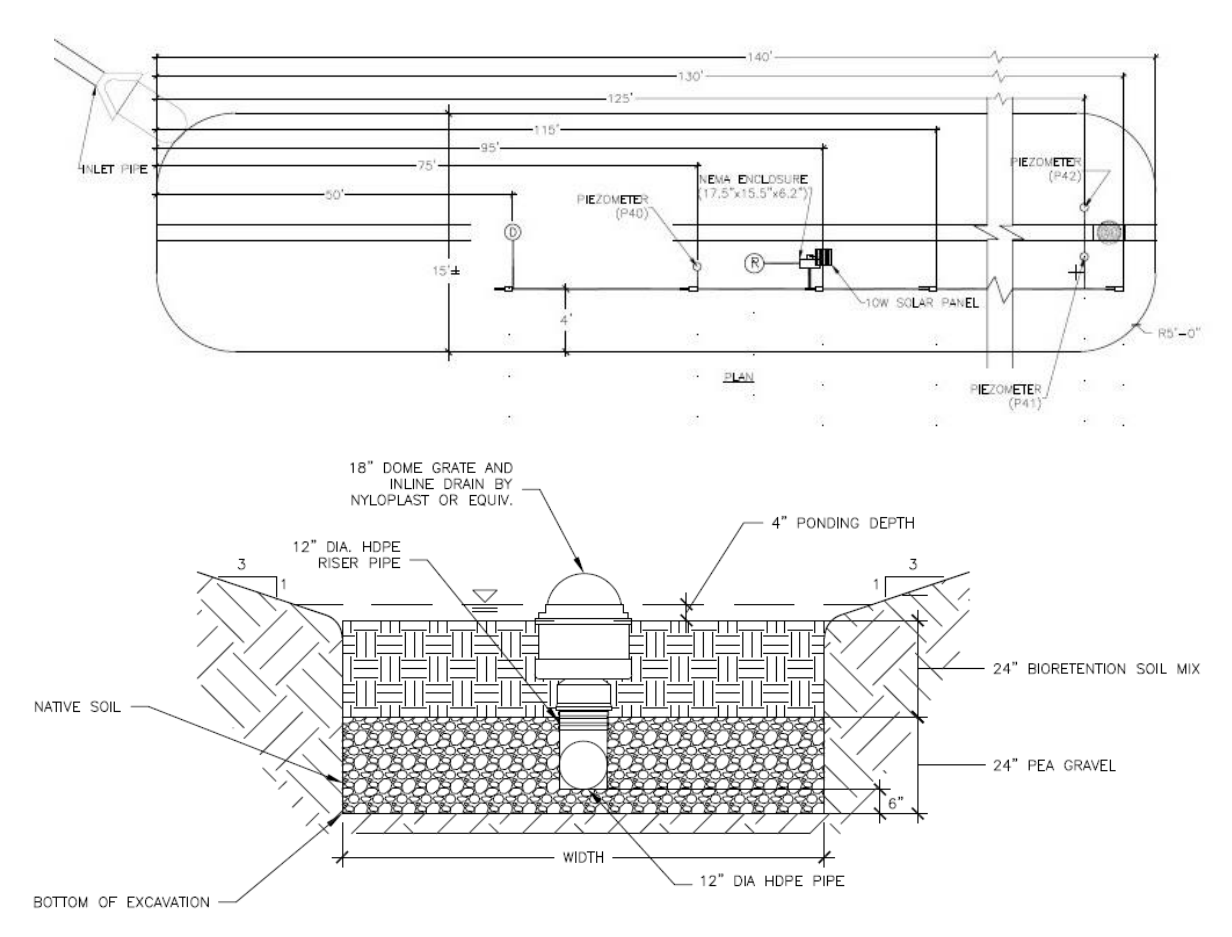


Figure 5: Plan view (top) and section view (bottom) of the Horne Street Bioretention System installed in Dover, NH.



Figure 6: Completed Horne Street System

Horne Street Monitoring Instrumentation

Several monitoring instruments were also installed in the system and include: nine time-domain-reflectometers (TDRs) to measure soil moisture, temperature and conductivity; three piezometers to measure water depth and temperature; a surface drain gage lysimeter, and inflow and outflow pressure transducers to measure influent and bypassed effluent that is not infiltrated. A rain gage is also installed at the site roughly centered within the basin. All instrumentation is connected to site-specific data loggers. A complete description of the instrumentation of the Horne Street Bioretention system is provided in the approved QAPP (attachment A).

Lowell Avenue Bioretention:

A bioretention system at the end of Lowell Avenue in Dover, NH was instrumented and monitored in accordance with the project's approved QAPP. During the initial monitoring phase of the project it was observed that minimal flow was recorded at the effluent monitoring location and it therefore appeared that somewhere water was being lost. It was first assumed that flow was infiltrating through the system and being captured by a nearby 6" perforated foundation drain that was installed by the City of Dover around the perimeter of the neighboring old waterworks building. During construction, a clay barrier was

installed between these two systems to prevent water from flowing towards this 6" perimeter drain. With minimal water passing the effluent location it was assumed that the clay barrier had failed. Upon further inspection it was discovered that the 12" effluent pipe connecting the high flow bypass tee to the outfall location had separated at one of the couplers and sank approximately 6 - 8". This location was upstream of the effluent monitoring location. This caused a large gap to open up between the coupler and the pipe which was enough to effectively drain the majority of the flows before reaching the effluent monitoring location; it is unknown when this occurred. As such, the flow data for this system was deemed unusable since without defensible and reliable effluent flows a water balance could not be developed.

Lowell Avenue Bioretention Monitoring Instrumentation

Several monitoring instruments were also installed in the system and include: nine time-domain-reflectometers (TDRs) to measure soil moisture, temperature and conductivity; three piezometers to measure water depth and temperature; a surface drain gage lysimeter, and inflow and outflow pressure transducers to measure influent and bypassed effluent that is not infiltrated. A rain gage is also installed at the site roughly centered within the basin. All instrumentation is connected to site-specific data loggers. A complete description of the instrumentation of the Horne Street Bioretention system is provided in the approved QAPP (attachment A).

Data Synthesis

Synthesis of the installed systems involved various approaches. One was to look at the entire time series data set as well as the cumulative probability distribution they represent (% of time flow, moisture content, temperature, conductivity were below a specific value). Another approach was to focus on specific events (rainfall, snowmelt). These discrete storms were defined by precipitation and the cessation of system effluent. The integration of hydrograph flows (inflows and outflows) for each storm yields the volume of water, from which volume balance could be computed. This information (% volume reduction) was then graphed and tabulated. The intent of the synthesis was to prepare and organize the raw data into a meaningful and useful format for further analysis.

Measured data consisted of a timestamp in a regular interval (1, 3, 5, or 10-minutes), influent and effluent data in gpm or depth, and rainfall depths. Inflows and outflows provided in gallons per minute (gpm) were summed for each storm and multiplied by the data time interval to obtain total storm volumes. For influent and effluent data provided as depth, flow rates were derived from the hydraulic rating curves developed at the tree pod location (Thelmar weir, generic weir, orifice, and in-field calibration). From the provided observed data, tabulation included:

- Storm label, and start date and time
- Season and month
- Storm and precipitation length (hours)
- Total storm rainfall (inches)
- Total rainfall volume: (gallons)
- Peak precipitation depth and time (inches, hours)
- Total storm influent and effluent volume (gallons)
- Storm peak flow: influent and effluent (gpm)
- Storm peak time: influent and effluent (hours)

- Volumetric moisture content
- Temperature
- Specific conductivity

Tabulated data was then used to calculate:

- Precipitation and storm time centroid (hours)
- Storm lag (p-q_{pi}) (hours)
- Influent/effluent lag (q_{pi}-q_{po}) (hours)
- Peak precipitation rate: Rational Method (gpm)
- Total loss volume for each calculation method (gallons)
- Total loss depth (inches)
- Volume reduction efficiency (%)
- Total peak flow reduction for each calculation method (gallons)
- Peak flow reduction efficiency (%)
- Cumulative Probability Distributions
- Temporal profiles of in-situ sensor throughout the monitoring period

Tree Box Filter

For the Tree Box, a broad-crested weir is at the influent location and a Thelmar weir in the 12-inch pipe for the effluent location. Initially to estimate flows, at the influent a simple rectangular weir equation was employed and at the effluent the manufacturer's rating curve. However initial data synthesis resulted in unbelievable volumes at both influent and effluent locations (much more than what fell from the sky on an impermeable surface); this called into question the validity of the rating curves. Therefore known flows were pumped into the system, and a rating curve was calibrated (depth of flow and flow) for low flows (up to 70 gpm). At the influent, the field-generated rating curve was used up to 70 gpm. Above 70 gpm, the broad-crested weir equation (8-inch crest length) was used up until the influent orifice hydraulically acted as an orifice (5 inches of depth on the weir) per FHWA guidelines. An orifice equation was used for depths of flow at the weir in excess of 5 inches. This calibrated rating curve yielded reasonable results for the influent when compared to the precipitation depth across the watershed. There were a few storms in which there was no measurable precipitation (at the site gage as well as the UNH Weather Station), yet there was influent. In some cases this was snow melt. In other cases there was no apparent reason, and therefore these storms were removed from the data set with the belief that the depth measurement (bubbler) was suspect.

The TREE POD effluent monitoring location was a Thelmar weir in a 12-inch pipe. The Thelmar weir comes with a factory suggested rating curve, however when this was employed, it gave very unrealistic values for flow and runoff volume. Therefore the Thelmar weir was field-calibrated up to a flow of 70 gpm by pumping water through the system. Above the water depth for 70 gpm, the weir equation was then used up until the orifice equation became the hydraulic control per FHWA methods. Employing this compound rating curve gave reasonable results when comparing influent to effluent volumes and to rainfall volume. There were a few storms in which there was much more outflow than inflow. In these

cases the storms were removed from the data set with the sentiment that the effluent depth measurement (bubbler) was suspect.

Total rainfall volume and peak flow were calculated using a drainage area for the Tree Box of 0.4773 acres, and a runoff coefficient of 0.85, for asphalt, for the Rational Method. The date range of the original synthesized data was from 6/12/2012 through 6/5/2014.

Horne Street Bioretention

The Horne Street effluent measurement location monitoring system was very similar to the effluent location for the TREEPOD: a Thelmar weir in a 12-inch diameter pipe. This location also had a field-calibrated rating curve to 70 gpm, and then the same weir and orifice rating curves, for higher flows, as for the TREEPOD effluent location.

The Horne Street influent location was challenging in that the first set-up used a Thelmar weir with a Solinst pressure transducer for two months. After that, the Solinst was paired with a pressure transducer behind the Thelmar weir. However the Thelmar weir would blow-out of the culvert in many storms due to high flows and the pressure build-up upstream of the weir. When the system was removed in December 2013, it was replaced in spring 2014 with a simple pressure transducer. It was believed that the Manning equation would yield reasonable inflows. Unfortunately, negative flow depths were recorded, possibly as a result of blockages on the transducer. At the same time, for much of this second season, the effluent flows were having transmission problems, and so most of that data was lost. For this reason, the inflow and outflow hydrograph data is unusable.

Influent data was measured as depth in feet and had a timestamp in either a 3-minute or 10-minute interval. Effluent had 1-minute or 10-minute time steps.

Analysis

Both sites were analyzed similarly; first looking at each full set of summary data, and then editing the set to exclude storms with missing data, or remove error data points (7999), or negative losses (not uncommon in the winter months...more water out than in). From the working data set, plots were constructed to visualize relationships and identify problem areas. Finally, assessing system hydrology and performing a water balance when possible.

Tree Box Filter

Of the two hundred originally delineated storms, some storms were combined since the effluent did not return to zero between storms. Other storms were removed from the data set due to suspicion about the runoff volumes. The reduced dataset resulted with 145 events. These 145 events were then further subdivided into non-snowmelt events (124) and snowmelt events (21). The snowmelt events were days with or without measurable precipitation, yet snow on the ground, melting temperatures, and measurable runoff.

Figure 7 depicts the volume reduction results for all TREEPOD events . The median volume reduction is 79% and the average volume reduction 64%. The cumulative volume reduction was 77%.

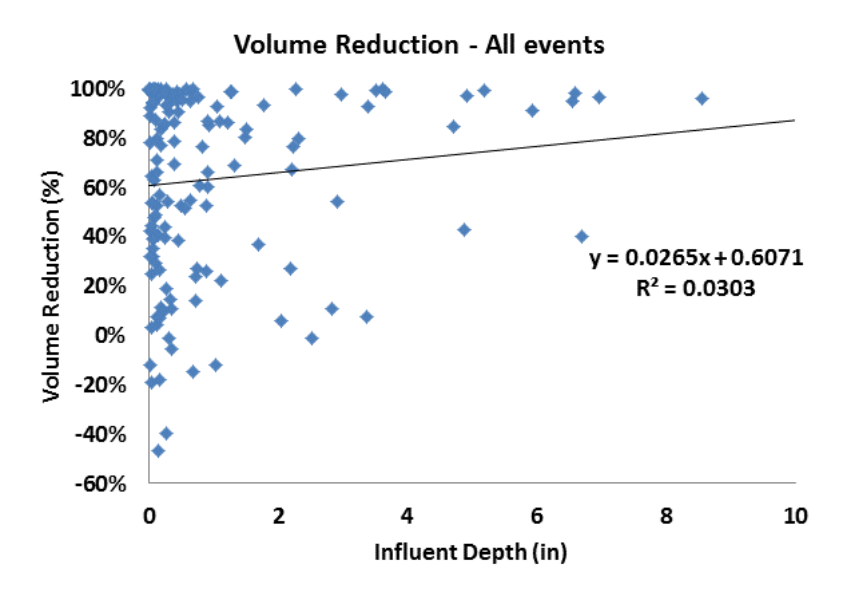


Figure 7: TREEPOD volume reduction versus runoff depth for all individual events.

Figure 8 depicts the peak flow reduction versus the precipitation depth for all events. The median peak flow reduction is 81% and the average peak flow reduction 63%.

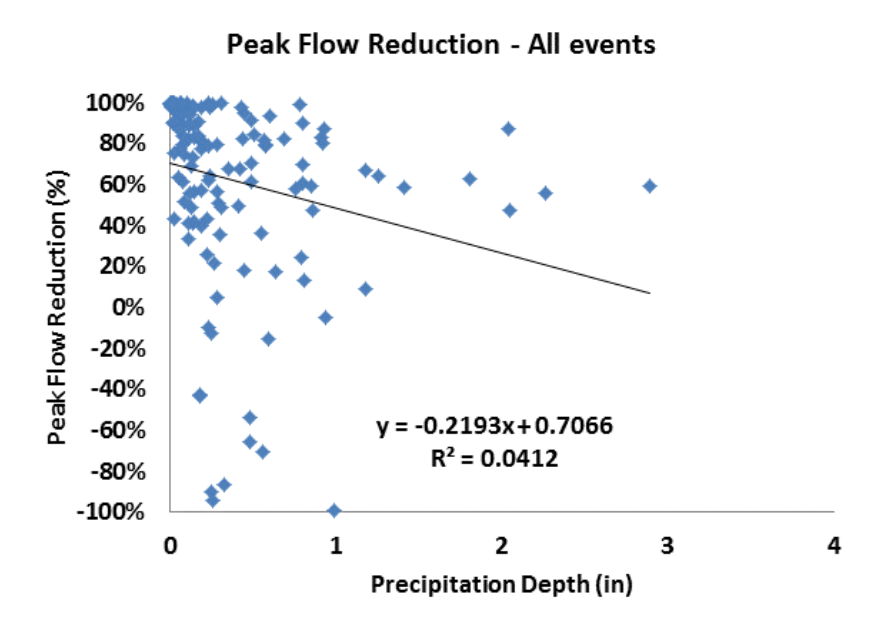


Figure 8: TREEPOD peak inflow versus peak outflow for all individual events.

Figure 9 depicts the volume reduction versus runoff depth for the non-snowmelt events. The median volume reduction is 65% and the average volume reduction 58%. The cumulative volume reduction was 64%.

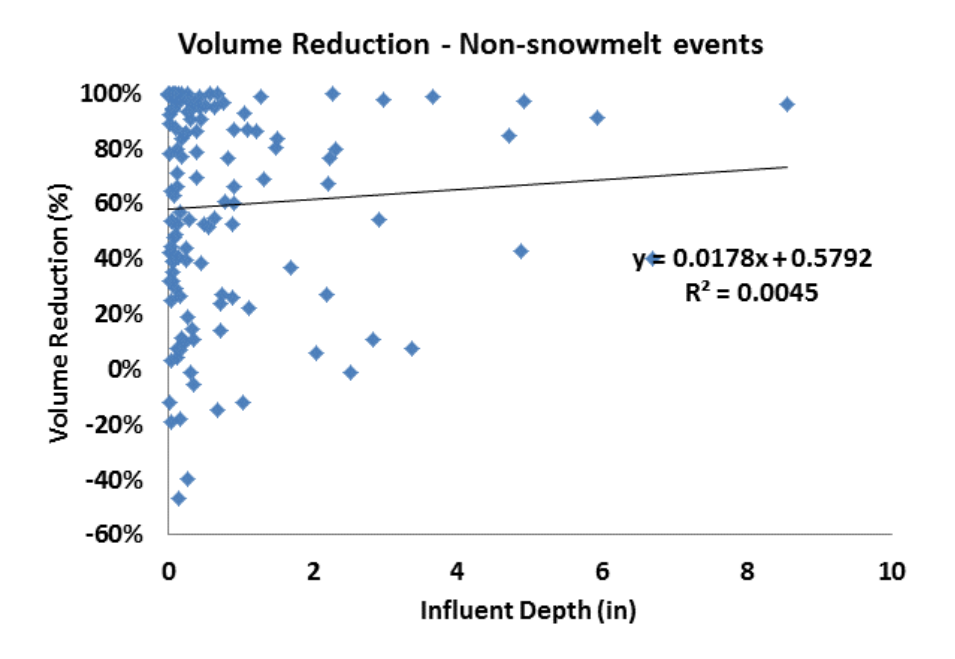


Figure 9: TREEPOD volume reduction versus runoff depth for non-snowmelt events.

Figure 10 depicts the peak flow reduction versus the precipitation depth for non-snowmelt events. The median peak flow reduction is 73% and the average peak flow reduction 57%.

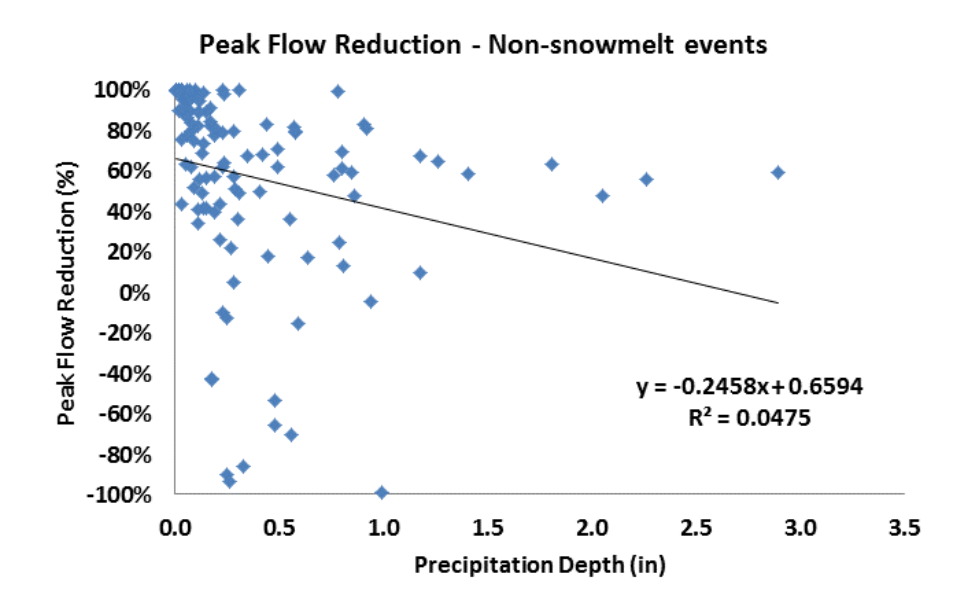


Figure 10: TREEPOD peak inflow versus peak outflow for non-snowmelt events

Page 19 of 75

Figure 11 depicts the volume reduction versus runoff depth for the snowmelt events. The median volume reduction is 96% and the average volume reduction 98%. The cumulative volume reduction was 96%.

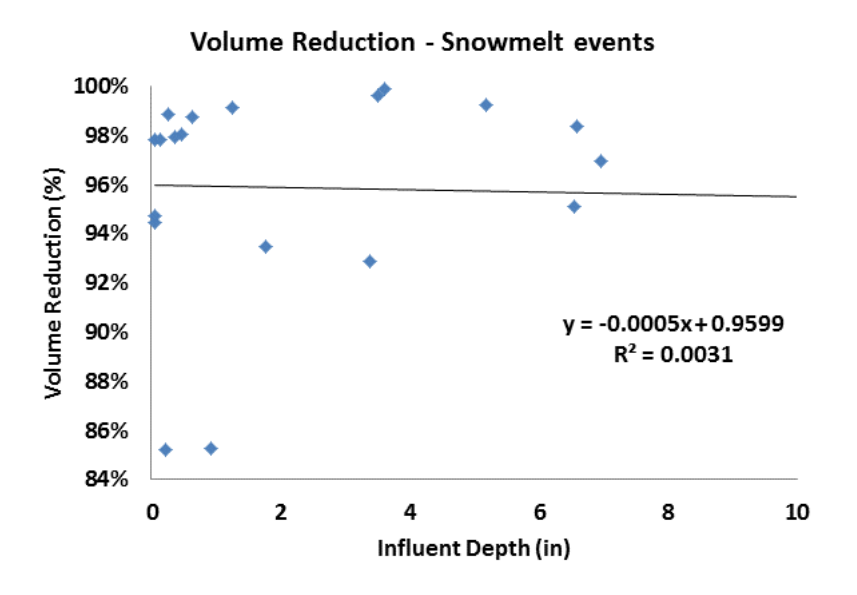


Figure 11: TREEPOD volume reduction versus runoff depth for snowmelt events.

Figure 12 depicts the peak flow reduction versus the precipitation depth for snowmelt events. The median peak flow reduction is 98% and the average peak flow reduction 94%.

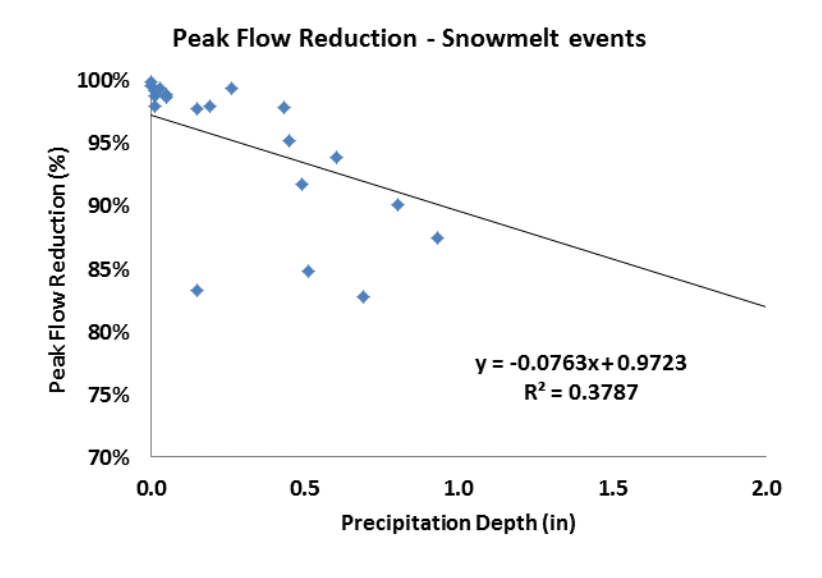


Figure 12: TREEPOD peak inflow versus peak outflow for snowmelt events.

Figure 13 depicts the lag time data for the Tree Pod for all storms. The lag time was determined by inspecting each storm for a peak inflow and respective outflow and subtracting the time stamps to get a time that it took the peak flow to move through the Tree Pod. The average lag time was 15.9 minutes with a median of 10 minutes. It is evident that the higher the rainfall peak intensity, the shorter the lag time.

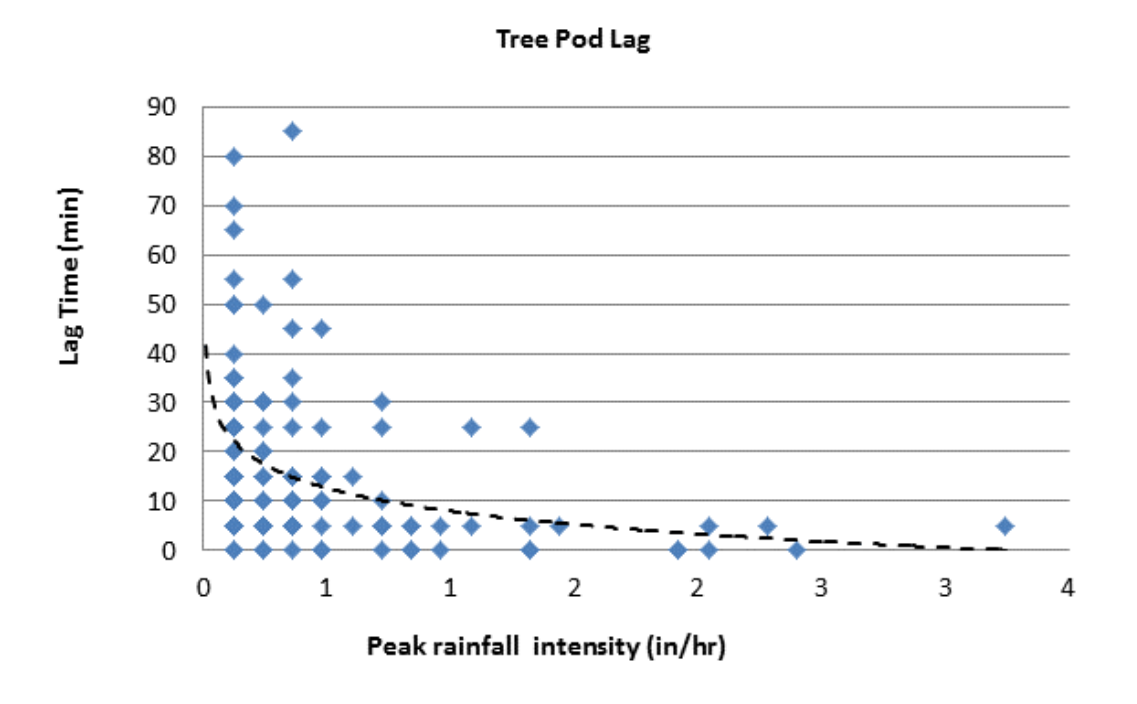


Figure 13: TREEPOD lag time versus peak rainfall intensity

Figure 14 displays the cumulative probability distributions for the Tree Pod volumetric moisture content. Included on this figure is the saturation volumetric moisture content estimated by EPA for just the soil media. The Tree Pod soil media VMC saturation value is 0.383. The saturation value for the stone layer is conventionally set at 0.4, but was not measured. Likewise, the saturation VMC for the underlying soil was not measured, but should be in the range of 0.3 to 0.5 (silty clay soil) and here was assumed to be 0.33. As can be seen from the figure, in general the driest (left-most) location is T01 - 6 in. below the soil media surface, followed by T02 and T03, both 1 foot below the soil media surface, with T02 being located closer to the influent. This would be expected due to soil drying near the surface between runoff events due to evaporation. T04 and T05 are near the base of the soil media and generally have wetter VMC than higher above.

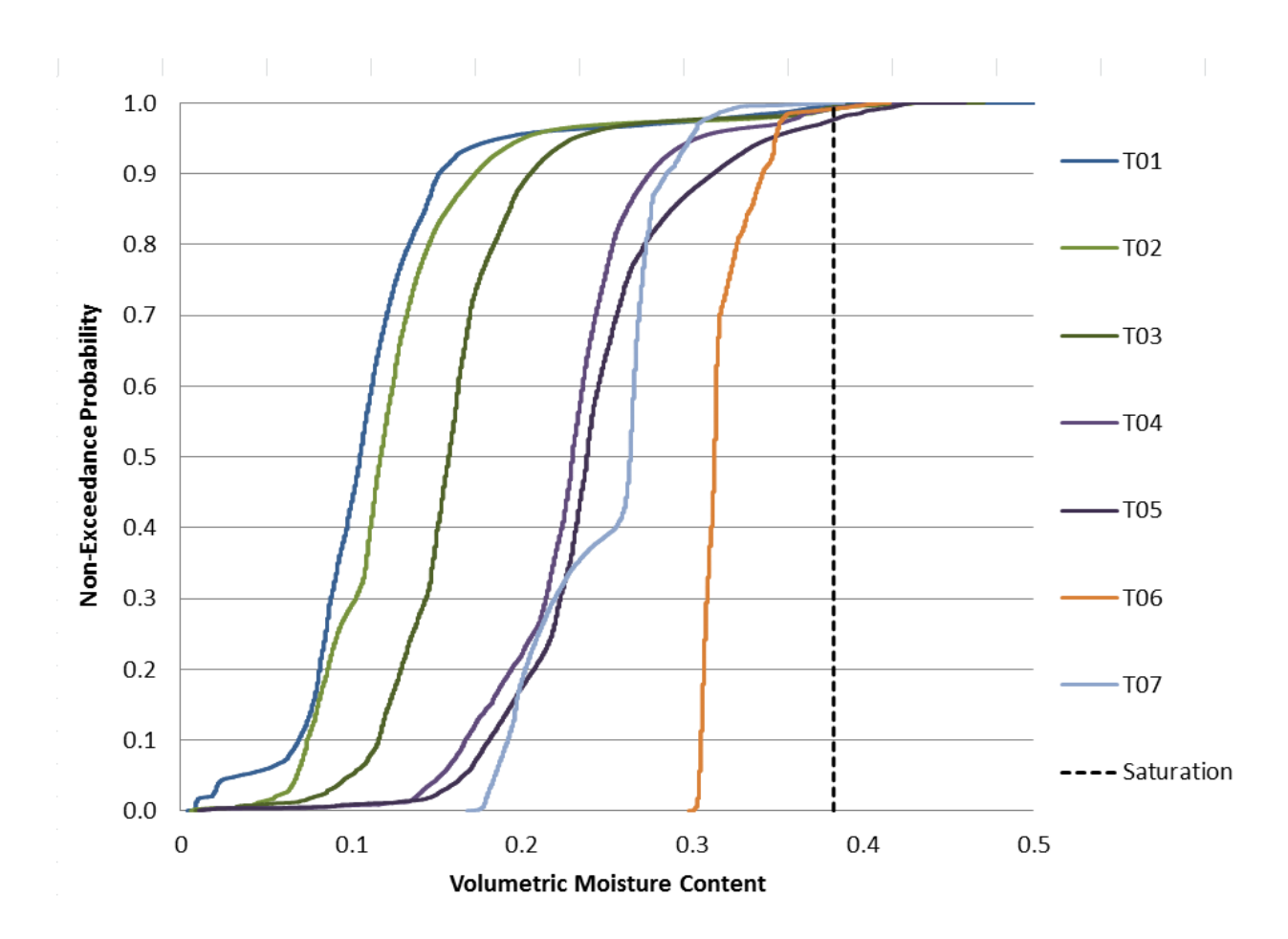


Figure 14: Cumulative probability distributions for TREEPOD volumetric moisture content

In studying the data for Figure 14, the non-exceedance probability or exceedance probability for the soil media can be directly identified and then compared to the probability of when inflows exceed the design flow. When inflows exceed the design inflow, it would be expected that the bioretention media would be at or close to saturation. The probabilities of the soil media reaching saturation may be found in Table 1. In previous UNHSC work on the moisture content characteristics of bioretention soil media and measuring VMC with TDR equipment, it was discovered that the wood chips act as solid particles however they themselves have porosity and may hold water thereby biasing the real VMC upwards. It is expected that the EPA calibration equation took this factor into account. However in the field situation, the TDR measures all the moisture in its sphere of influence and it is possible that at moisture contents measured in the field lower than the saturation moisture content measured in the lab, that the primary porosity of the media is saturated, but because the wood chips are not, TDR readings indicate that the system is not saturated.

TDR ID	TRD Location	Saturated VMC	Non-Exceedance probability at saturation (%)	Exceedance probability at saturation (%)
T01	6-in below top of media	0.383	99.7	0.3
T02	12-in below top of media	0.383	99.1	0.9
T03	12-in below top of media	0.383	99.4	0.6
T04	21-in below top of media	0.383	99.2	0.8
T05	21-in below top of media	0.383	97.6	2.4
T06	1-ft into underlying soil	0.33	81.8	19.2
T07	1-ft into underlying soil	0.33	99.5	0.5

Table 1: Measured probabilities when the soil median achieves saturation.

Figure 15 displays the cumulative probability distribution for days when there was measurable inflow. 83.5% of the data was no flow data. In addition on Figure 15 is the design flow for the Tree Pod of 36 gallons per minute (gpm). The figure and data indicate that of the times when the Tree Pod saw influent, 36.3% of the time the flow exceeded the design flow and therefore there should have been ponding on the surface and potentially saturated flow throughout the Tree Pod media. To compare this to the previous VMC data, the cumulative probability distribution for all flow data appears in Figure 16. Here it can be seen that 36 gpm is exceeded 6% of the time which greatly exceeds the right-hand values in Table 1 for all soil media sensors. This implies then that even though there may be ponding at the surface, in general the Tree Pod soil media flows under unsaturated flow conditions.

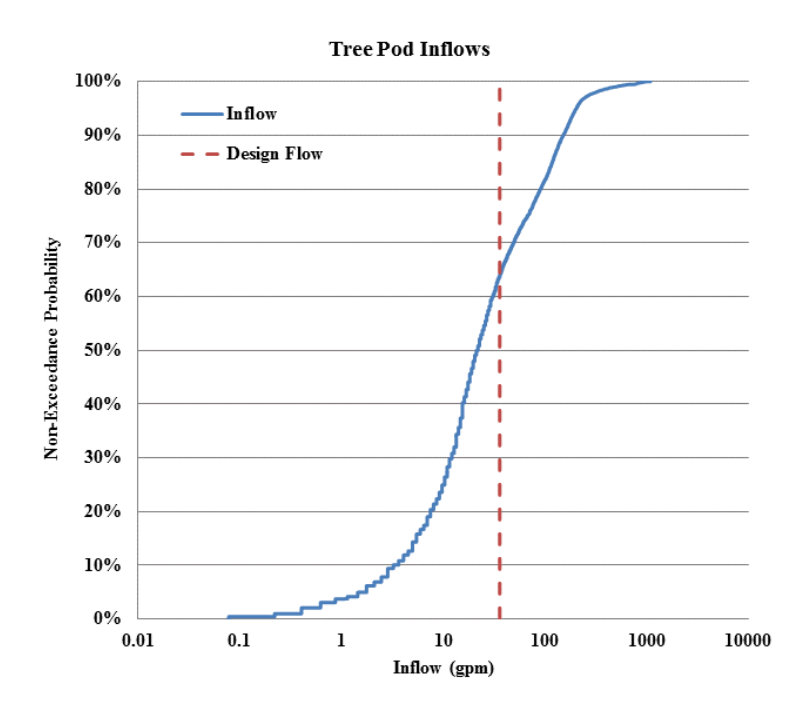


Figure 15: Cumulative probability distribution for non-zero TREEPOD inflows.

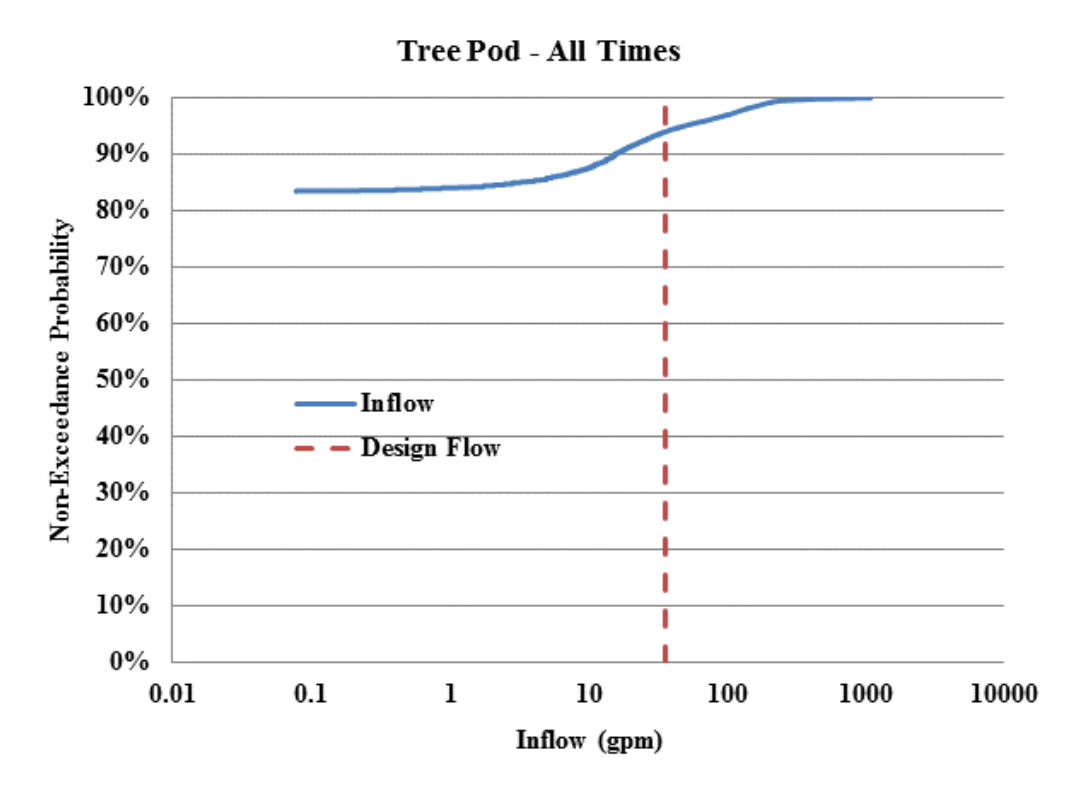


Figure 16: Cumulative probability distribution for all TREEPOD inflows.

Figure 17-22 demonstrate data collected for a summer rainfall event that had two bursts of precipitation. Figure 17 shows the inflow and outflow hydrographs. The dramatic peak flow and hydrograph volume reductions are evident. Note that the first peak was small (47 gpm) and on the order of the design flow and yielded very little outflow. The second inflow peak was over 1,000 gpm, far in excess of the design flow of 36 gpm. This means that during the second burst of rainfall water ponded on the surface and also flowed into the overflow weir in the system. The outflow hydrograph for the first burst peaks at 5 gpm and for the second burst 317 gpm, demonstrating that there was overflow for the second burst. The peak flow reduction for this storm was 70.5% and there was a 66% volume reduction.

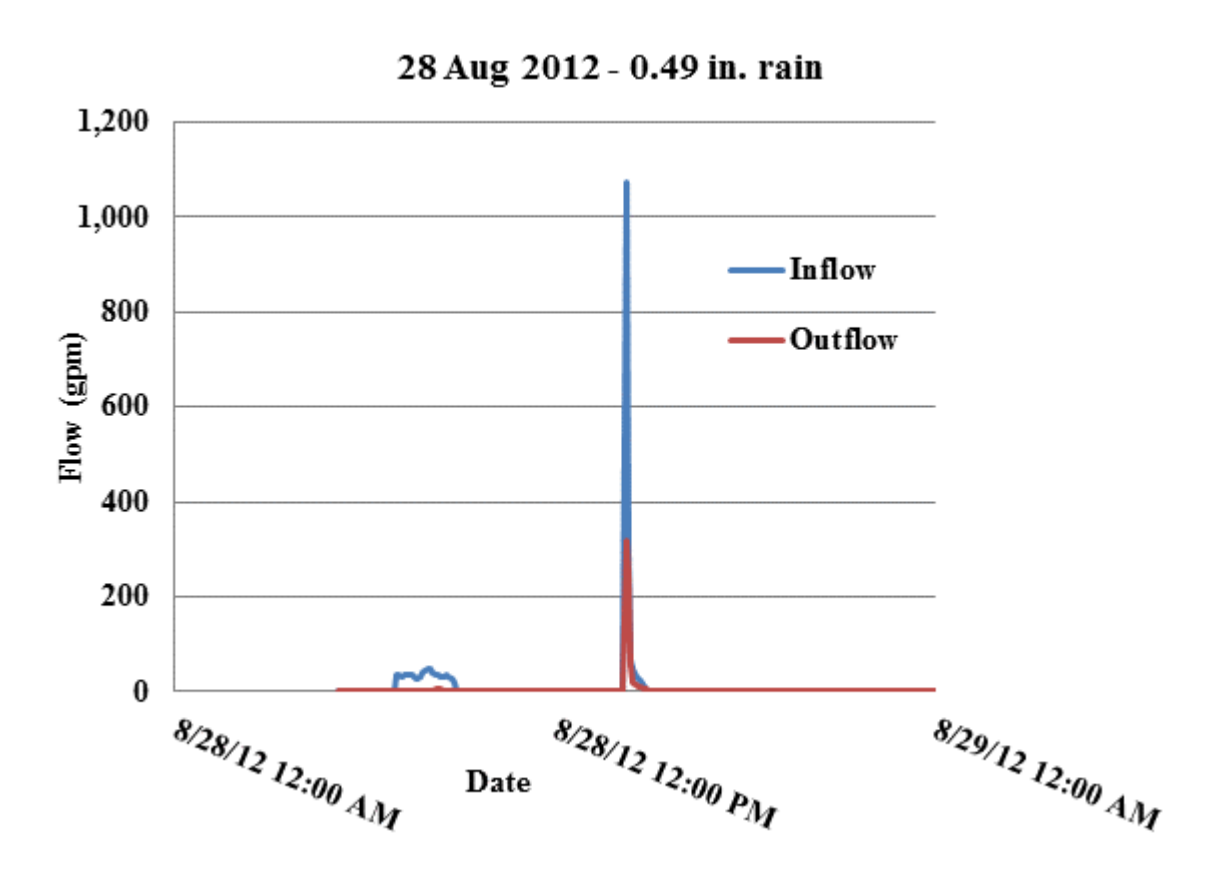


Figure 17: TREEPOD inflow and outflow hydrographs for 28 August 2012 event.

The VMC data for all sensors is plotted in Figure 18 to demonstrate that displaying all data on one plot makes it challenging to interpret. Figure 19 plots the data from one sonde for each depth in order to demonstrate the hydrograph movement through the soil media. The shallowest depth VMC picked up quickly for both rainfall bursts. But at 1 ft depth, only the second burst raised VMC. Because the stone layer filled with water during the first burst, the VMC in the lower part of the soil media reacted to both bursts. The soil media did not achieve saturation except at its base, most-likely due to saturation in the stone.

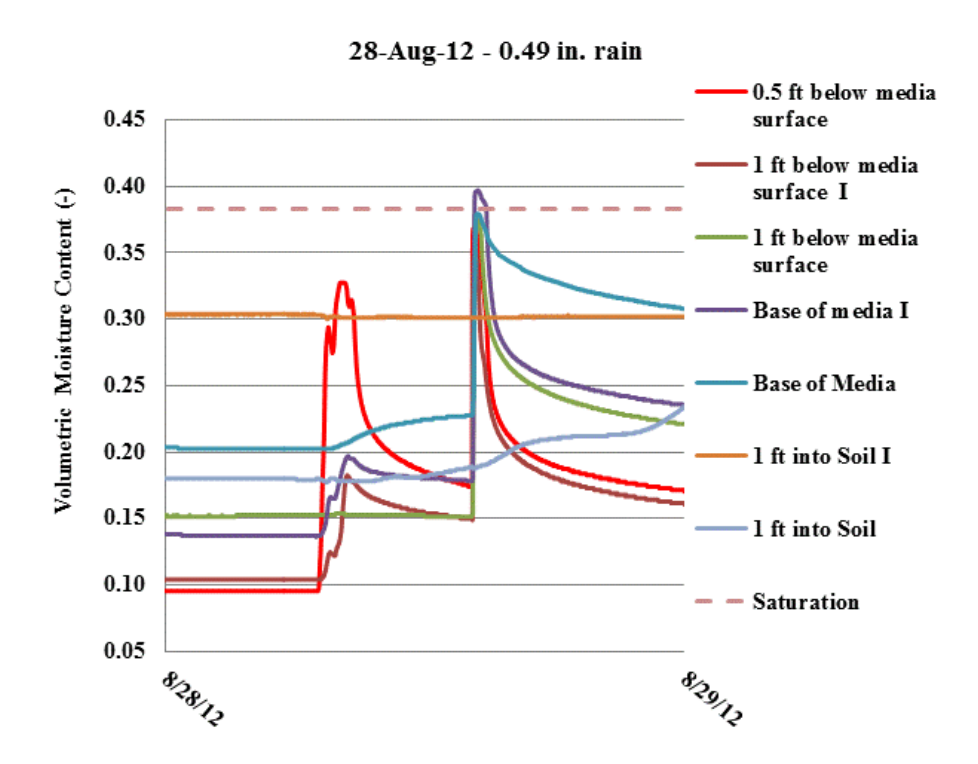


Figure 18: All TDR sensor VMC TREEPOD data for 28 August 2012 event.

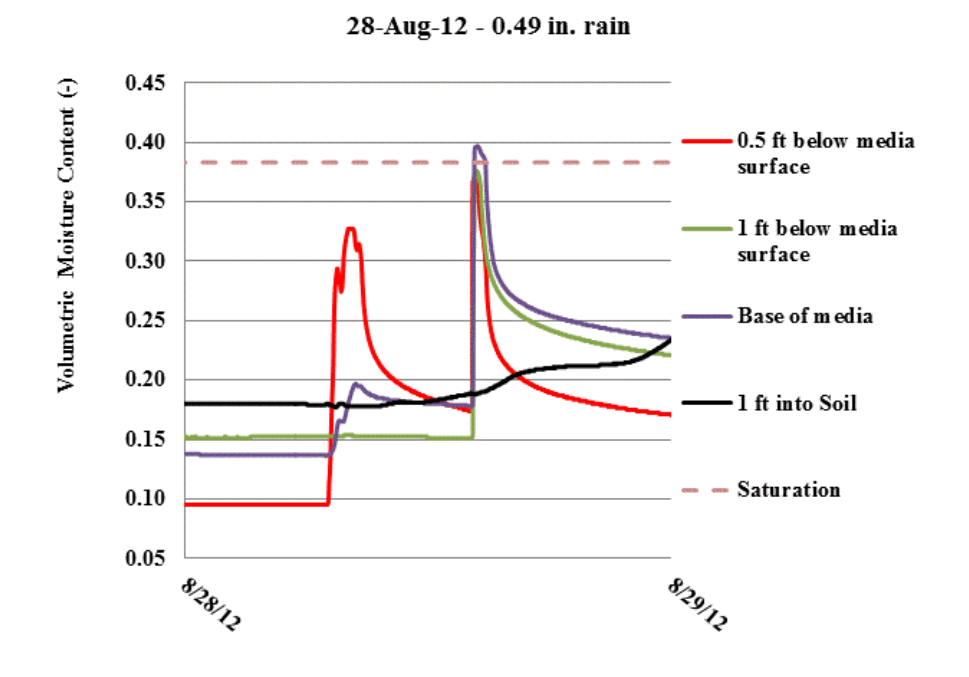


Figure 19: Selected TDR sensor VMC TREEPOD data for 28 August 2012 event.

Figure 20 shows the VMC for the 28 August 2012 storm for TDR equipment buried one foot below the soil media surface. The sonde closet to the inlet responded on the first and second rainfall burst whereas the sonde farthest from the inlet only responded to the second burst. This implies that inflow infiltrates soon after it enters the soil media system and does not spread evenly over the surface until inflows much larger than the design flow occur. Saturation did not occur at this depth.

28-Aug-12 - 0.49 in. rain

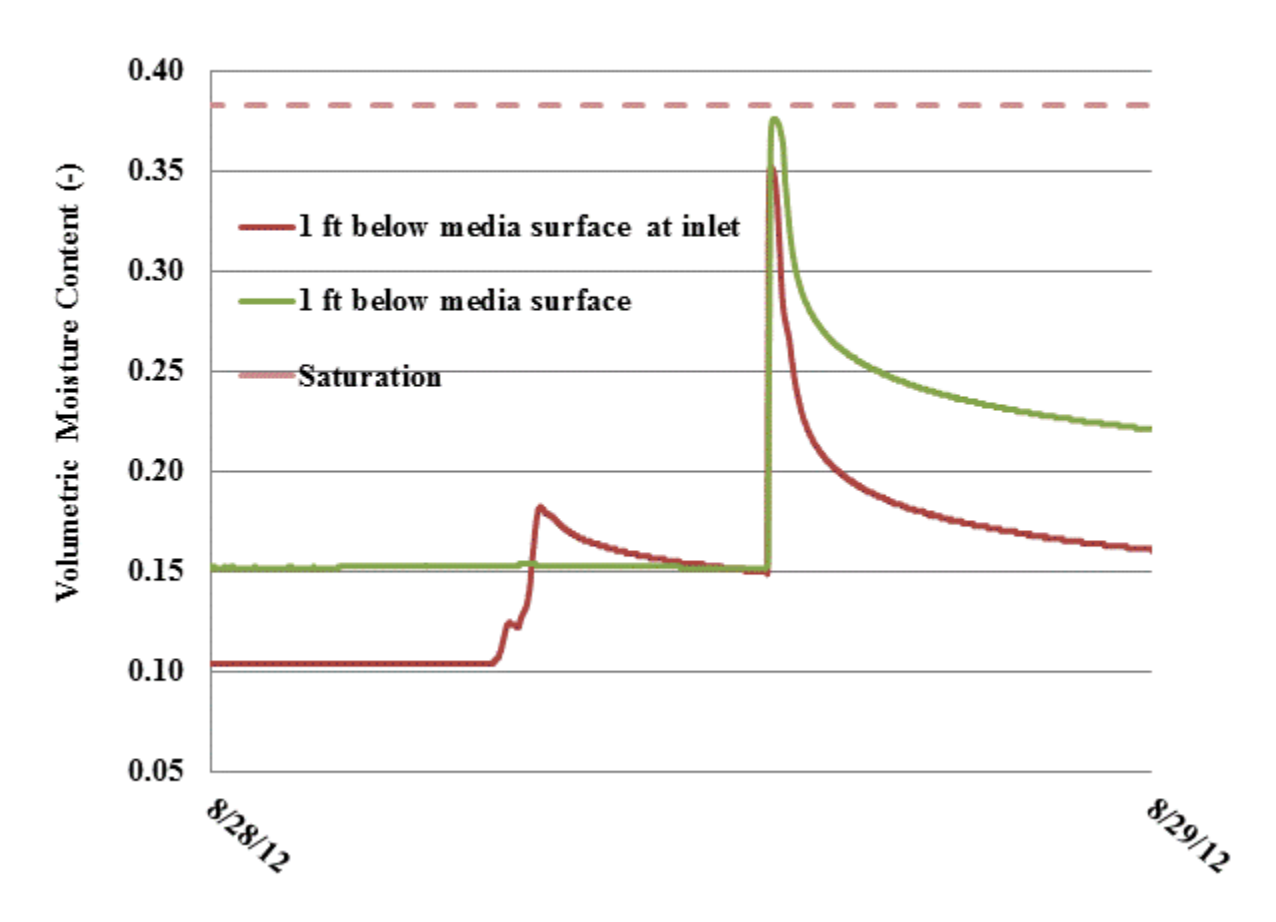


Figure 20: TREEPOD TDR sensor VMC data for 1 ft below the soil media surface data for 28 August 2012 event.

Figure 21 shows the temperature profile for this storm through the soil media and into the underlying soil. Included in this plot is the air temperature. The temperature in the soil below slightly increased demonstrating the temperature buffering capacity of infiltration system which is located below the earth's surface.

28-Aug-12 - 0.49 in. rain -0.5 ft below media surface -1 ft below media surface -Base of media -1 ft into Soil -Air

Figure 21: TREEPOD temperature profile for the 28 August 2012 event.

Figure 22 displays the water level data in wells installed in the Tree Pod system. The data indicate there was surface ponding for the second burst of rain and not the first, as reflected in the VMC data. The data also indicate that the stone layer was filling with water for both bursts, and almost completely drained between bursts. Lastly there was also a short-lived response in the underlying soil for the second burst.

28-Aug-12 - 0.49 in. rain

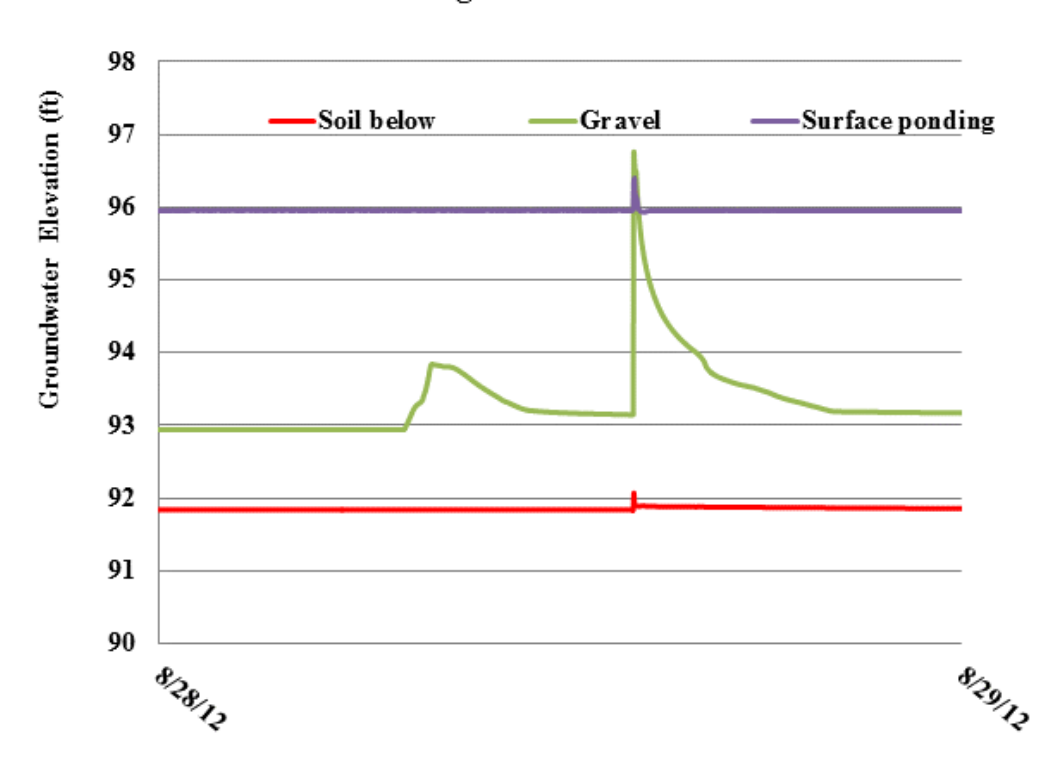


Figure 22: TREEPOD well water levels for the 28 August 2012 event.

Figures 23-27 show similar event data for a very small rainfall event on 30 May 2014. The rainfall depth was 0.12 inches. The inflow peak was 207 gpm and the outflow peak was 94 gpm. At this inflow rate, there also was overflow in the Tree Pod system. The peak flow reduction was 56% and the volume reduction 87%.

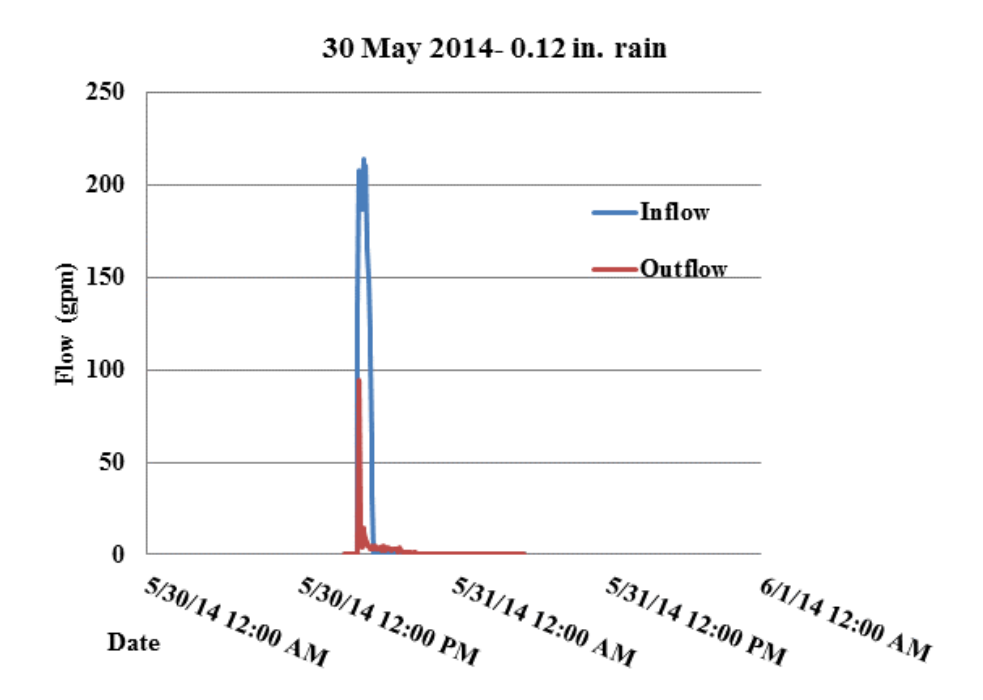


Figure 23: TREEPOD inflow and outflow hydrograph for the 30 May 2014 event.

Figure 24 shows the VMC profile for the 30 May 2014 event. Even with overflow, the soil media did not achieve saturation. Also, the underling soil VMC did not react to the storm.

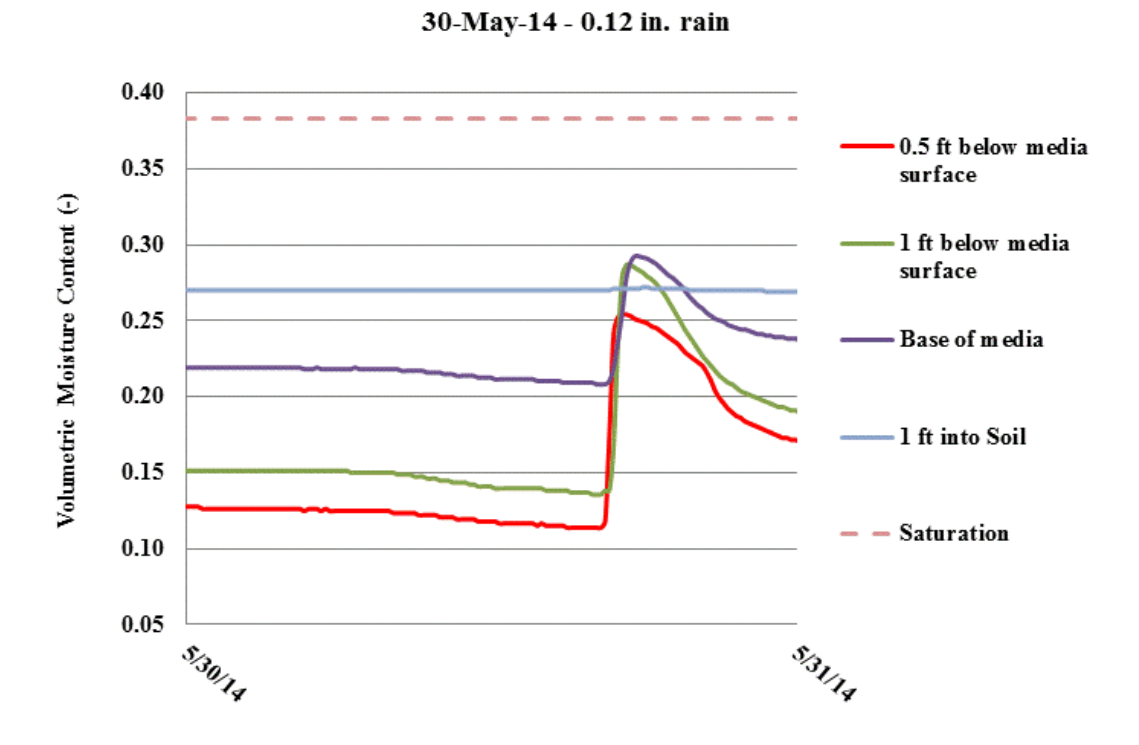


Figure 24: TREEPOD VMC profile for 30 May 2014 event.

At the one foot depth both VMC sensors reacted almost the same, yet neither achieved saturation as demonstrated in Figure 25.

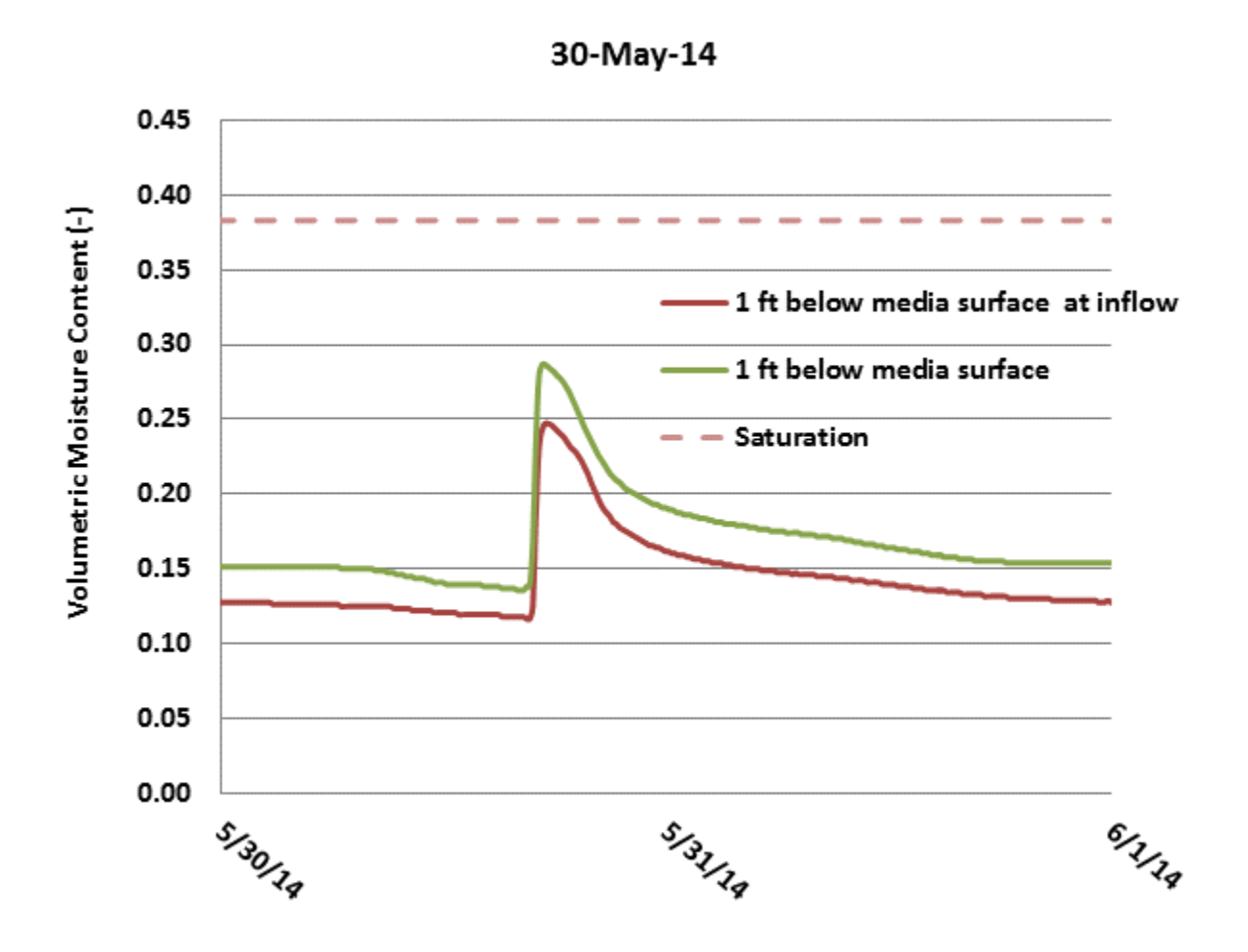


Figure 25: TREEPOD VMC data at one foot depth into the soil media for the 30 May 2014 storm.

Figure 26 depicts the well water level data for the 30 May 2014 storm. There was surface ponding as expected from the inflow hydrograph as well as saturation in the stone layer. The latter drained fairly quickly.

30-May-14 - 0.12 in. rain

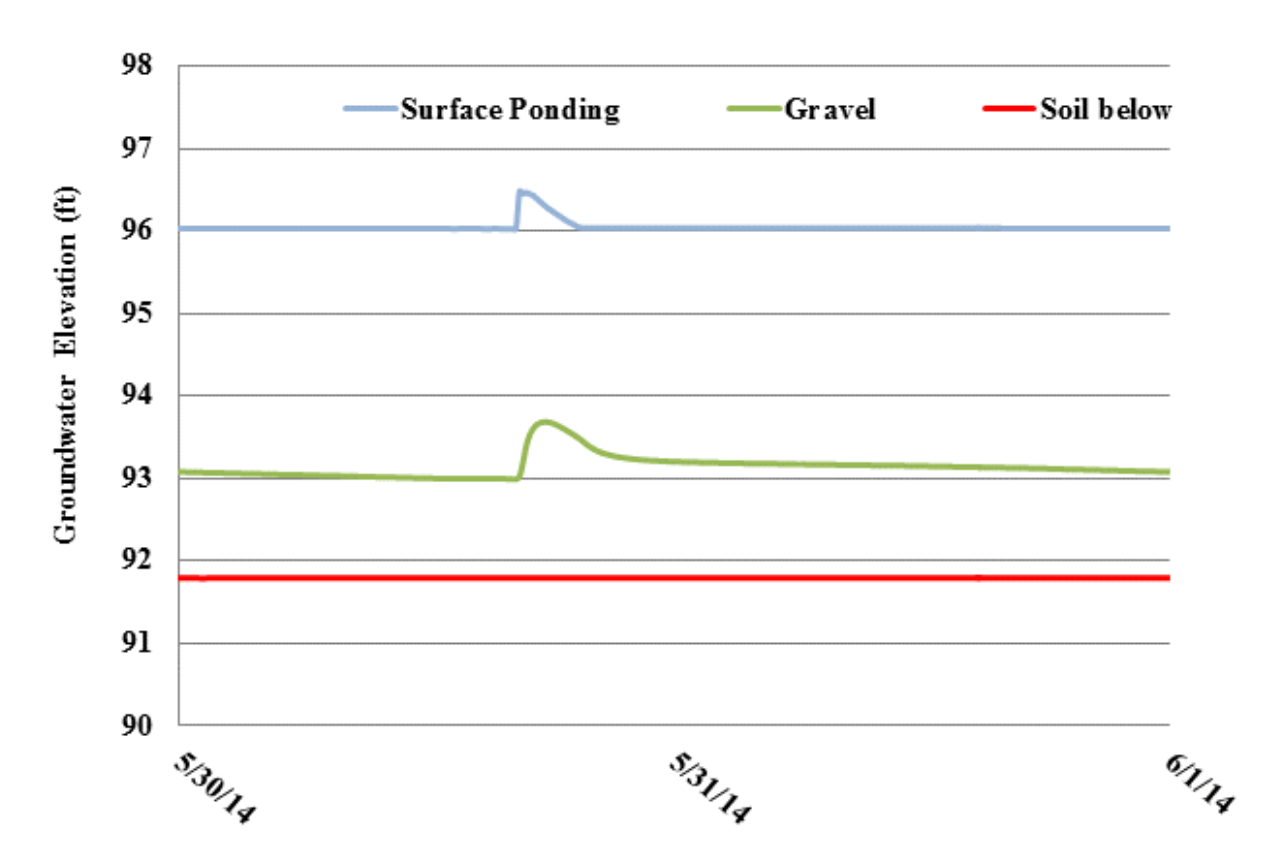


Figure 26: TREEPOD water level data for the 30 May 2014 event.

Figure 27 displays the temperature sensor data for the 30 May 2014 storm. The runoff event can be tracked by the 0.5 foot depth sensor (red curve) and followed through the soil profile even into the underlying soil. Again, there is excellent temperature buffering afforded by the system as demonstrated by the small change in temperature in the underlying soil.

30-May-14 - 0.12 in. rain

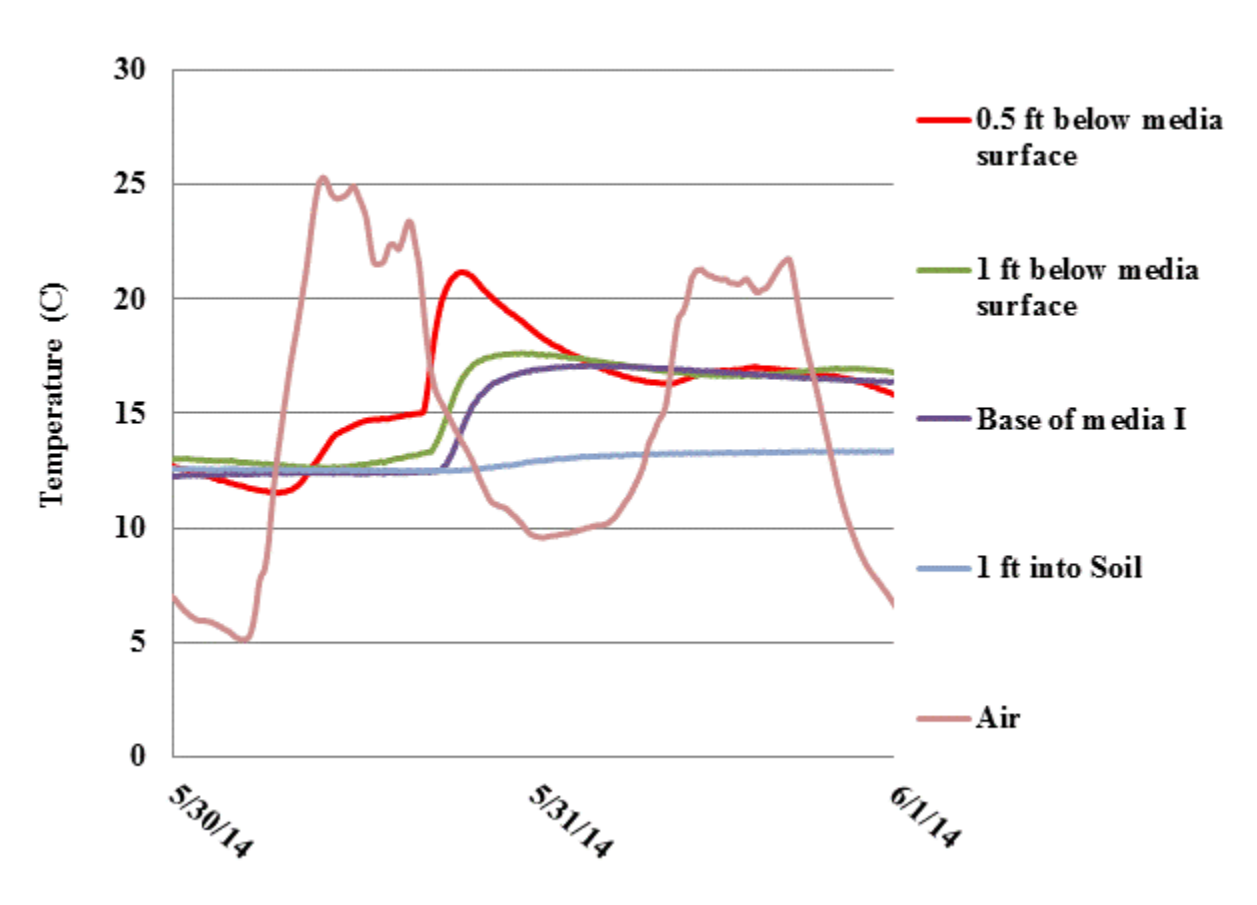


Figure 27: TREEPOD temperature profile for the 30 May 2014 event.

Figures 28-33 demonstrate a snowmelt event. The inflow hydrograph peak was on the order of the design flow and therefore overflow most likely did not occur. Peak flow reduction averaged 95% over these days and total volume reduction was 95%. There was 0.69 in. of rain late on 21 February 2014.

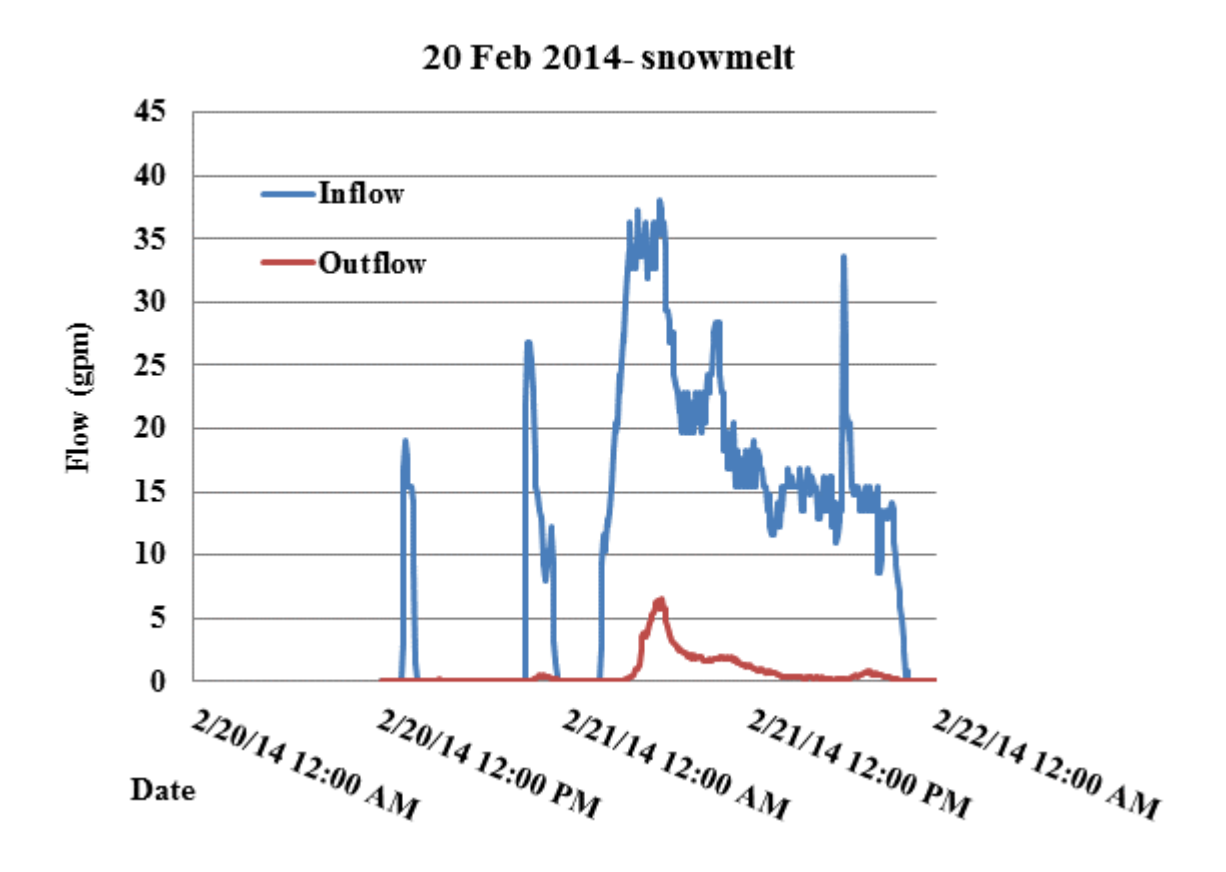


Figure 28: TREEPOD inflow and outflow hydrographs for 20 February 2014 event.

The VMC profile for the 20 February 2014 event shows near saturated conditions (Figure 29). This is in part due to frozen soil. The underlying soil VMC is at the highest point of the year also potentially reflecting near frozen conditions. Since the stone is free draining, cold air may enter here and start frost from that elevation. The VMC data reflects daily snowmelt with the most dramatic responses closer to the soil media surface. Some sensors were not working during the early part of this event.

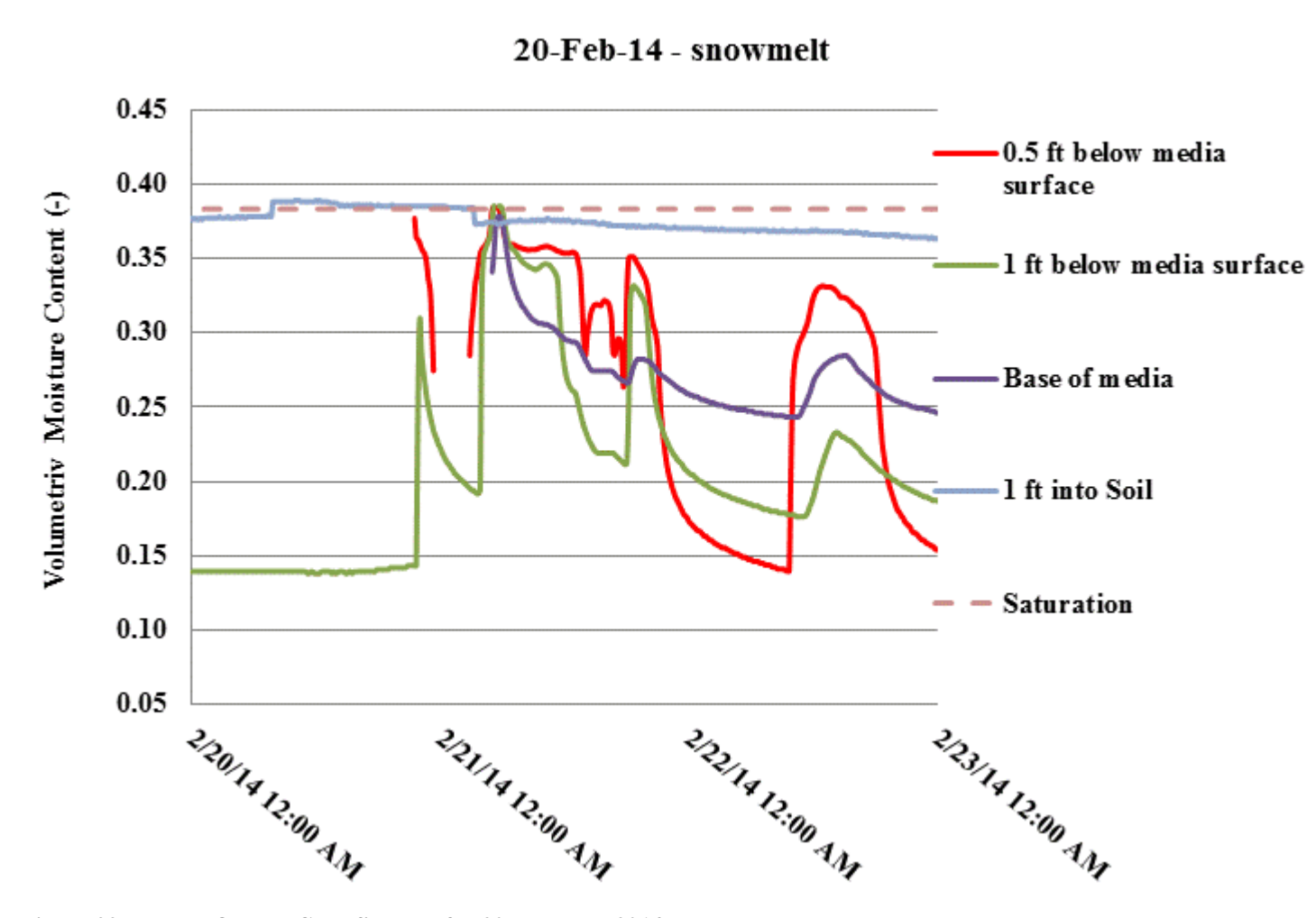


Figure 29: TREEPOD VMC profile data for 20 February 2014 event.

At the one foot soil media depth, both sensors react similarly and show the diurnal variation in runoff (Figure 30).

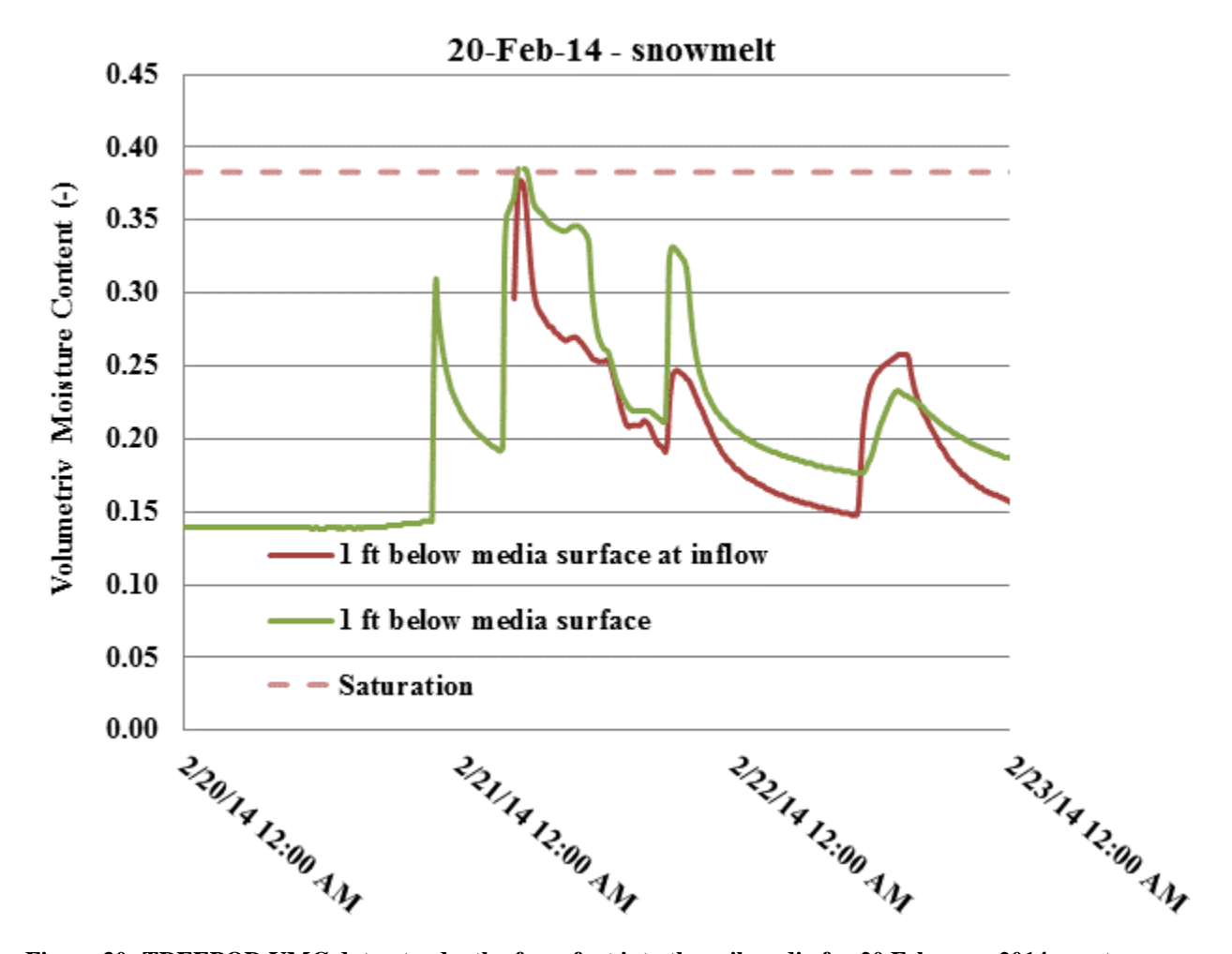


Figure 30: TREEPOD VMC data at a depth of one foot into the soil media for 20 February 2014 event.

The well water level data in Figure 31 indicates surface ponding starting on the 21st but not on the day before. The stone layer manifests water accumulation throughout the melt (Figure 31).

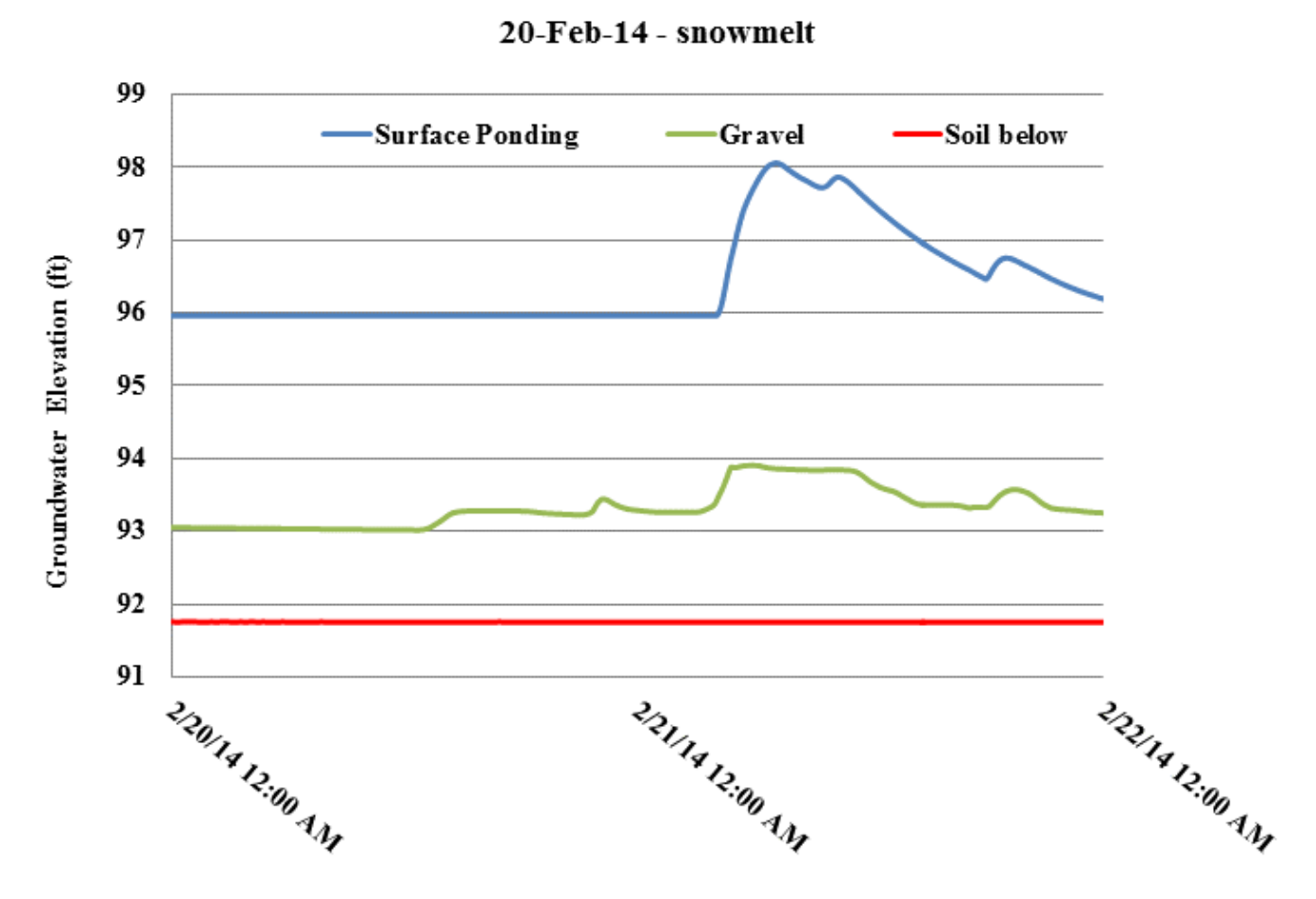


Figure 31: TREEPOD well water level data for 20 February 2014 event.

Figure 32 displays the temperature profile for the 20 February 2014 event. Although there was meltwater runoff on the 20^{th} , there was not enough to completely thaw out the system and would explain the very low outflow that day. All levels responded to the very cold runoff by lowering their temperatures almost to the freezing level.

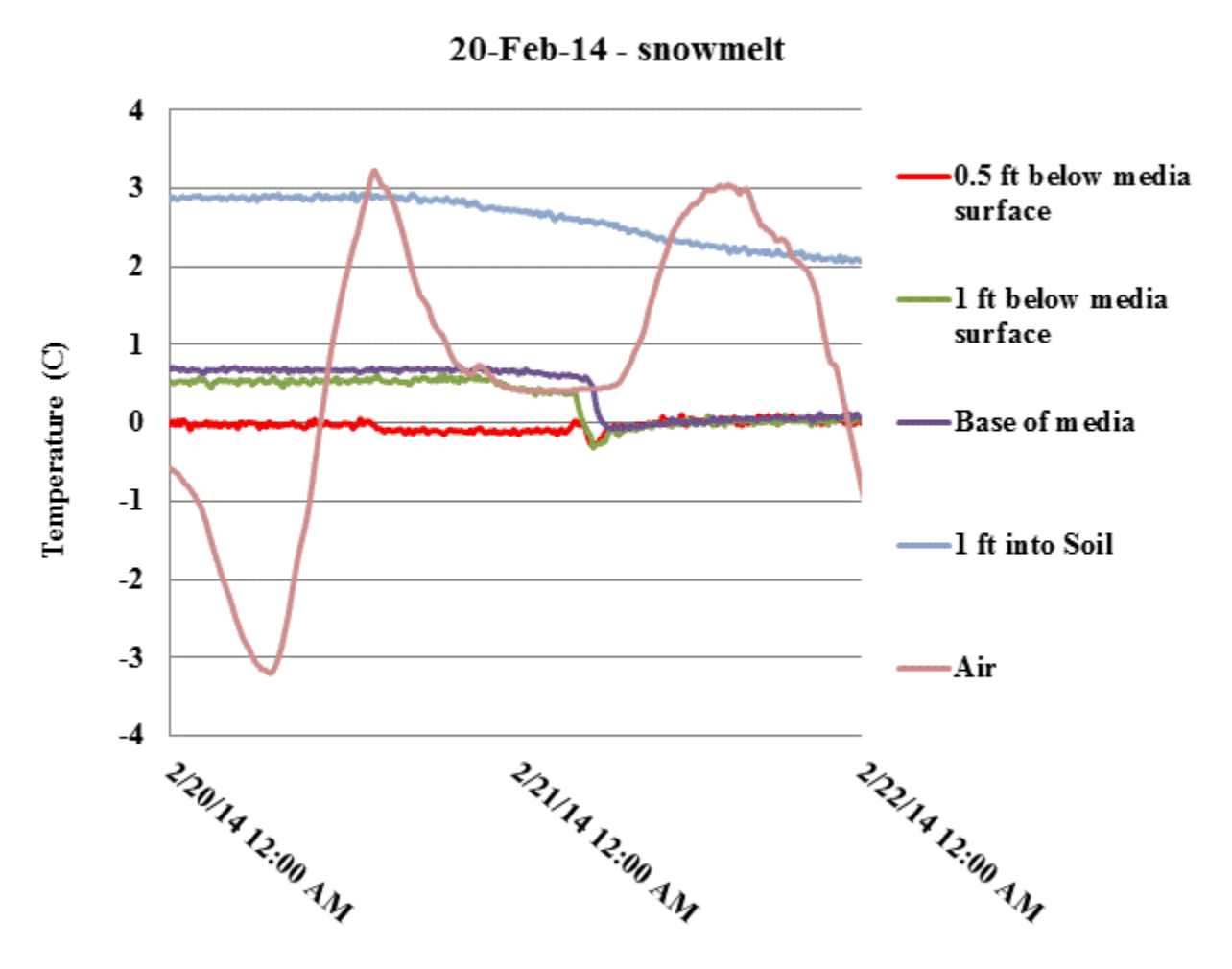


Figure 32: TREEPOD temperature profile for 20 February 2014 event.

Figure 33 displays the profile of electrical conductivity (in decaSeimens per meter). Conductivity can be used as a surrogate for the amount of dissolved salts in the runoff. The Shallow depth sensors react each day most dramatically. Once there is significant melt on the 21st, the deepest sonde then dramatically responds most likely reflecting the meltwater accumulating in the stone layer. The high conductivities are the result of the use of salt on the parking lot surfaces in the winter. It is also noted that the underlying soil has a high value that is maintained throughout the event.

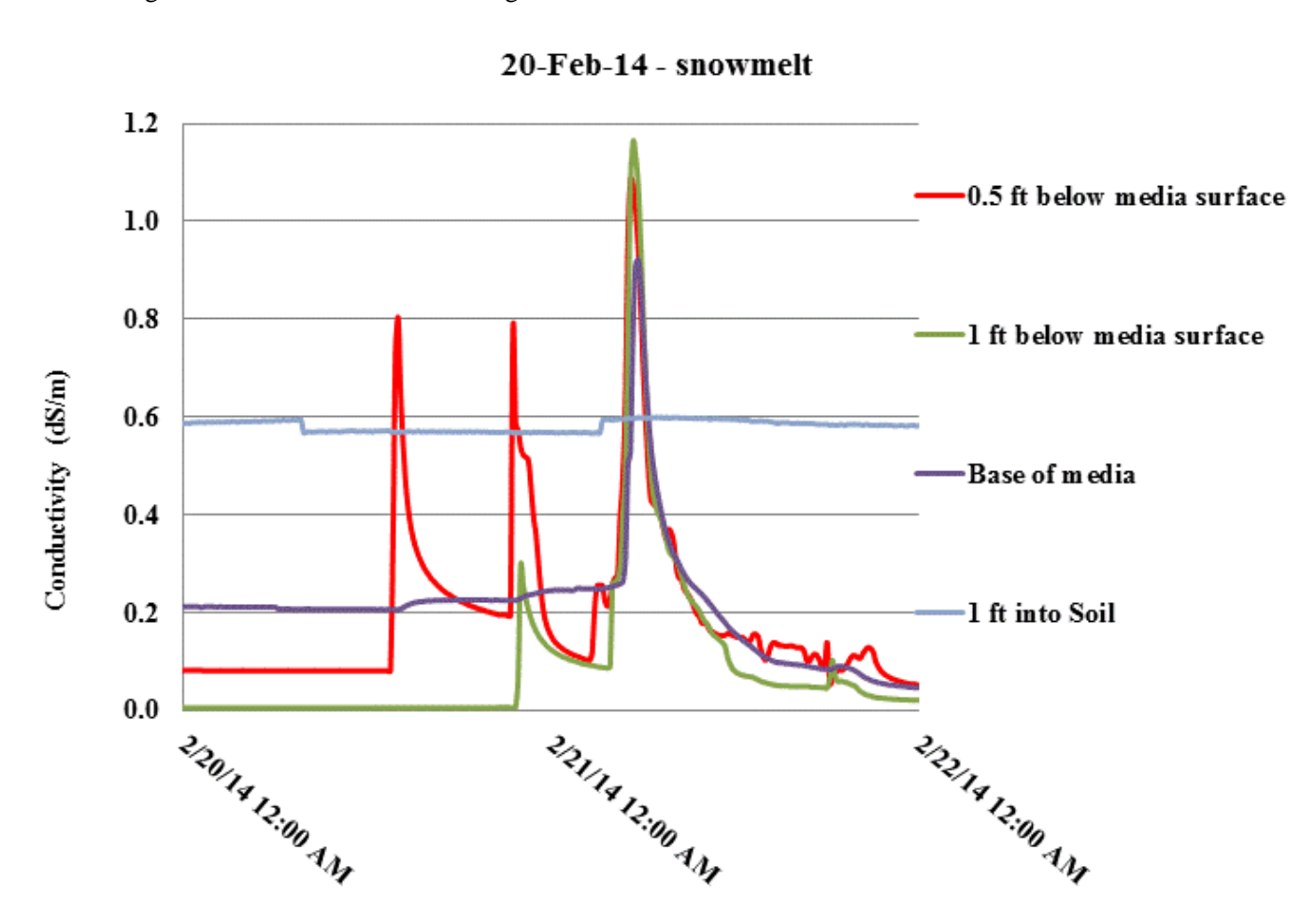


Figure 33: TREEPOD electrical conductivity profile for 20 February 2014 event.

Horne Street Bioretention

The Horne Street bioretention system had a full summary set of 40 storms. The data was reviewed as a whole with three different influent calculation methods (manufacturer supplied Thelmar curve, Manning's Equation, power regression field calibration curve), and two effluent methods (manufacturer supplied Thelmar curve, power regression field calibrated curve). Influent and effluent comparisons originally indicated significant mean volume reductions (> 90%).

Upon further assessment of the 3 calibrations used to develop this data it was determined that there were rectifiable issues with the calibrations used to translate influent and effluent flow and for now until additional calibration work is developed these results should not be considered defensible.

Volumetric Moisture Content

For Horne Street bioretention data presentation and discussion, an important facet of the system to understand is that the surface of the system is sloped at 1% and in order to minimize inflow moving directly to the far end of the system and prematurely bypassing, three internal berms (4-inch height) were constructed. Nests of monitoring equipment were installed in spatial relation to these berms. The berms are approximately located 60 feet, 90 feet and 120 feet from the inlet. Monitoring equipment was located at 50, 75, 95, 115, 125, and 130 feet from the inlet. This means that equipment at 50 feet was in the most upstream cell close to a berm. Equipment at 75 feet is just upstream of the middle berm (at 90 feet). The equipment at 75 feet would not react until water spilled over the first berm and entered the second cell upstream of the second berm. The equipment at 95 feet and 115 feet are upstream of the third berm (at 120 feet) and the equipment at 125 feet and 130 feet are downstream of the third berm and upstream of the end of the system.

Figure 34-36 displays the cumulative probability distributions for the Horne Street Bioretention system volumetric moisture content at various longitudinal and vertical cross-section locations. Included on this figure is the saturation volumetric moisture content estimated by EPA for just the soil media. The Horne Street Bioretention system soil media VMC saturation value is 0.416. The saturation value for the stone layer is conventionally set at 0.4, but was not measured. Likewise, the saturation VMC for the underlying soil was not measured, but should be in the range of 0.3 to 0.5 (silty clay soil) and here was assumed to be 0.4. As can be seen from Figure 34 which plots data from TDR sondes buried mid-depth in the biomedia, in general the system gets drier the further away from the inlet location: T01, T02, and T03 have higher median VMC than T04 and T05 and in general the entire distribution of the first three sensors is to the right (wetter) than the latter two. This would be expected due to soil inundation being most prominent and more consistent nearer the inlet (cells 1 and 2. Also of note is that the soils are consistently

dryer than the underlying stone and the underlying native soil (silty clay soil) [Figures 35 and 36]. Drying near the surface between runoff events due to evaporation would seem to be the primary reason with soils furthest from the inlet less inundated and drier.

In studying the data for Figures 34-36 below, the non-exceedance probability or exceedance probability for the soil media can be directly identified and then compared to the probability of when inflows exceed the design flow. The probabilities of the soil media reaching saturation may be found in Table 2. In previous UNHSC work on the moisture content characteristics of bioretention soil media and measuring VMC with TDR equipment, it was discovered that the wood chips act as solid particles however they themselves have porosity and may hold water thereby biasing the real VMC upwards. Here the laboratory calibrated VMC was 0.416 and was rarely exceeded throughout the 2 year monitoring period. A second saturation value was developed from the characteristics of the estimated soil moisture characteristic curve using the Arya-Paris model. This second saturation value is 0.267 for the Horne Street biomedia. From the data plots two patterns emerged, first that the biomedia is progressively dryer as the distance from the influent increase. Second the VMC of the base of the stone and the relative lack of extreme variability of the VMC of the native soil indicates that the underling stone (below the invert of the underdrain) and soils are likely saturated or very close to saturation. Despite inconclusive data on the water balance of the system we know that volume reductions were demonstrated at this site. Volume reduction pathways include infiltration through the native soils but also may include significant exfiltration through the sides of the system.

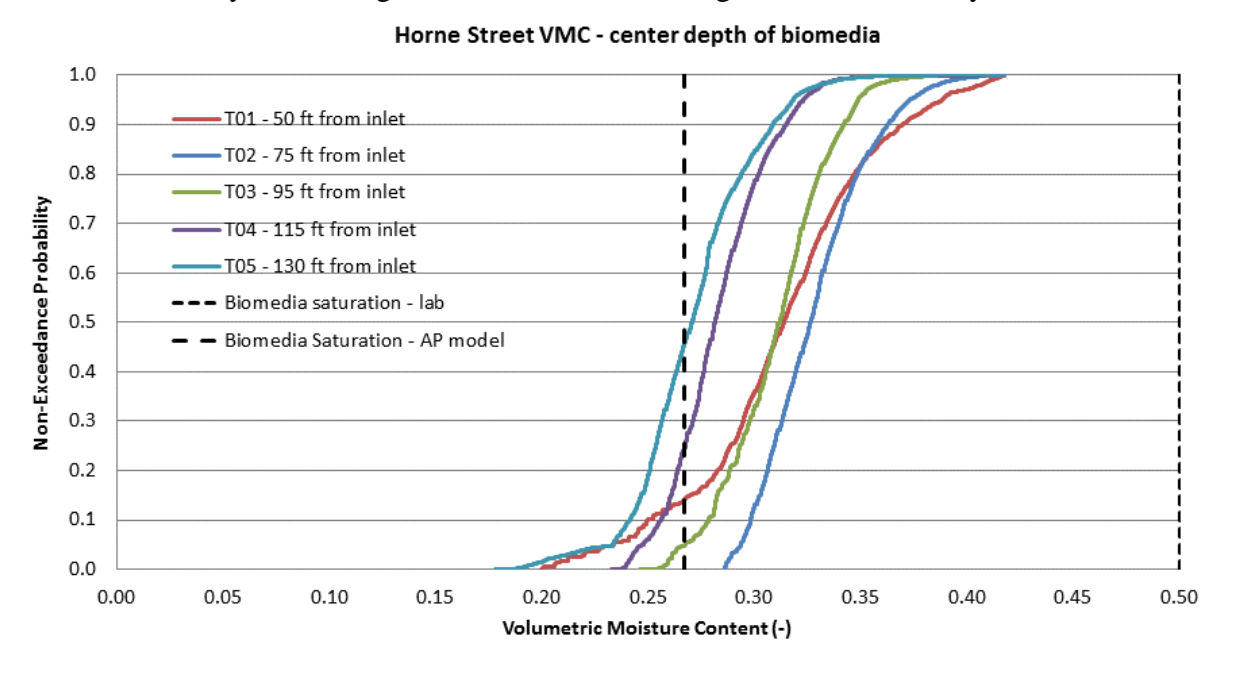


Figure 34: Cumulative probability distributions for Horn Street Bioretention volumetric moisture content through the longitudinal profile of the system at the center of the Bioretention Soil Mix (BSM) depth.

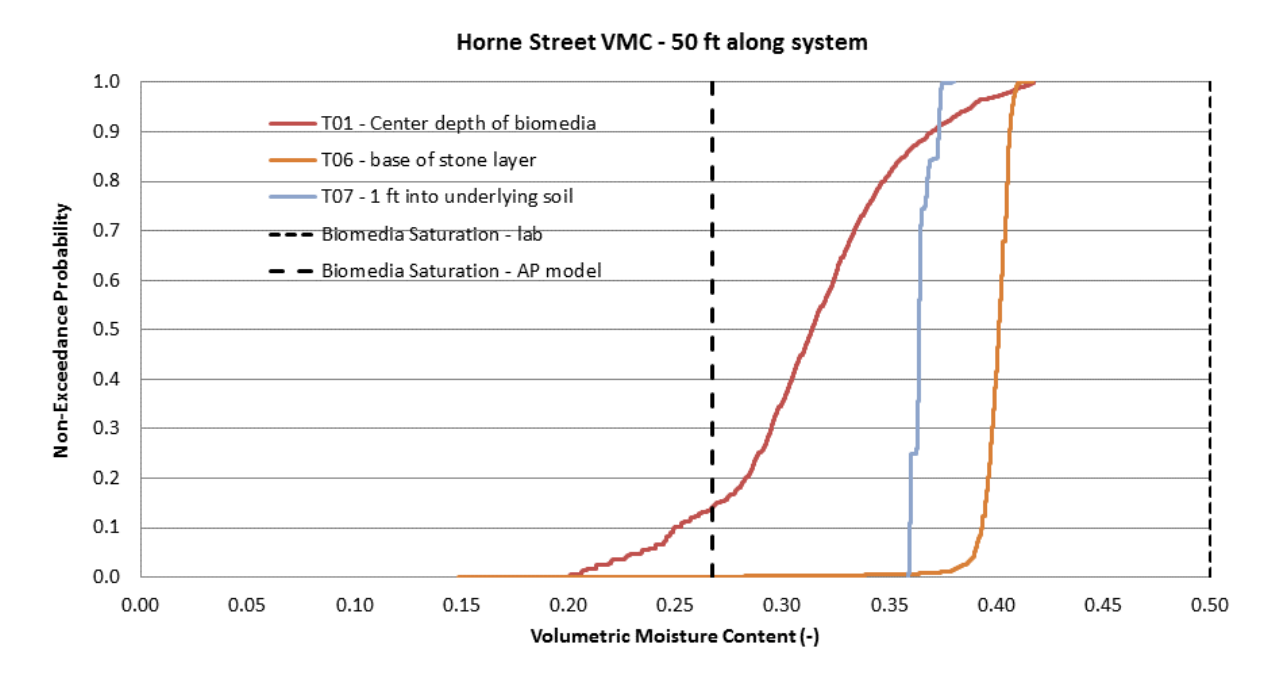


Figure 35: Cumulative probability distributions for Horn Street Bioretention volumetric moisture content through the vertical cross section of the system closest to the inlet.

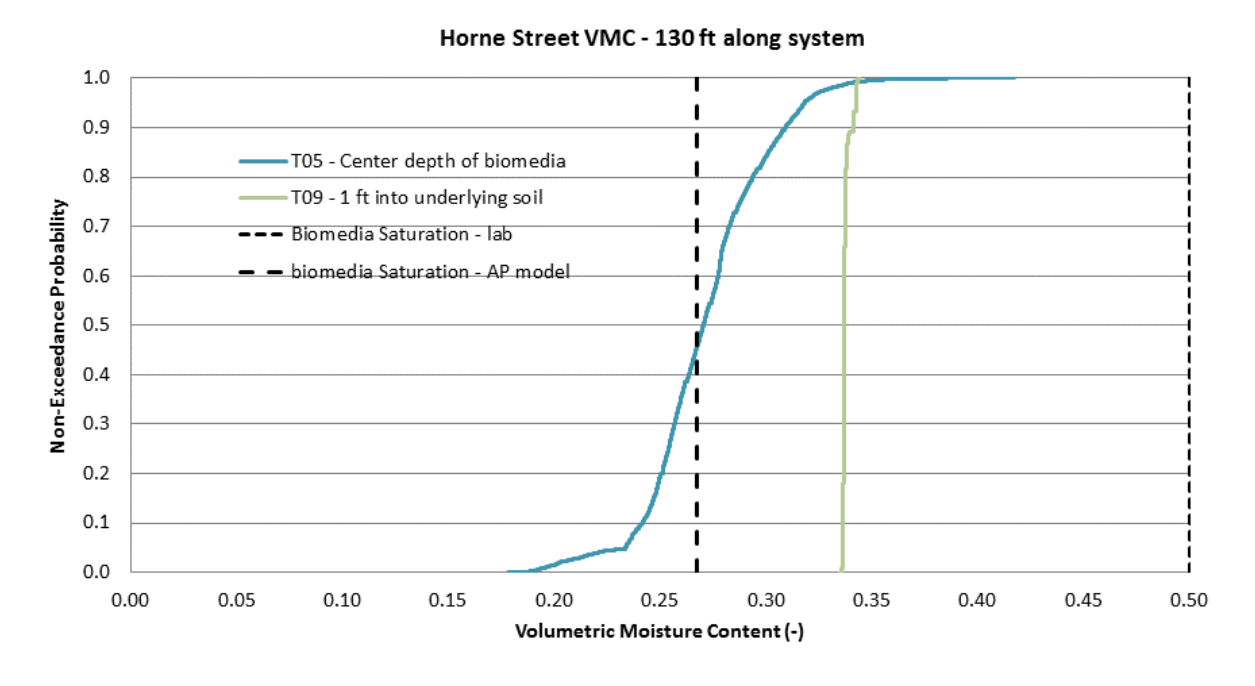


Figure 36: Cumulative probability distributions for Horn Street Bioretention volumetric moisture content through the vertical cross section of the system closest to the outlet

Table 2: Measured probabilities when the soil media achieves saturation (EPA field measured saturation = 0.416 for biomedia, 0.4 for underlying soil, and stone layer).

TDR ID	TDR Location	Non-Exceedance probability at saturation (%)	Exceedance probability at saturation (%)
T01	1ft below surface of media – 50ft from inlet	99.56	0.44
T02	1ft below surface of media – 75ft from inlet	99.96	0.04
Т03	1ft below surface of media – 95ft from inlet	99.995	0.005
T04	1ft below surface of media – 115ft from inlet	99.99	0.01
T05	1ft below surface of media – 130ft from inlet	99.994	0.006
Т06	At gravel / underlying soil interface – 50ft from inlet	38.2	62.8
Т07	1ft below system in native soils – 50ft from inlet	40.0	60.0
Т08	1ft below system in native soils – 95 ft from inlet	40.0	60.0
Т09	1ft below system in native soils – 130 ft from inlet	100	0

The VMC sensors are installed at various longitudinal and vertical locations within the Horne Street Bioretention system are plotted in Figure 37. The location closest to the inlet shows higher variability in VMC values than the downstream location closest to the outlet. This is expected and indicates that areas closes to the inlet are inundated first and far more frequently than downstream areas of the system. It can be inferred from the figures that while nearly all storms inundate the area 50' from the inlet, many do not even reach the BSM closes to the outlet. The VMC levels in the base of the stone layer demonstrate variability indicating reactions to the BSM infiltrating runoff from above and subsequent exfiltration either through the native soils or more probable through the system sides. There is also a very clear depression of the VMC data during winter months presumably from interference from water with high concentrations of chloride that interferes with the dialectical current. The overall lack of variability of the VMC

data associated with the TDRs in the underlying soils indicate that exfiltration is likely dominated by the system sides and the slotted underdrain.

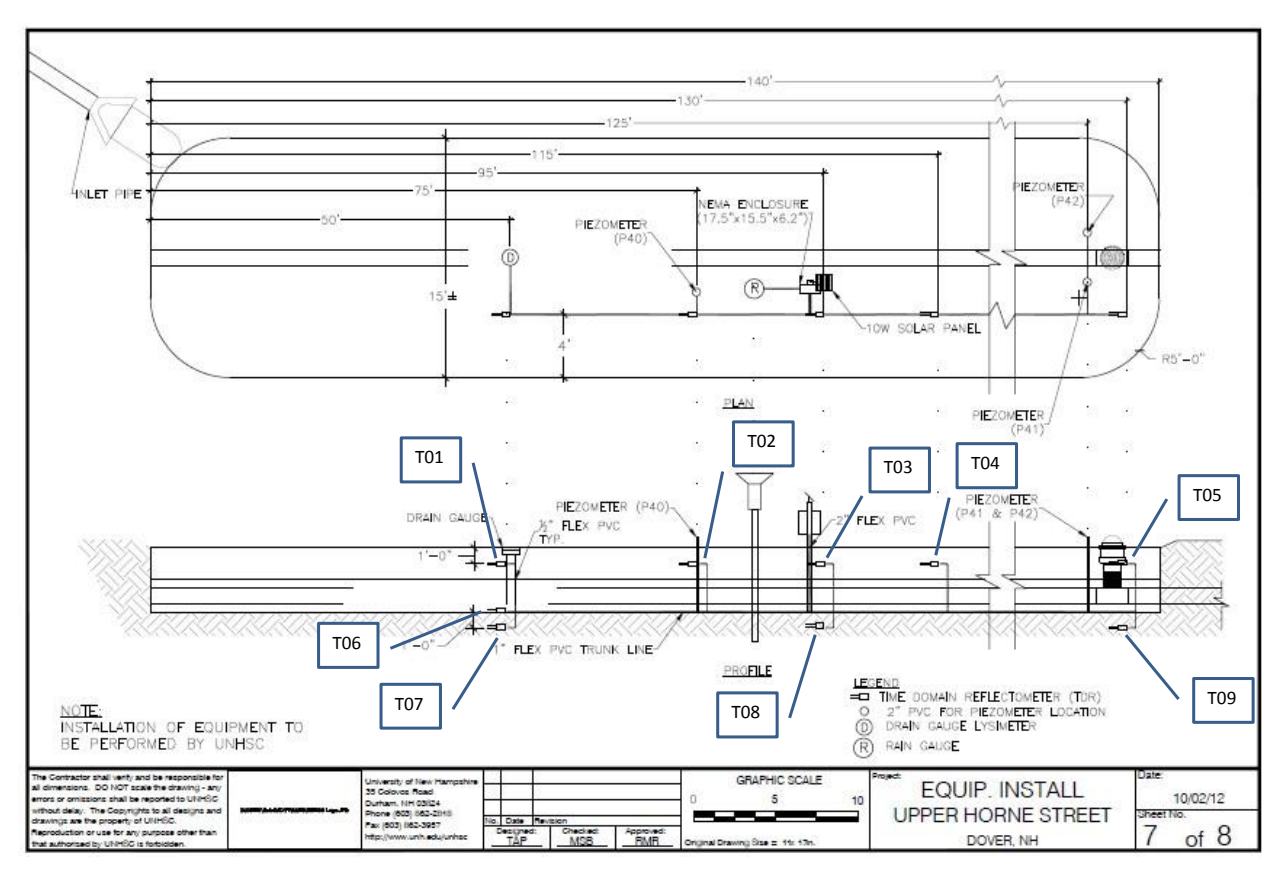


Figure 37: Locations of Sensors at the Horne Street Bioretention system

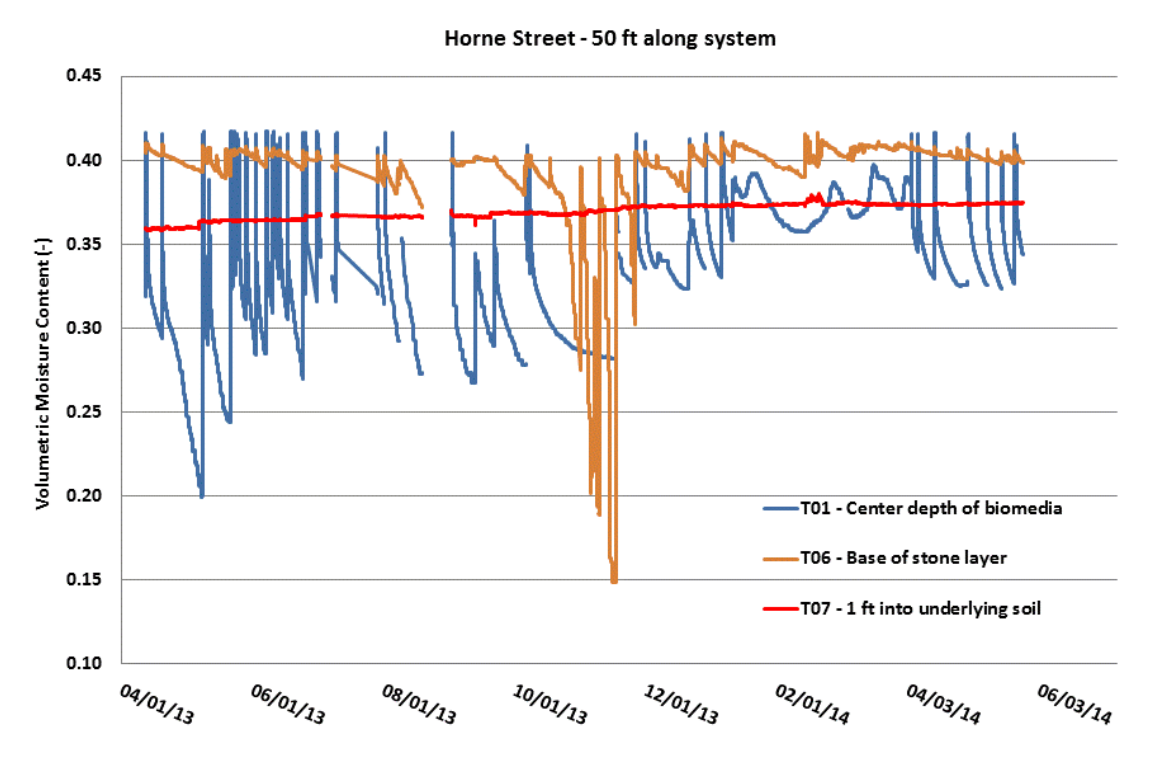


Figure 38: All TDR Sensor VMC Bioretention System Data 50 ft from the inlet for Storms recorded between May 2013 and May 2014.

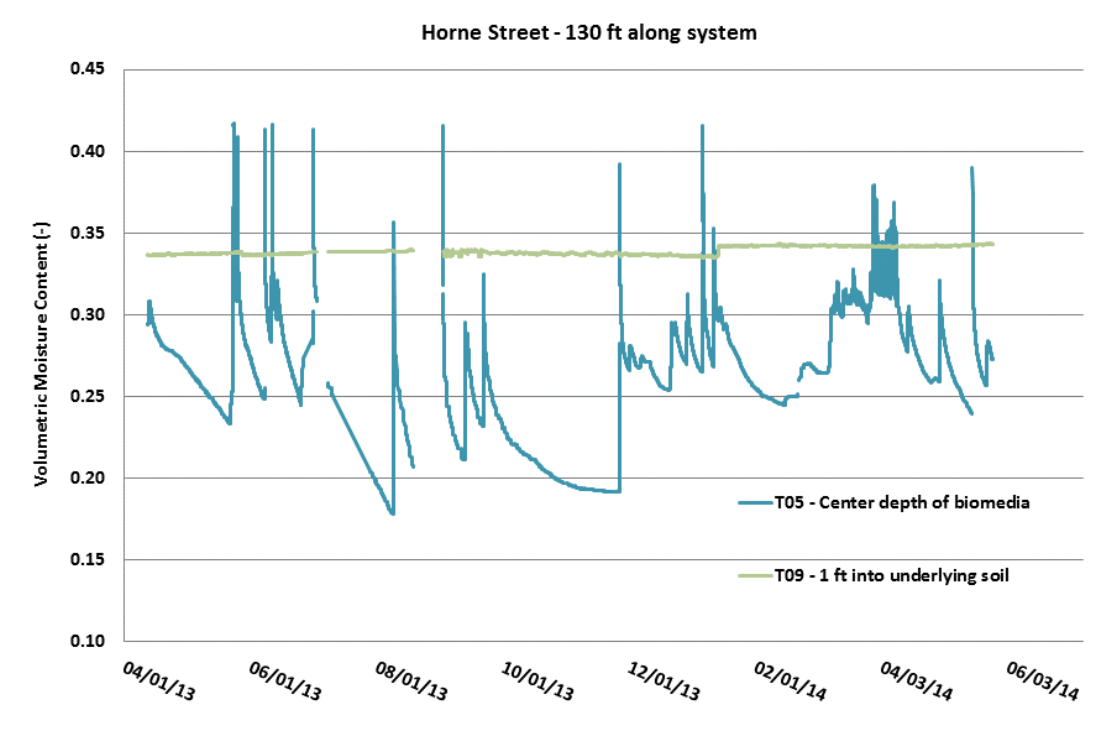


Figure 39: All TDR Sensor VMC Bioretention System Data 130 ft from the inlet for Storms recorded between May 2013 and May 2014.

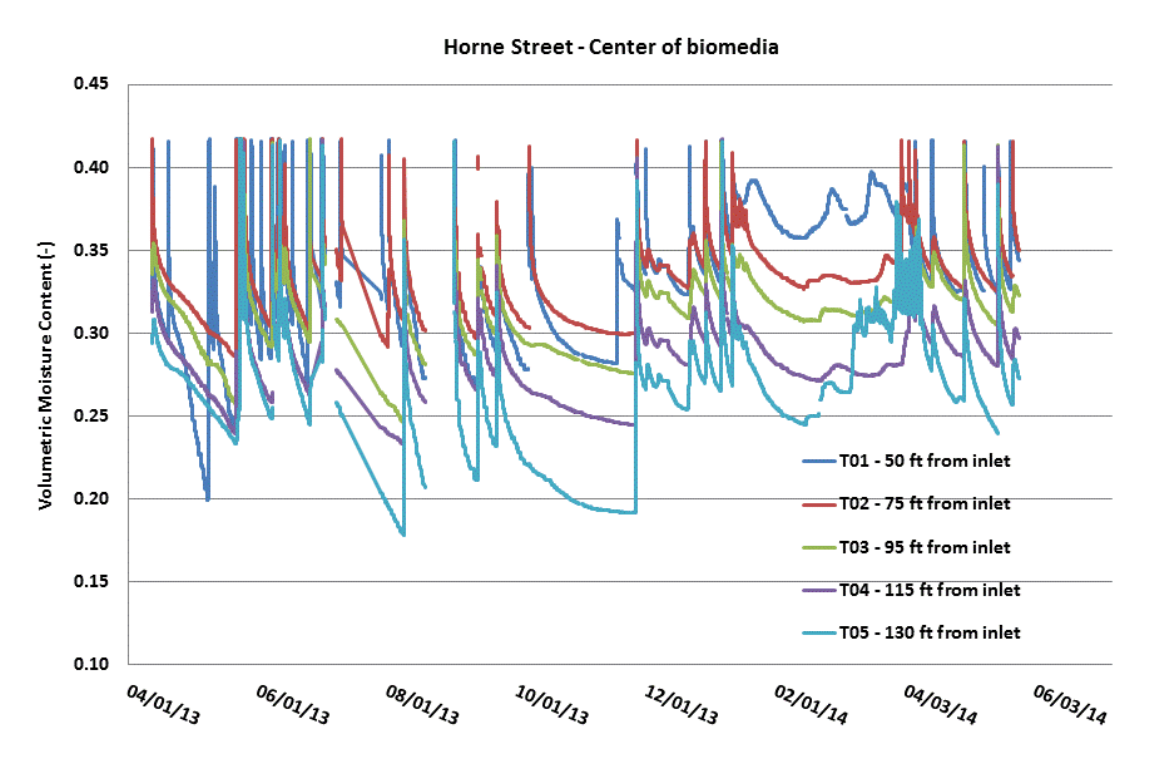


Figure 40: All TDR Sensor VMC Bioretention System Data at various longitudinal locations within the system at the center of the BSM for Storms recorded between May 2013 and May 2014.

Temperature

Figures 41-43 displays the cumulative probability distributions for the Horne Street Bioretention system temperature data at various longitudinal and vertical cross-section locations. Air temperature data are added for reference to the cross-section stations.

The temperature distribution in the longitudinal profile at the center of depth of the BSM shows some buffering at the temperature extremes (hotter and colder) as the sensors get further from the inlet location. This would be presumably be due to the parallel trend toward drier less inundated soil conditions as the sensors get further from the inlet location as well as a reflection of runoff water temperatures throughout the year. Temperatures of the BSM close to the stormwater inlet are more influenced by incoming water whereas locations further from the inlet would be influenced more by air and subsurface temperatures and in effect be more buffered by ground temperatures. In the same manner sensors in the vertical cross-sections (50 ft and 130 ft from the inlet) demonstrate the temperature buffering capacity of the subsurface where median temperatures trend toward cooler conditions the deeper the sensor station. The exception occurs where the distributions cross at the temperature extremes and are related again toward buffering capacity of the subsurface, air temperature, and runoff temperature.

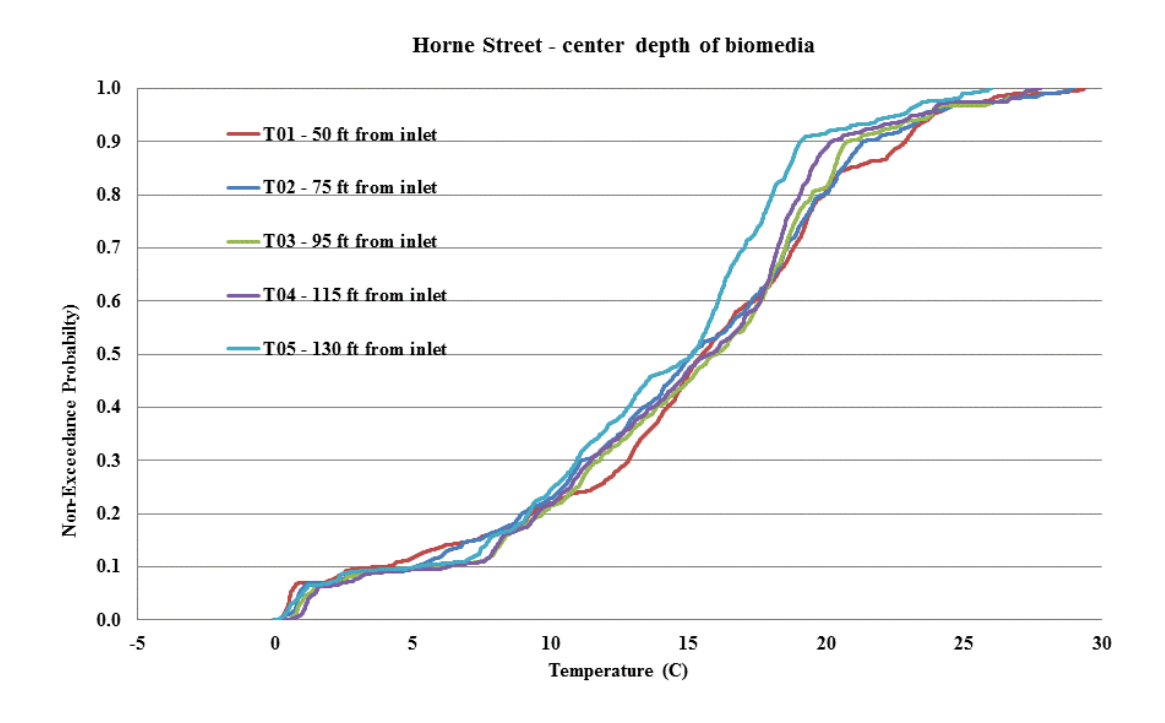


Figure 41: Cumulative probability distributions for Horn Street Bioretention temperature through the longitudinal profile of the system at the center of the Bioretention Soil Mix (BSM) depth.

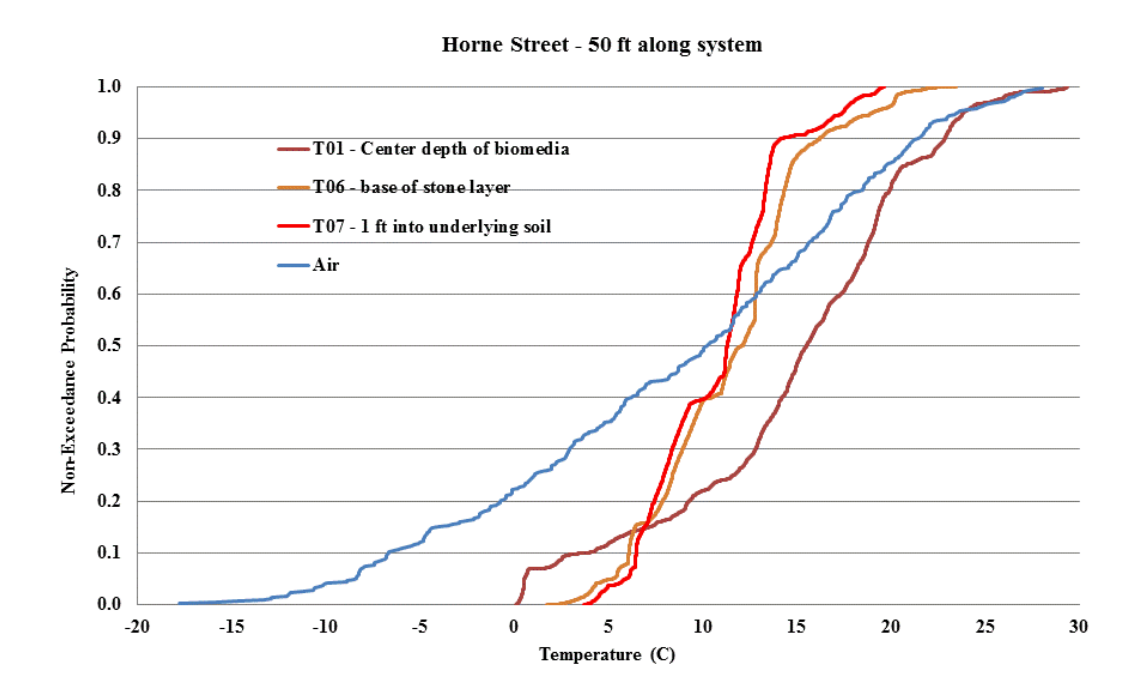


Figure 42: Cumulative probability distributions for Horn Street Bioretention temperatures through the vertical cross section of the system closest to the inlet.

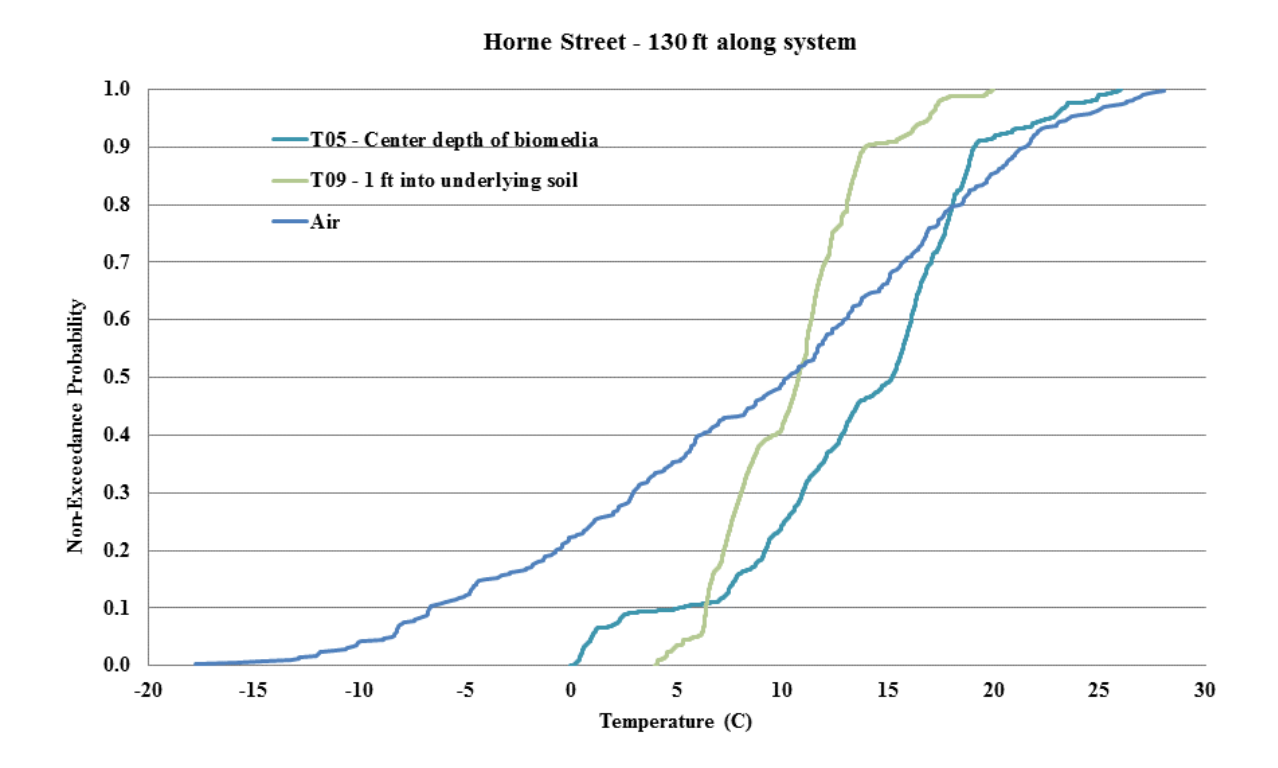


Figure 43: Cumulative probability distributions for Horn Street Bioretention temperatures through the vertical cross section of the system furthest from the inlet.

The time series of temperature data for all sensors installed at various longitudinal and vertical cross-sections within the Horne Street Bioretention system are plotted in Figures 44-48. As with the cumulative probability distributions seasonal temperature plots demonstrate buffering (flattening of the variability) of the temperature with the increasing depth of the sensors. A lag in peak and minimum temperatures with depth is also evident. The seasonal buffering of depth is clear where the time series cross: shallow sensors demonstrate greater influence to fluctuating air/surface temperatures between seasons. The stone layer temperature almost parallels that of the underlying soil temperature except during periods of runoff.

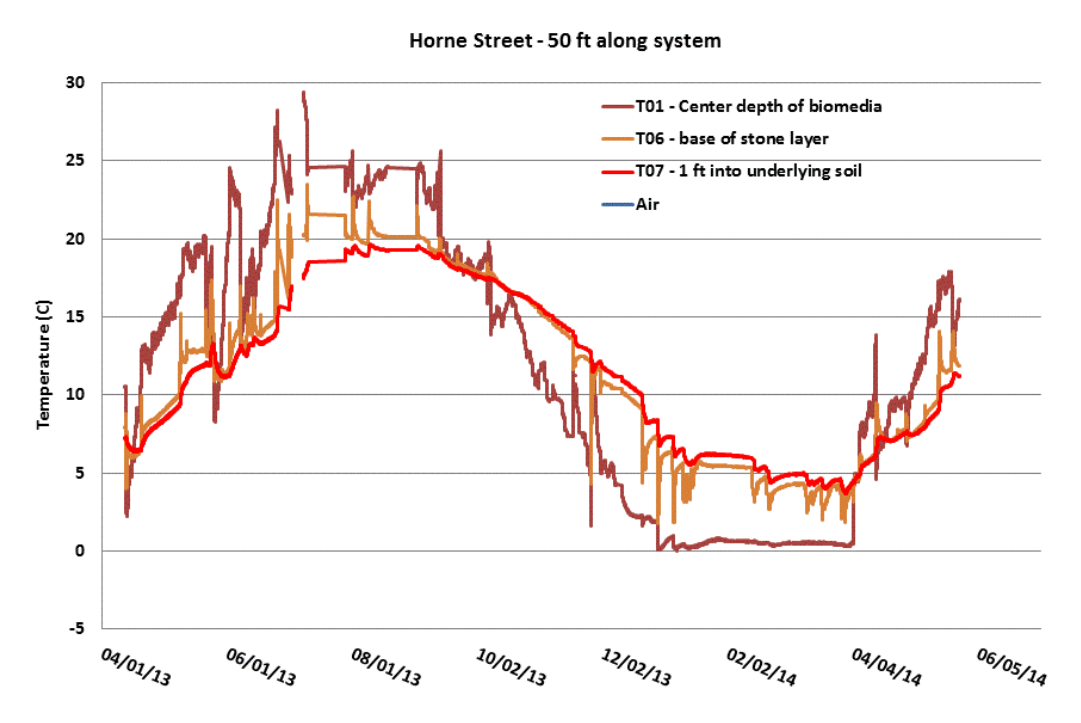


Figure 44: All Temperature Sensor Bioretention System Data 50 ft from the inlet for the period of recorded between May 2013 and May 2014.

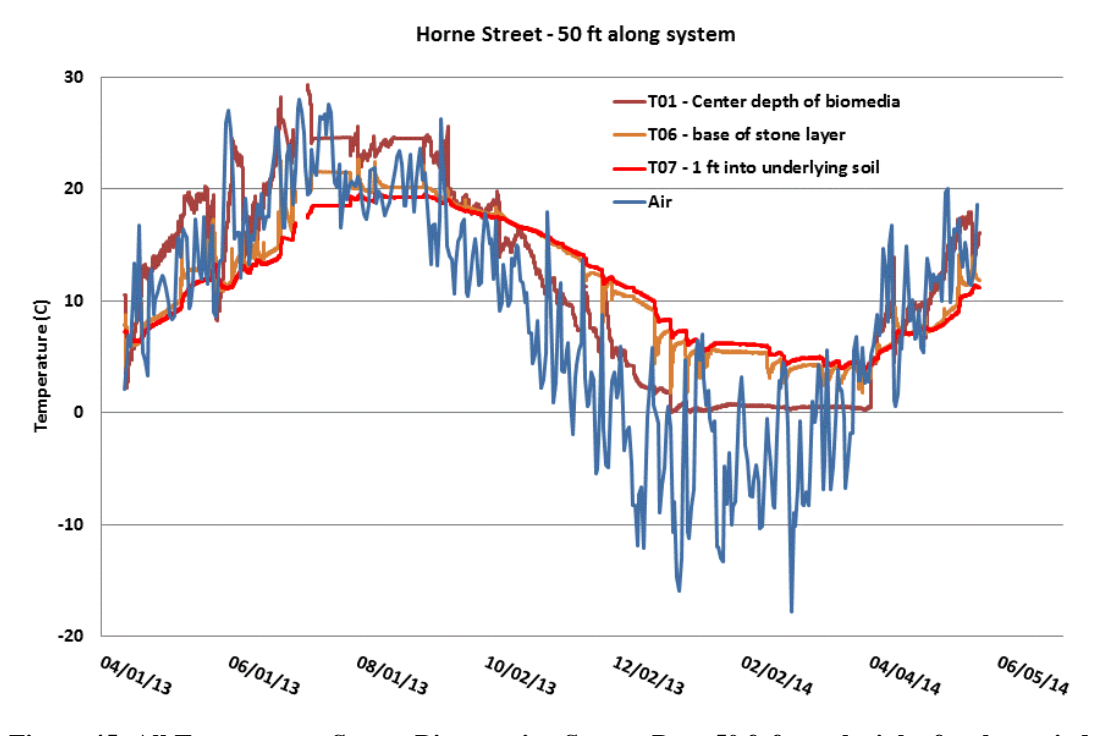


Figure 45: All Temperature Sensor Bioretention System Data 50 ft from the inlet for the period of recorded between May 2013 and May 2014 with ambient air temperature data added for reference.

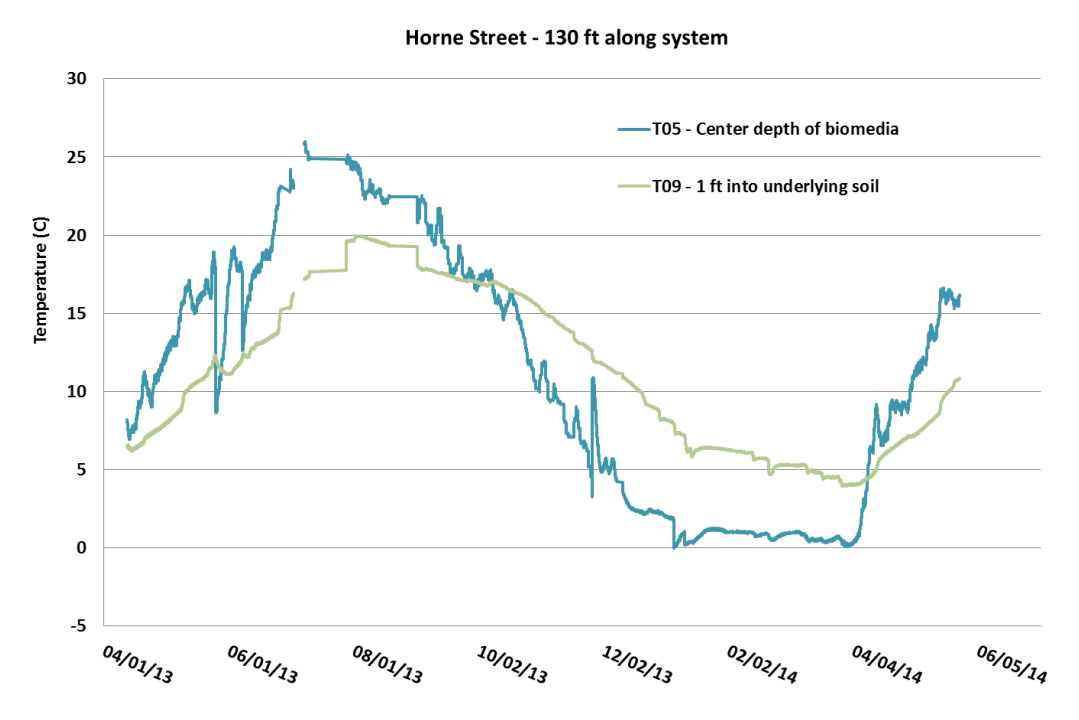


Figure 46: All Temperature Sensor Bioretention System Data 130 ft from the inlet for the period of recorded between May 2013 and May 2014.

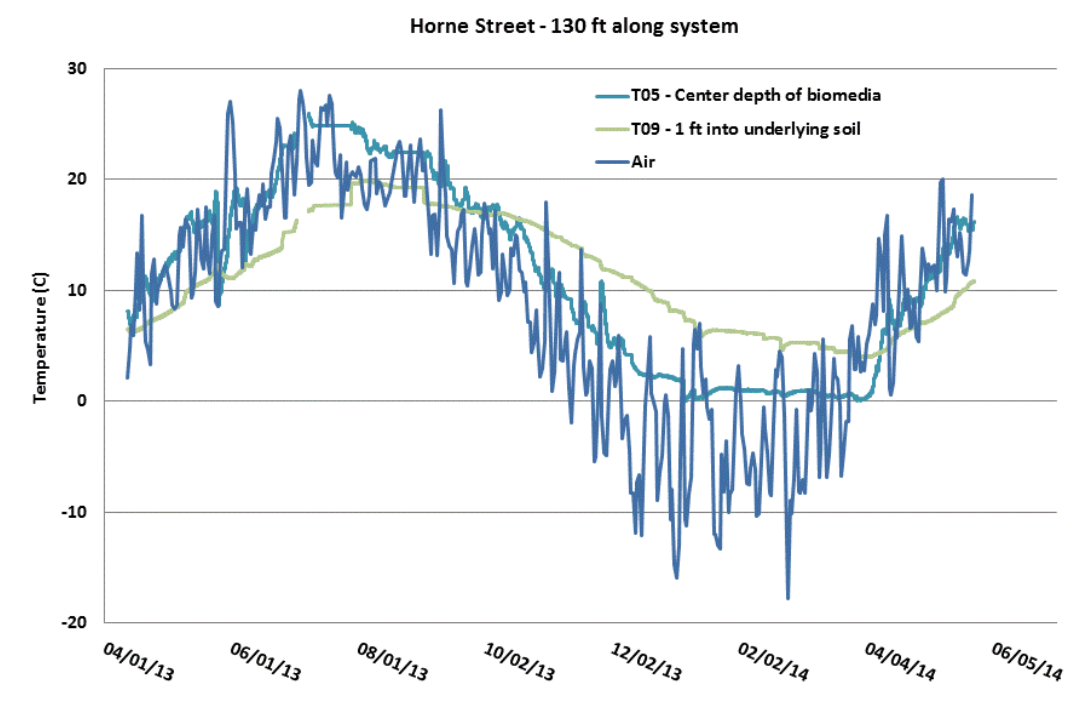


Figure 47: All Temperature Sensor Bioretention System Data 130 ft from the inlet for the period of recorded between May 2013 and May 2014 with ambient air temperature data added for reference.

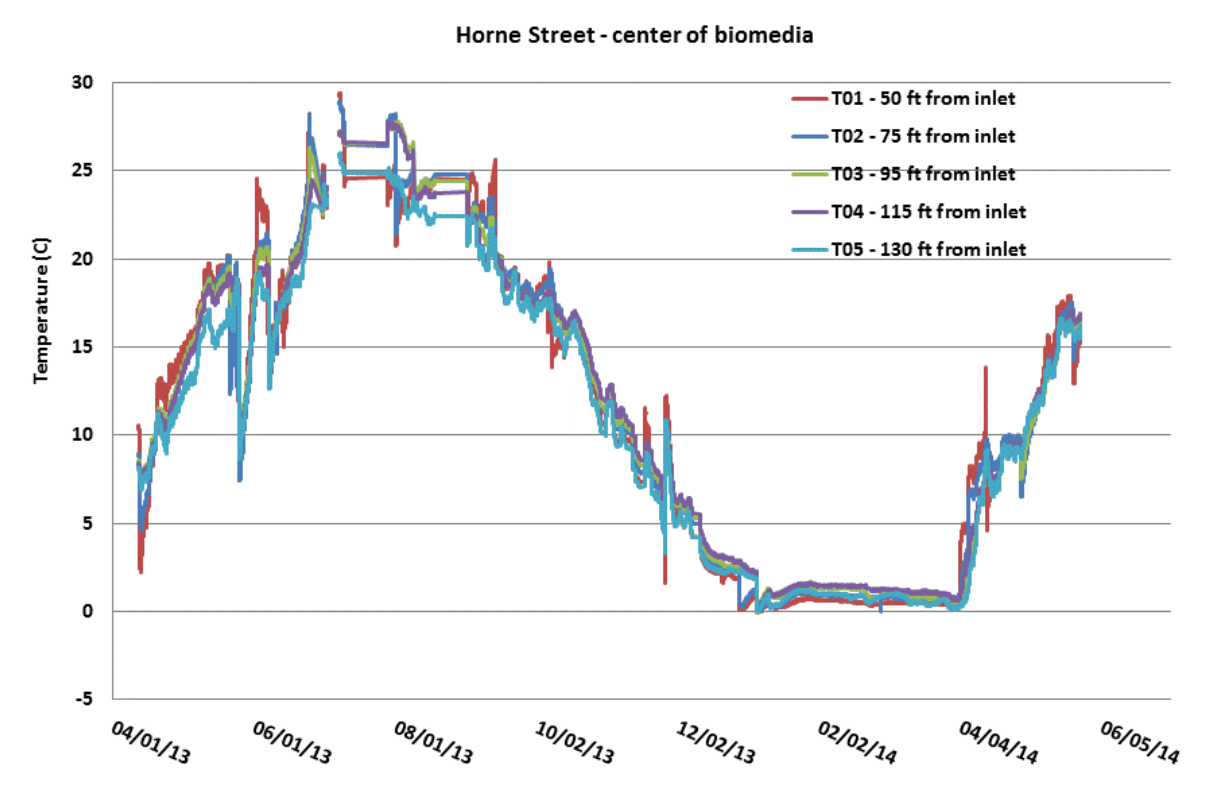


Figure 48: All Temperature Sensor Bioretention System Data at the center of the BSM across the longitudinal profile of the system for the period of recorded between May 2013 and May 2014.

Conductivity:

Figure 49-51 displays the cumulative probability distributions for the Horne Street Bioretention system conductivity data at various longitudinal and vertical cross-section locations.

The conductivity distributions in the longitudinal profile at the center of depth of the BSM shows that conductivity is relatively consistent within the system and median conductivity trends lower toward the inlet and toward the outlet likely for different reasons. Median conductivity at the inlet is likely lower due to dilution from increased inundation whereas conductivity closest to the outlet is likely lower due to dryness and lack of inundation. At high conductivities (associated with the use of salt in the winter) the location closest to the inlet reflects the high chloride levels associated with winter deicing events. Much winter runoff occurs at very low flowrates and therefore the first cell of the bioretention system receives the majority of the runoff during this time along with the attendant salt load.

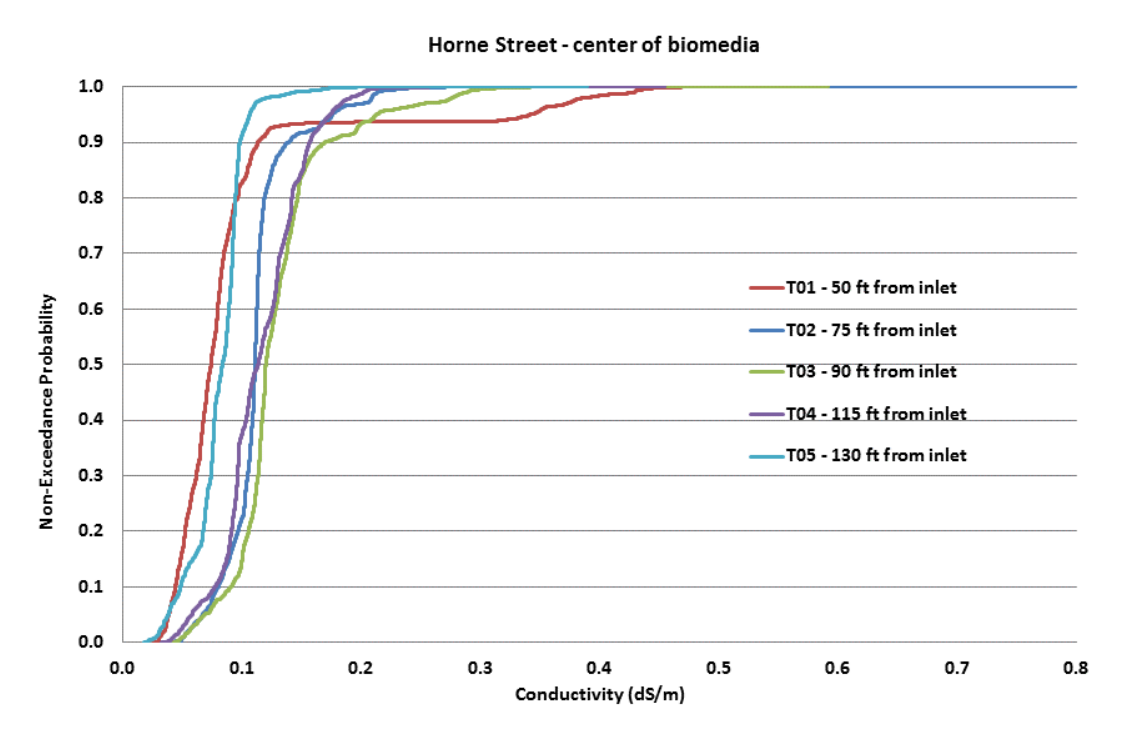


Figure 49: Cumulative probability distributions for Horne Street Bioretention conductivity through the longitudinal profile of the system at the center of the Bioretention Soil Mix (BSM) depth.

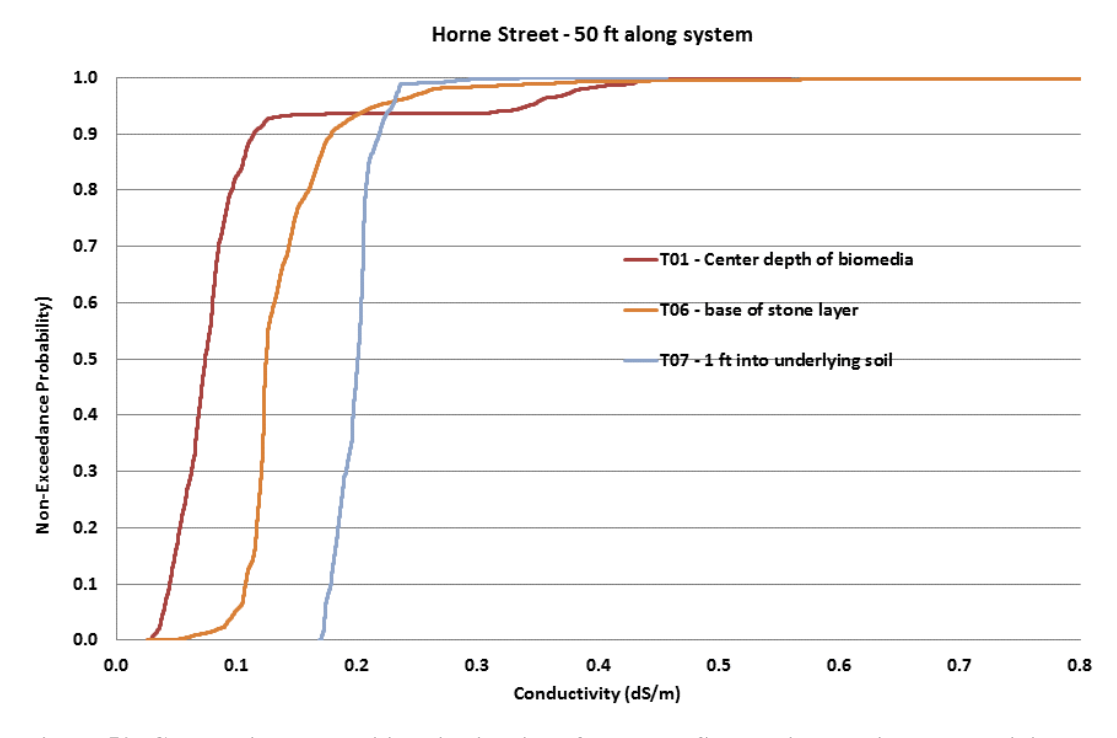


Figure 50: Cumulative probability distributions for Horne Street Bioretention conductivity levels through the vertical cross section of the system closest to the inlet.

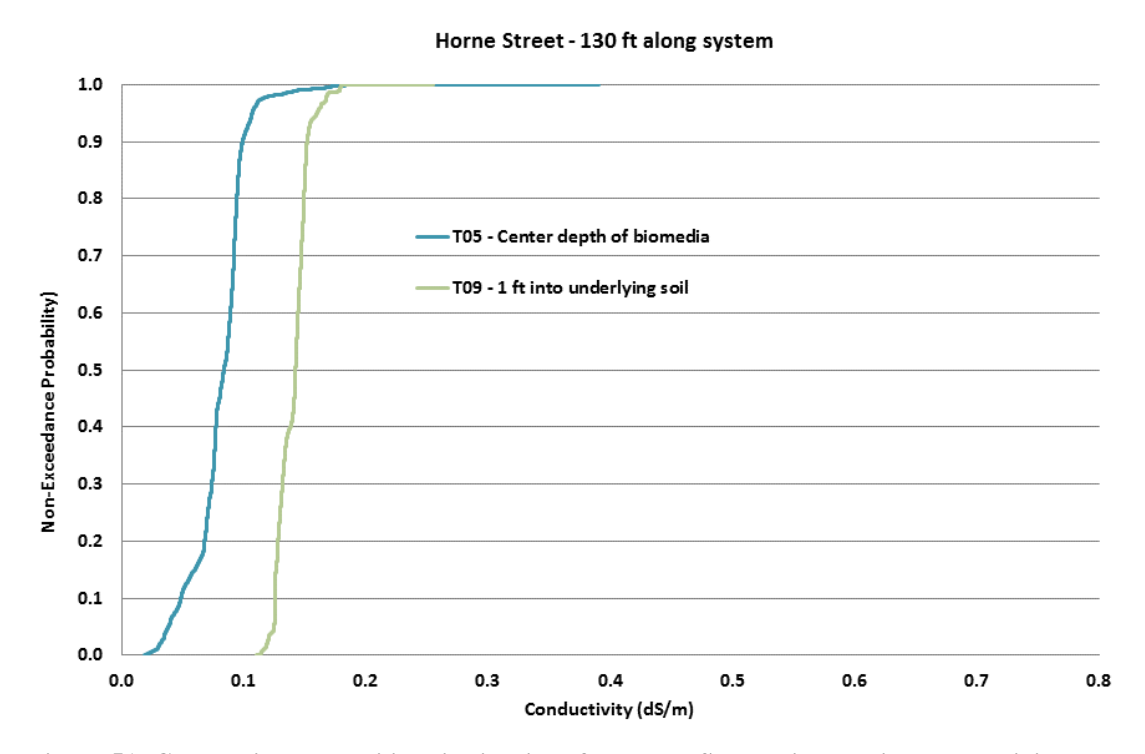


Figure 51: Cumulative probability distributions for Horne Street Bioretention conductivity levels through the vertical cross section of the system furthest from the inlet.

The conductivity data for all sensors installed at various longitudinal and vertical cross-sections within the Horne Street Bioretention system are plotted in Figures 52-54. Conductivity plots demonstrate seasonal spikes of conductivity associated with the onset of winter. This is to be expected as conductivity is positively influenced by chloride associated with winter deicing activities. Like the cumulative probability distributions, conductivity levels are in general lower toward the inlet and outlet locations due to dilution and drier conditions respectively. Seasonal fluxes reverse these trends where locations closest to the inlet exhibit higher conductivity in the winter season due to chloride laden runoff. Also of note is that throughout the system cross section conductivity fluxes are greatest toward the surface and depressed the deeper the sensor level. Of interest is the elevated conductivity response during the winter months of the TDR sensors within the native soils indicating that there is a vertical infiltration pathway through the native soils. Also of note is the conductivity response of the TDR sensors within the native soils at the 130' sensor location with no corresponding response from the TDR sensor above at the 130' sensor location in the center of the BSM. This indicates that there is a horizontal flow pathway through the stone reservoir course in the subsurface of the system that extends from the upstream end of the system. This pathway through the stone layer is likely the primary runoff hydraulic route particularly during low intensity rain events or low flow conditions such as persist in winter melt conditions.

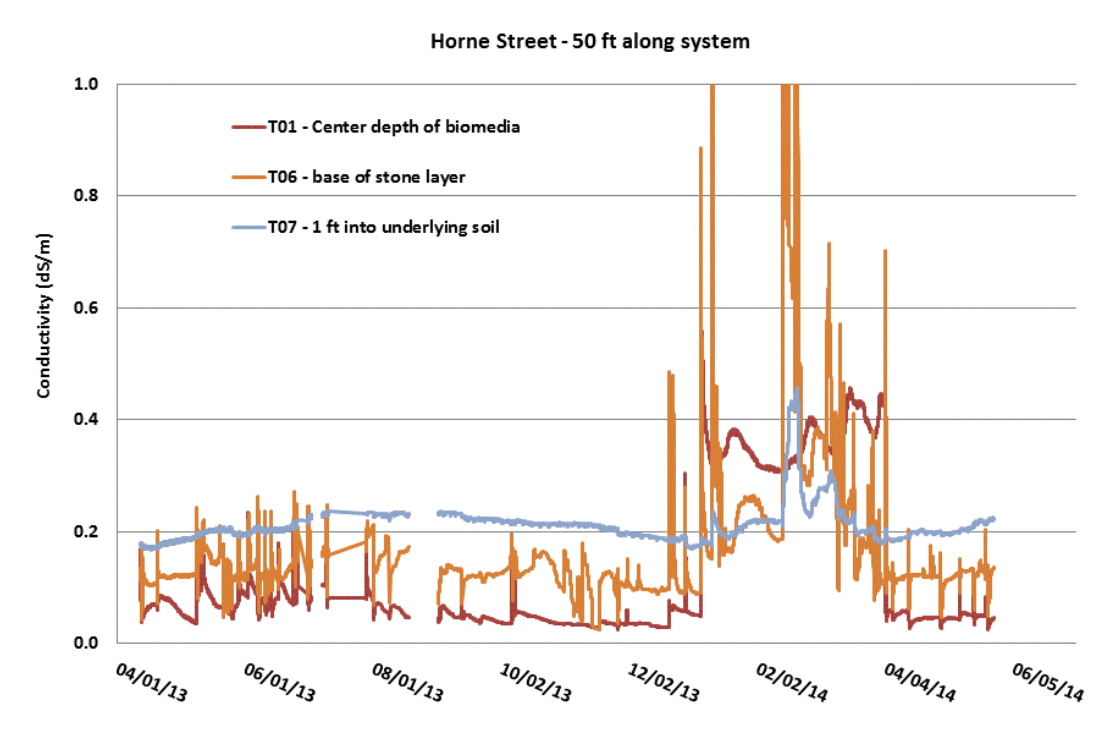


Figure 52: All Conductivity Sensor Bioretention System Data 50 ft from the inlet for the period of recorded between May 2013 and May 2014.

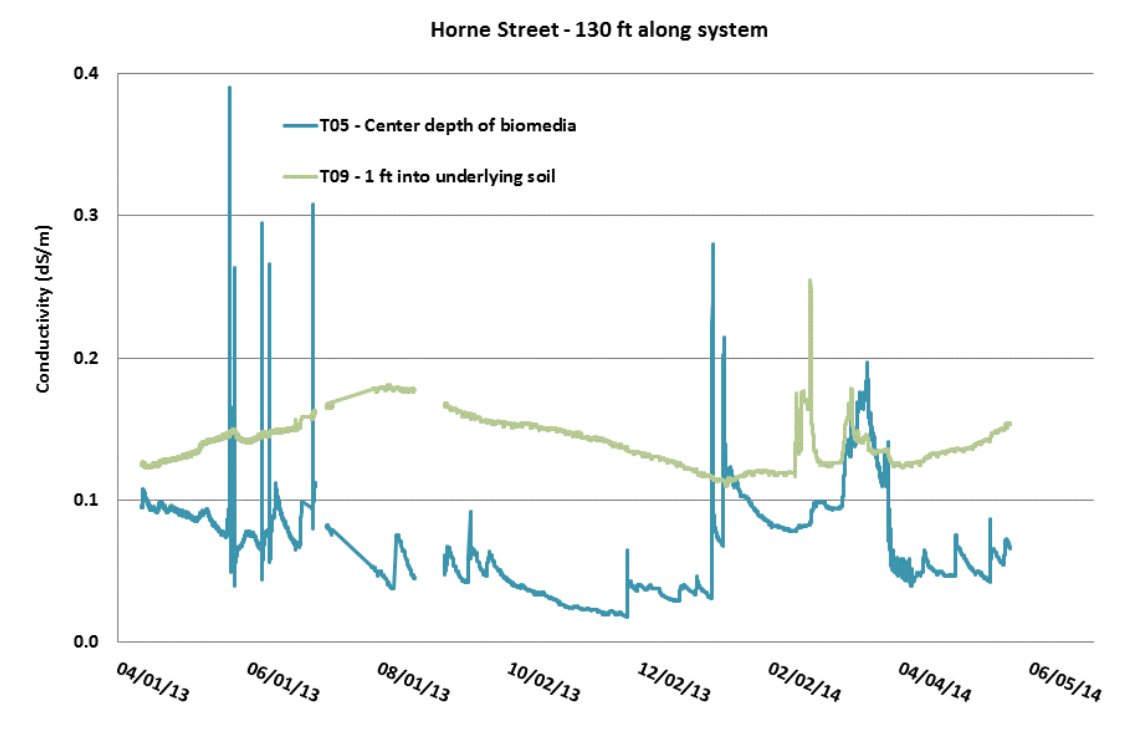


Figure 53: All Conductivity Sensor Bioretention System Data 130 ft from the inlet for the period of recorded between May 2013 and May 2014.

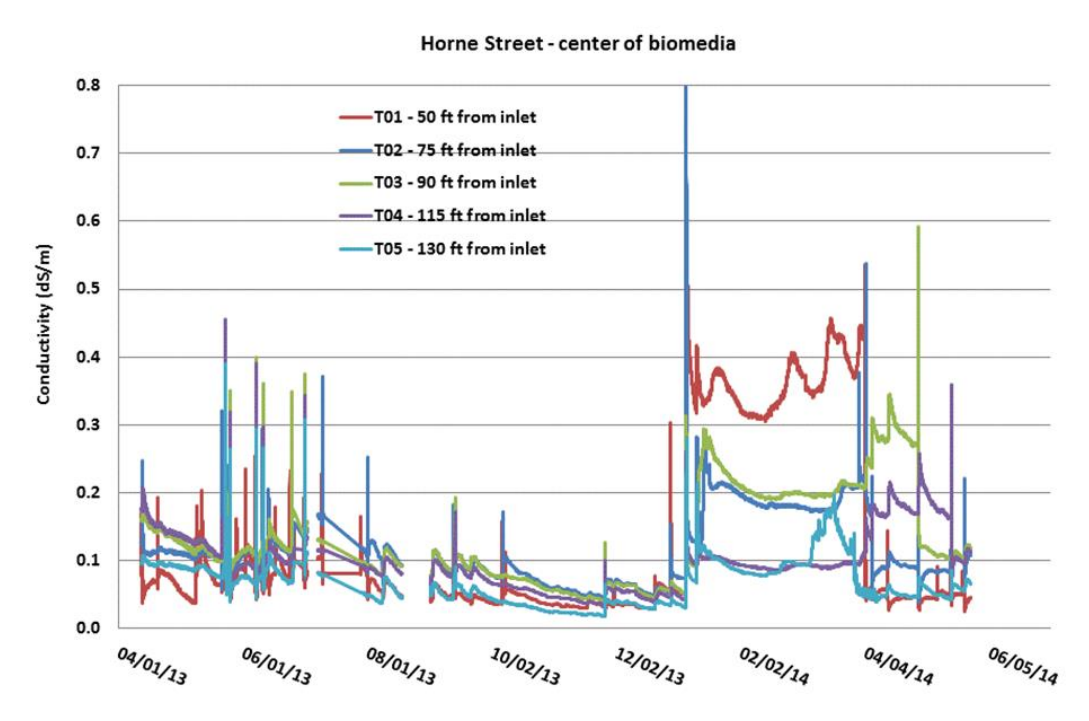


Figure 54: All Conductivity Sensor Bioretention System Data at the center of the BSM across the longitudinal profile of the system for the period of recorded between May 2013 and May 2014.

Figure 55-63 are VMC, temperature, and conductivity data for selected runoff events during the monitoring period. The first event is a 0.6 inch summer thundershower. VMC responds as expected with cells one and two (biomedia sensors T01 and T02) showing infiltration and cells three and four not (sensors T03, T04, and T05).

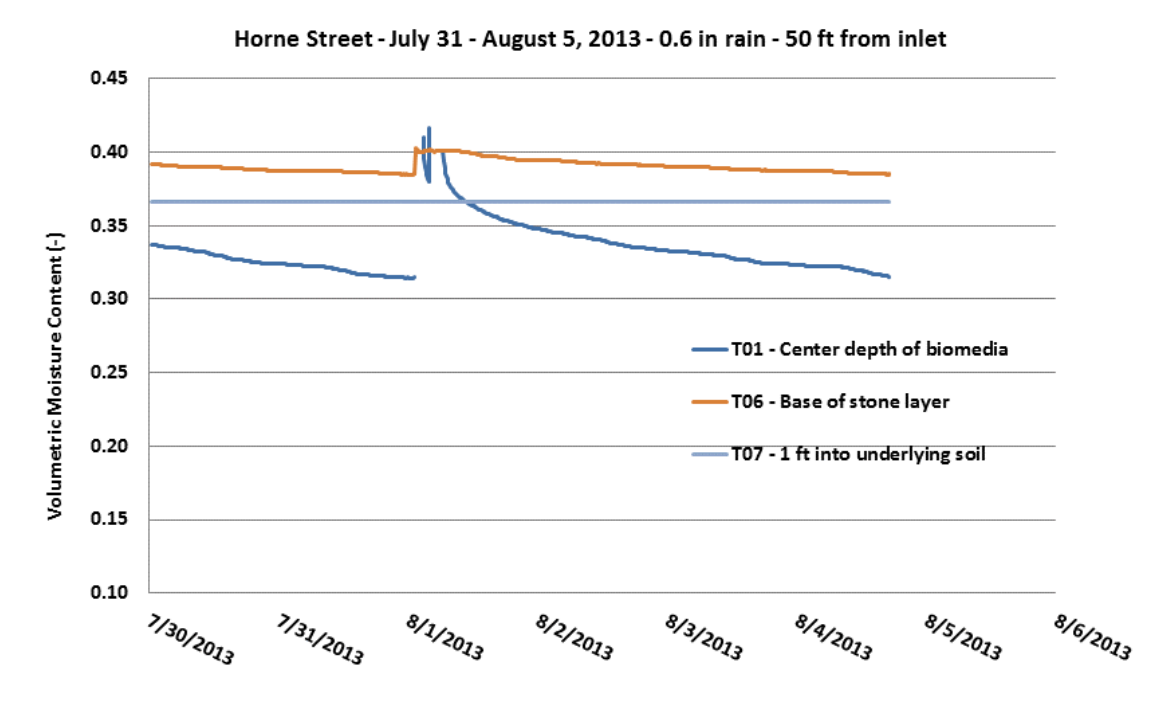


Figure 55: VMC data for the Horne Street Bioretention system closest to the inlet for selected runoff events during the monitoring period.

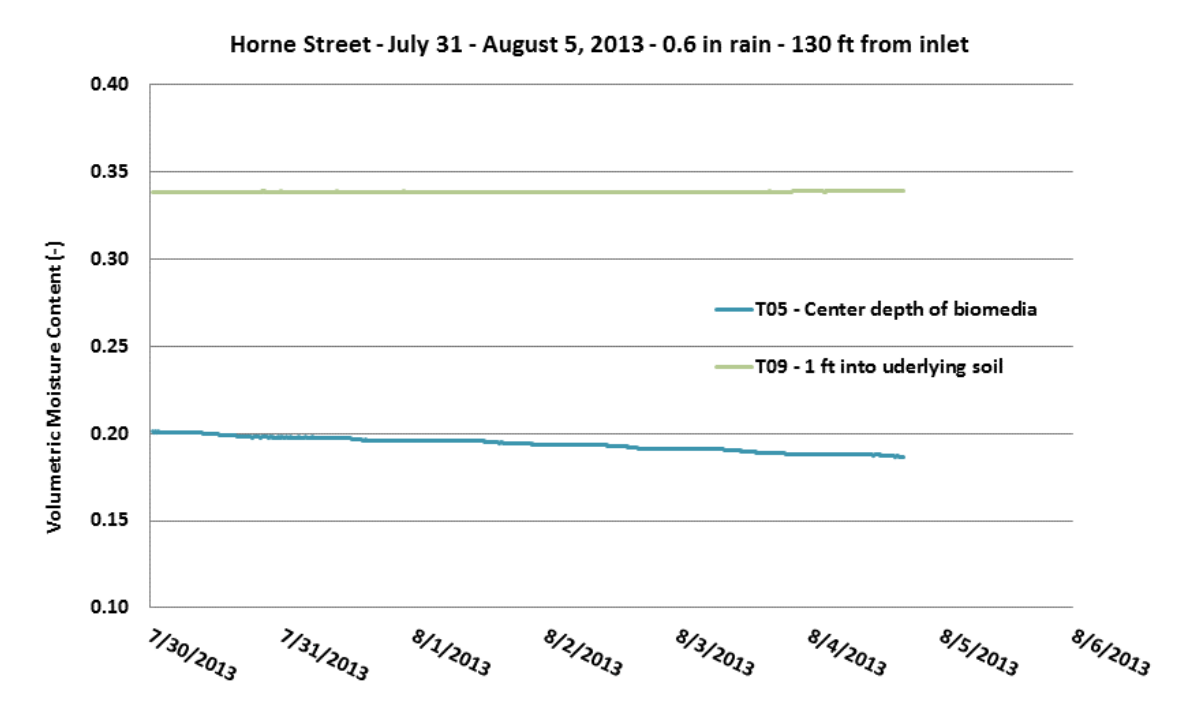


Figure 56: VMC data for the Horne Street Bioretention system furthest from the inlet for selected runoff events during the monitoring period.

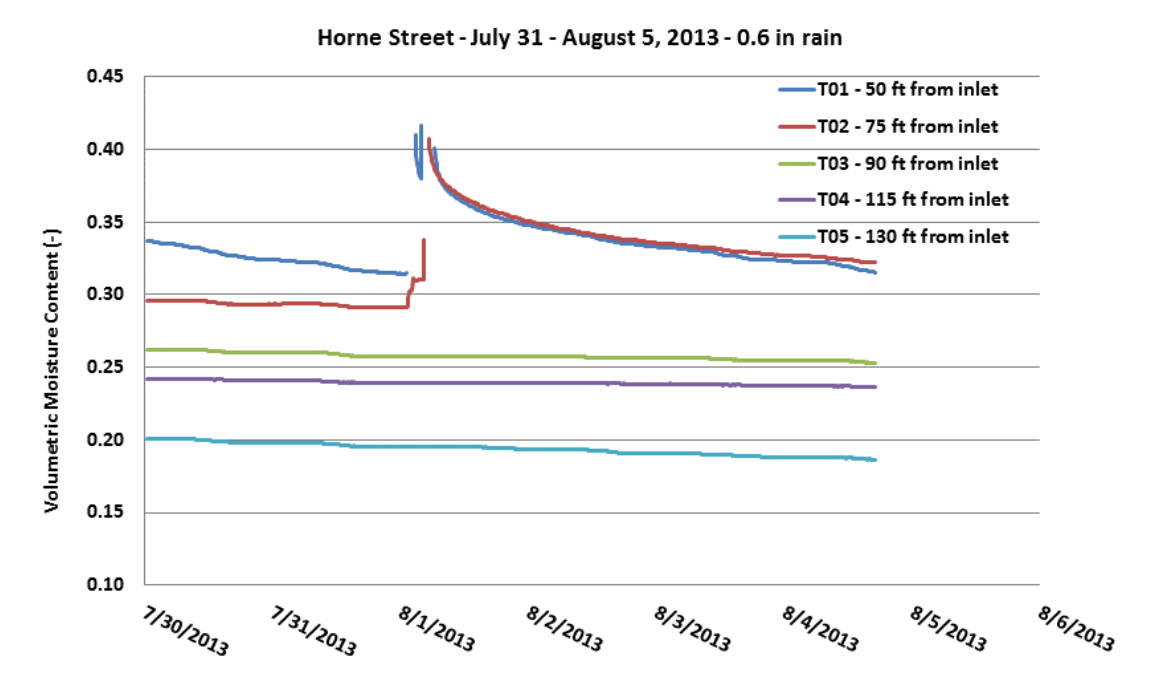


Figure 57: VMC data for the Horne Street Bioretention system at the center of the BSM across the longitudinal profile of the system for selected runoff events during the monitoring period.

The temperature data for the July 31 to August 5 event reflect diurnal variability which becomes interrupted at all levels by the runoff. As the underlying soil also responds, this may reflect both infiltration as well as conduction.

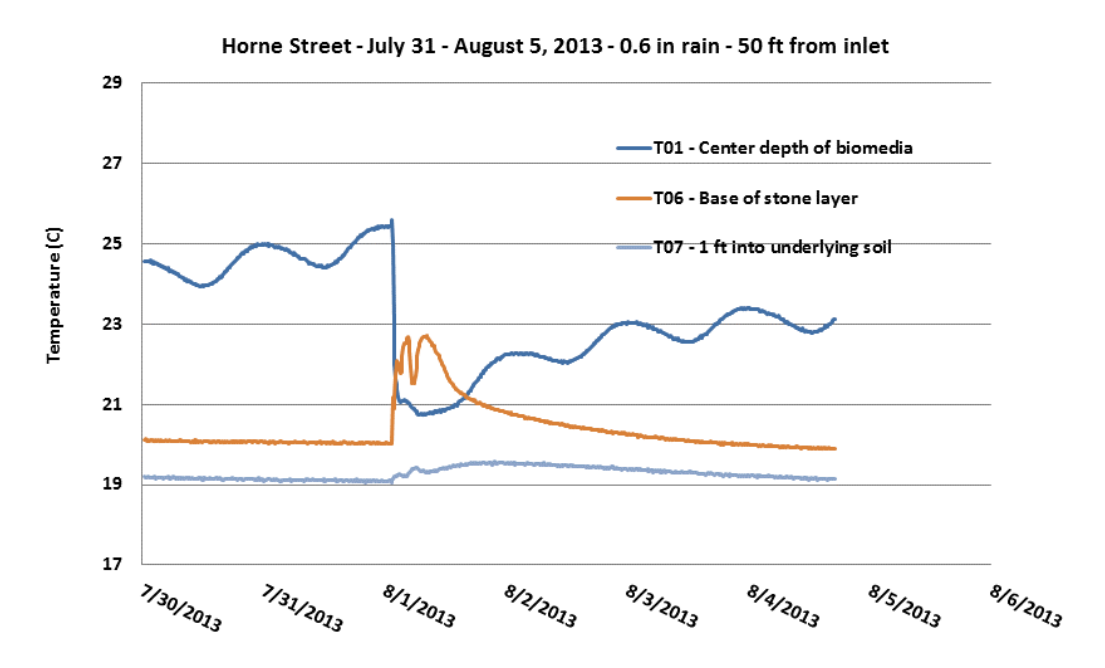


Figure 58: Temperature data for the Horne Street Bioretention system closest to the inlet for selected runoff events during the monitoring period.

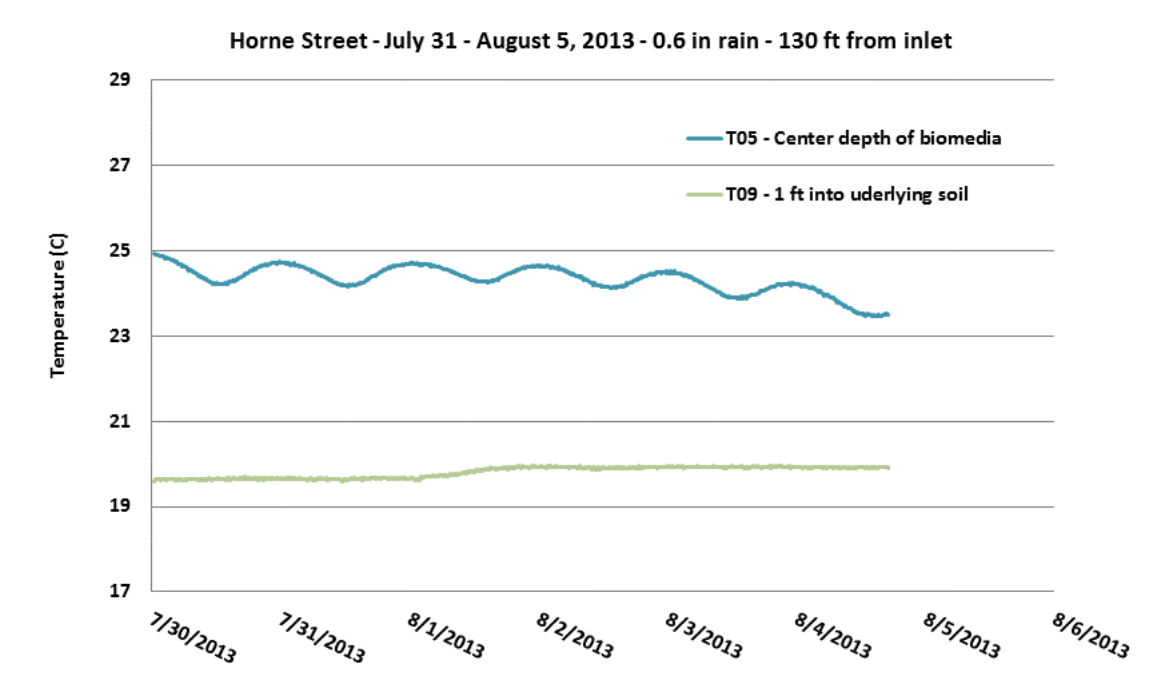


Figure 59: Temperature data for the Horne Street Bioretention system furthest from the inlet for selected runoff events during the monitoring period.

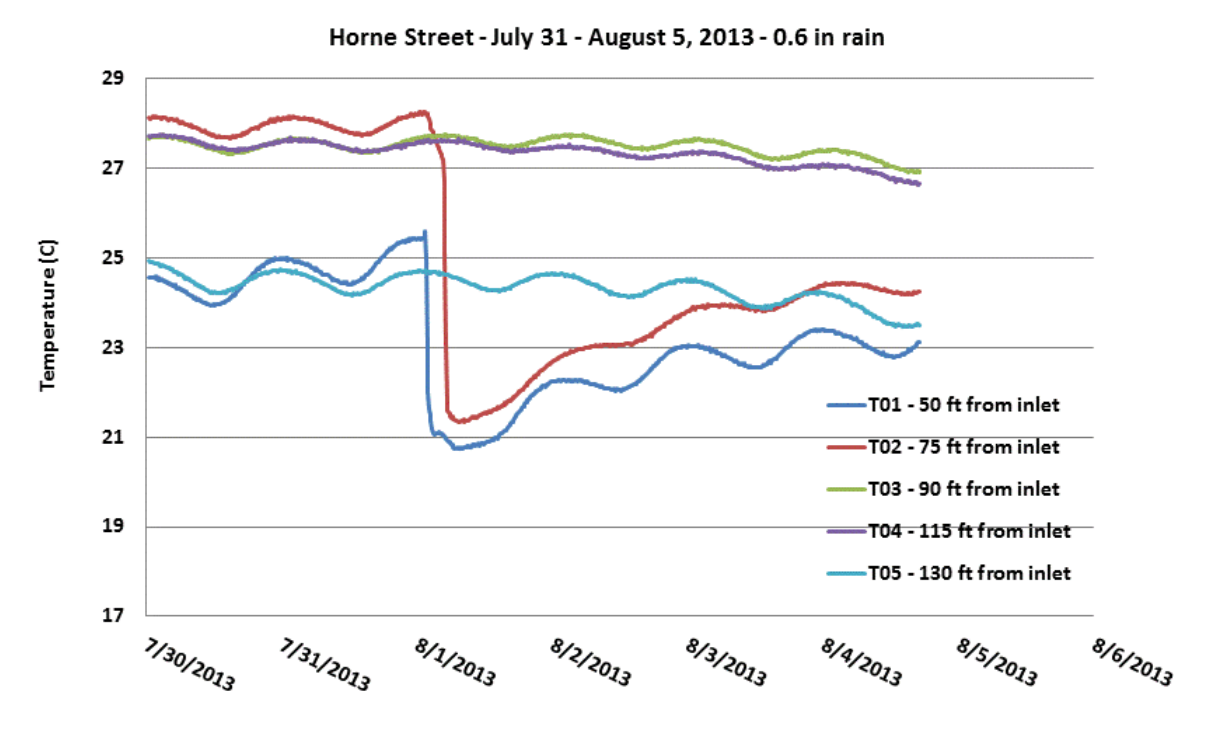


Figure 60: Temperature data for the Horne Street Bioretention system at the center of the BSM across the longitudinal profile of the system for selected runoff events during the monitoring period.

The conductivity data for the July 31 to August 5 event is also manifested at all depths close to the inlet. Since this is a summer event, runoff has lower conductivity than resident water, and therefore all layers demonstrate that diluted runoff has entered, including infiltration into the soil. At the far end of the system from the inlet, runoff does not seem to have impacted the conductivity. The lower conductivity of the biomedia in this location may be more reflective of direct precipitation.

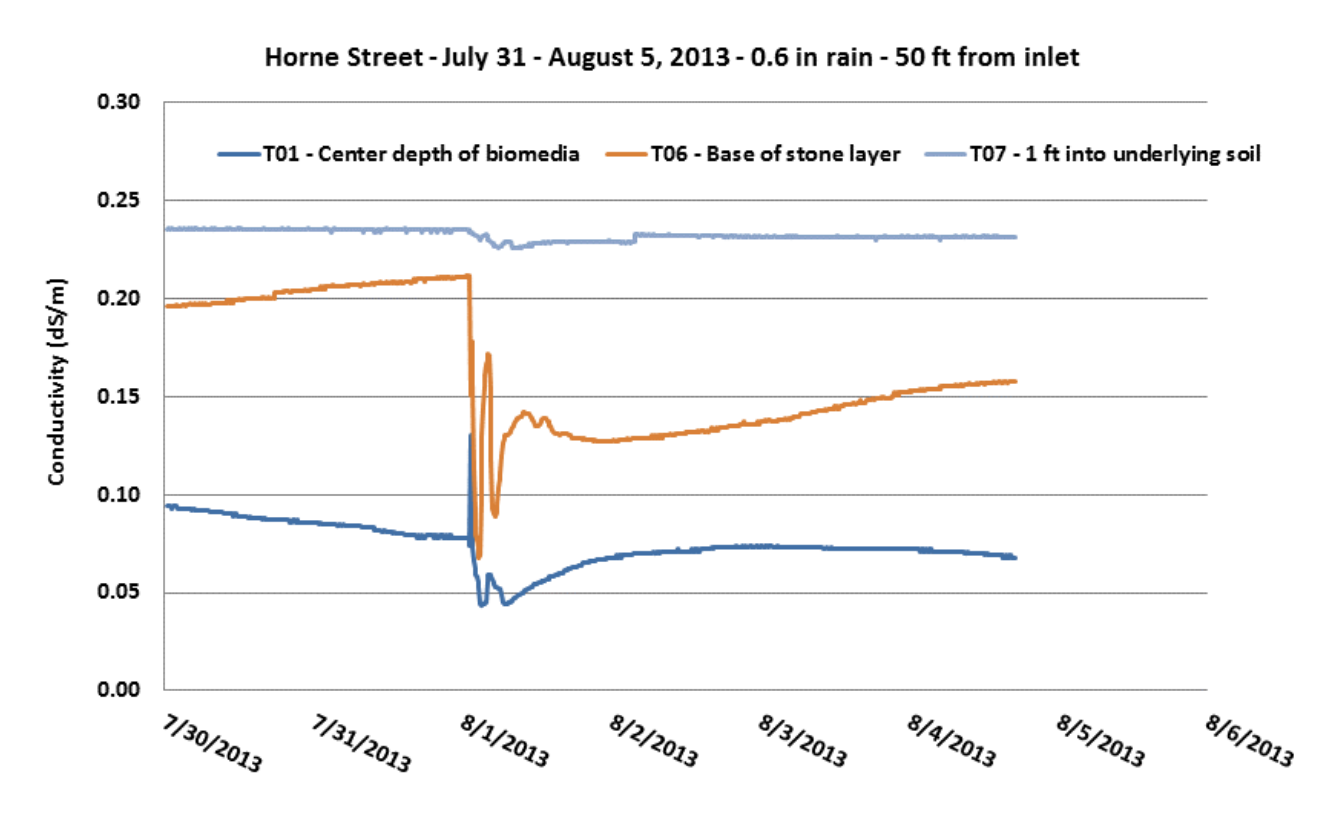


Figure 61: Conductivity data for the Horne Street Bioretention system closest to the inlet for selected runoff events during the monitoring period.

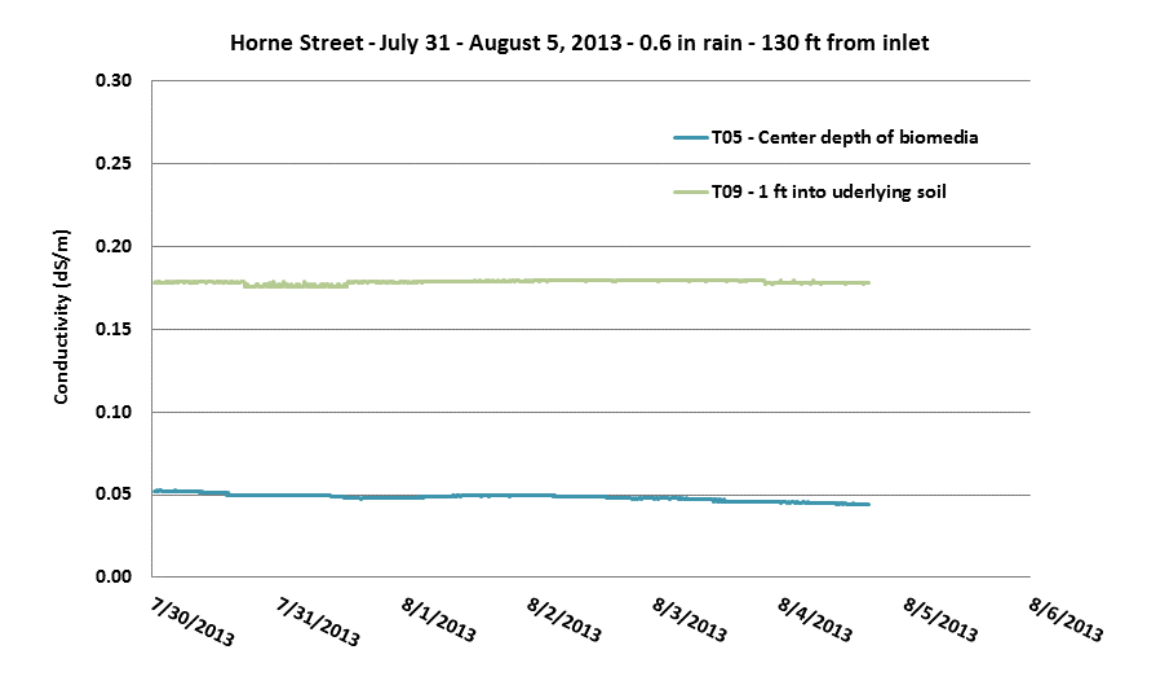


Figure 62: Conductivity data for the Horne Street Bioretention system furthest from the inlet for selected runoff events during the monitoring period.

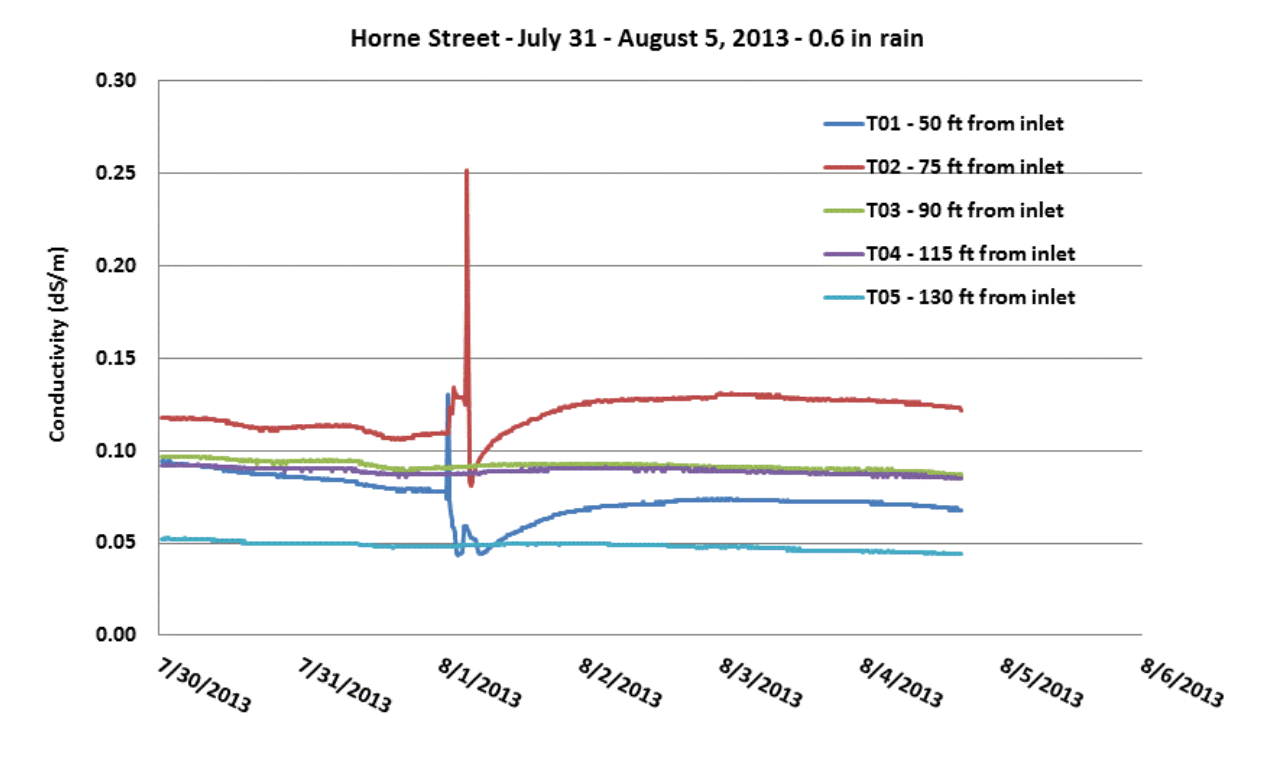


Figure 63: Conductivity data for the Horne Street Bioretention system at the center of the BSM across the longitudinal profile of the system for selected runoff events during the monitoring period.

The February 5, 2014 event is a snowfall event. The period 2-9 February 2014 had only this one event with no runoff. The storm precipitation data is shown in Figure 64 and the air temperature for this storm in Figure 65. VMC and temperature data are fairly stable at all sensors. The shallow temperature sensors show some variability during daylight hours except the day of the storm. Even though the readings are positive, the VMC data for all biomedia sensors reflect frozen soil conditions at the surface, and the sensors closest to the inlet have the highest VMC with VMC reducing the farther from the inlet.

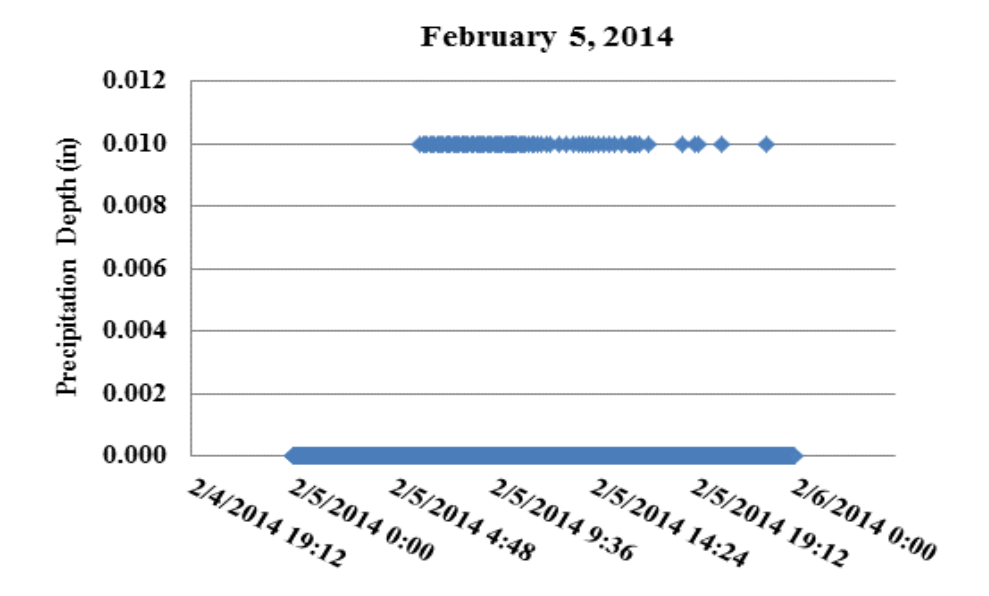


Figure 64: Water equivalent rainfall precipitation for a selected snowfall event.

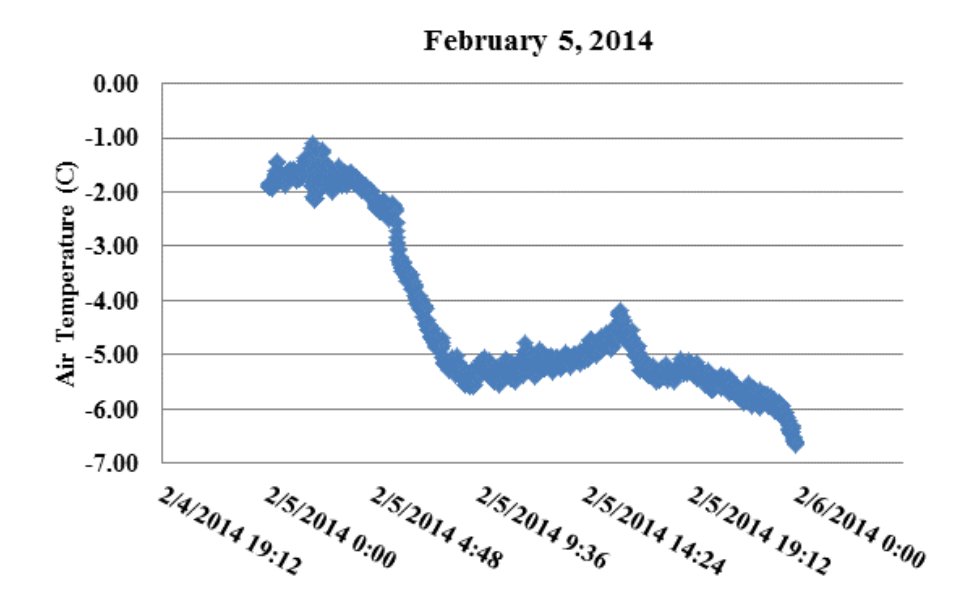


Figure 65: Ambient air temperature data for a selected snowfall event.

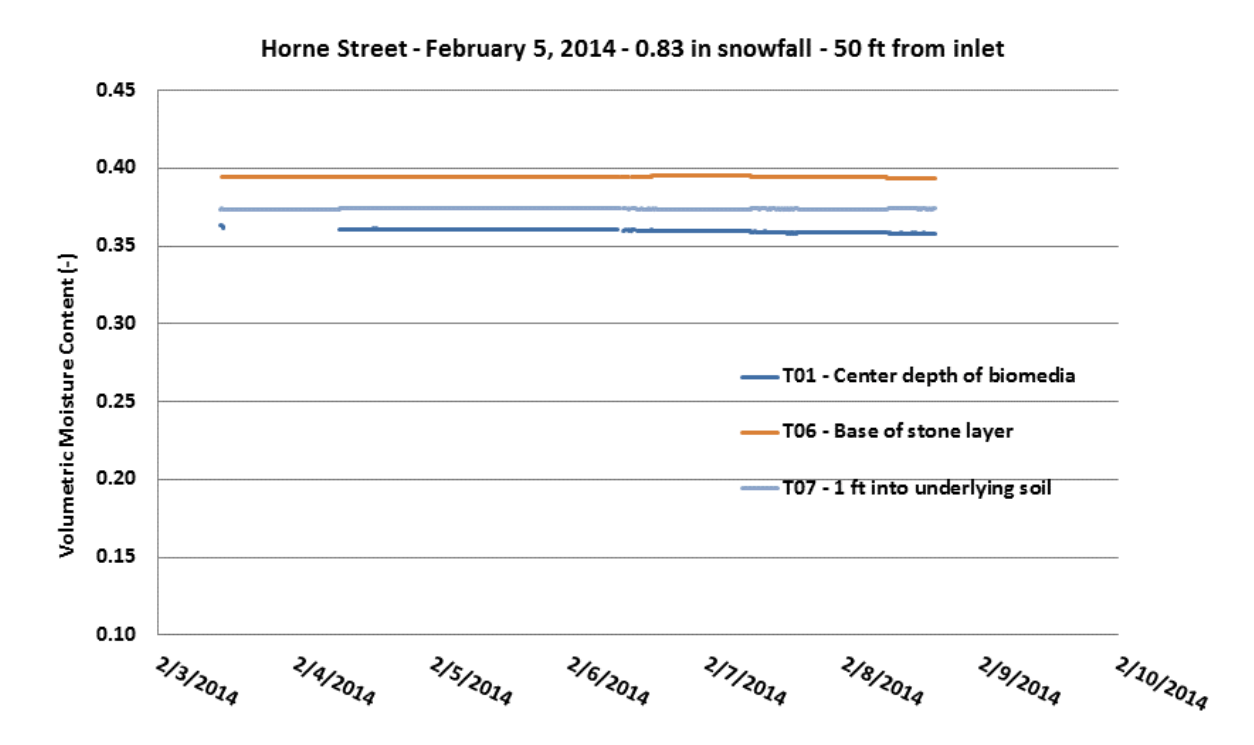


Figure 66: VMC data for the Horne Street Bioretention system closest the inlet for a selected snowfall event.

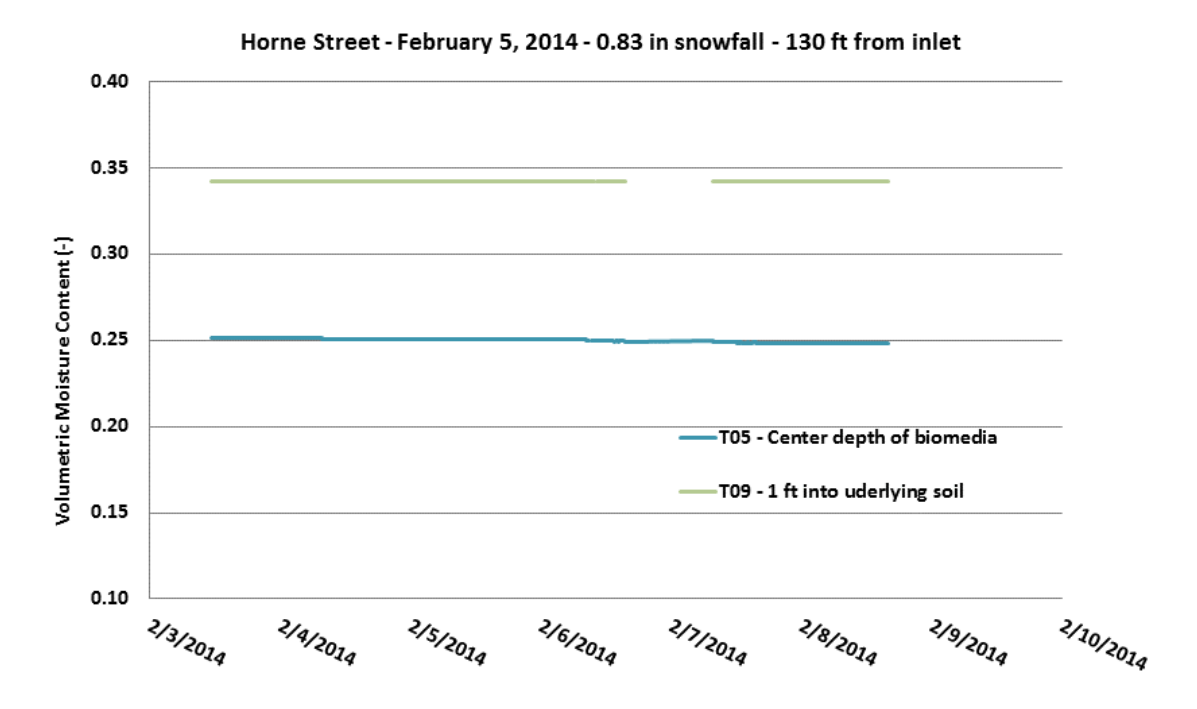


Figure 67: VMC data for the Horne Street Bioretention system furthest from the inlet for a selected snowfall event.

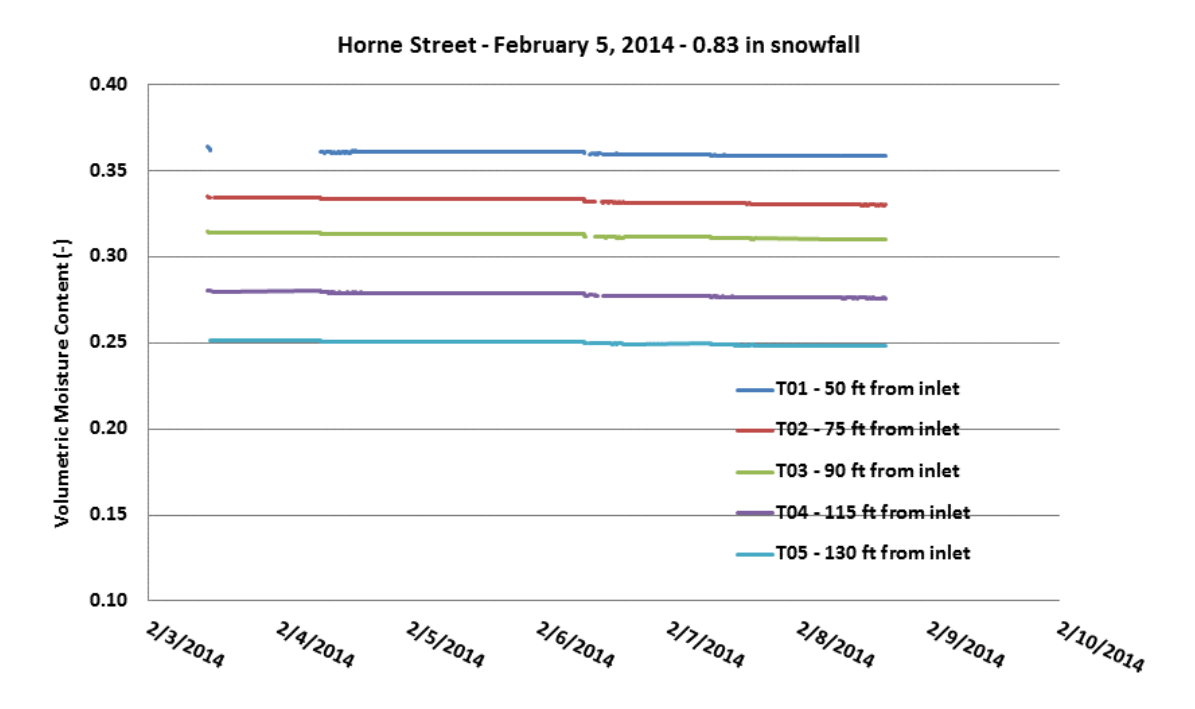


Figure 68: VMC data for the Horne Street Bioretention system at the center of the BSM across the longitudinal profile of the system for a selected snowfall event.

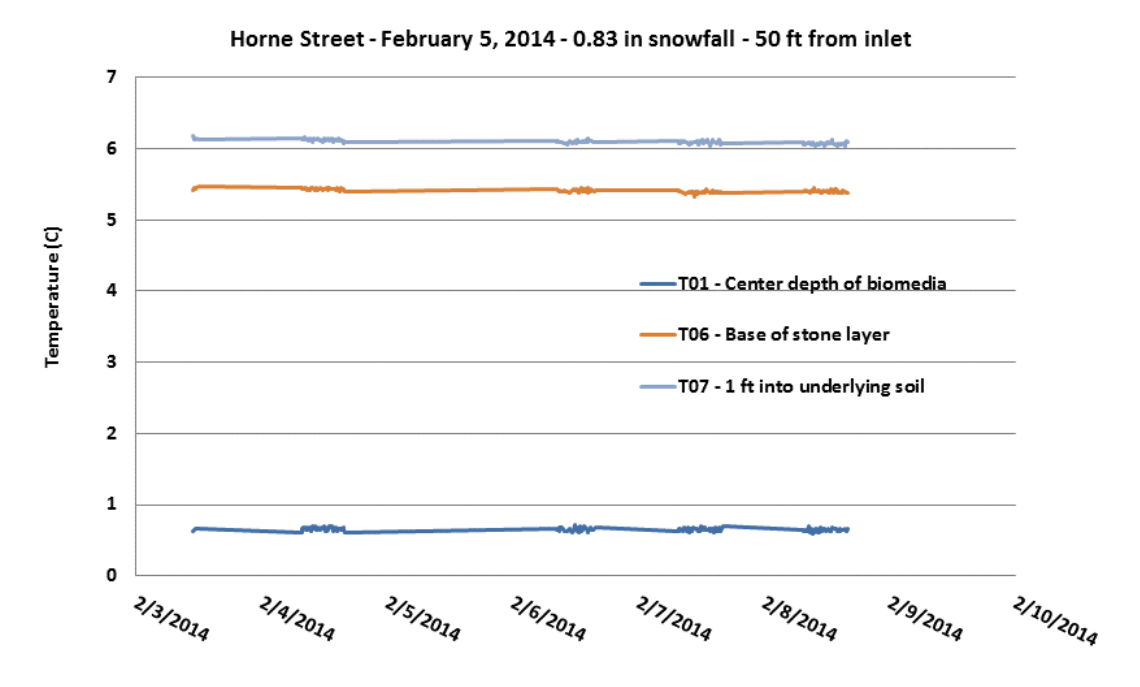


Figure 69: Temperature data for the Horne Street Bioretention system closest to the inlet for a selected snowfall event.

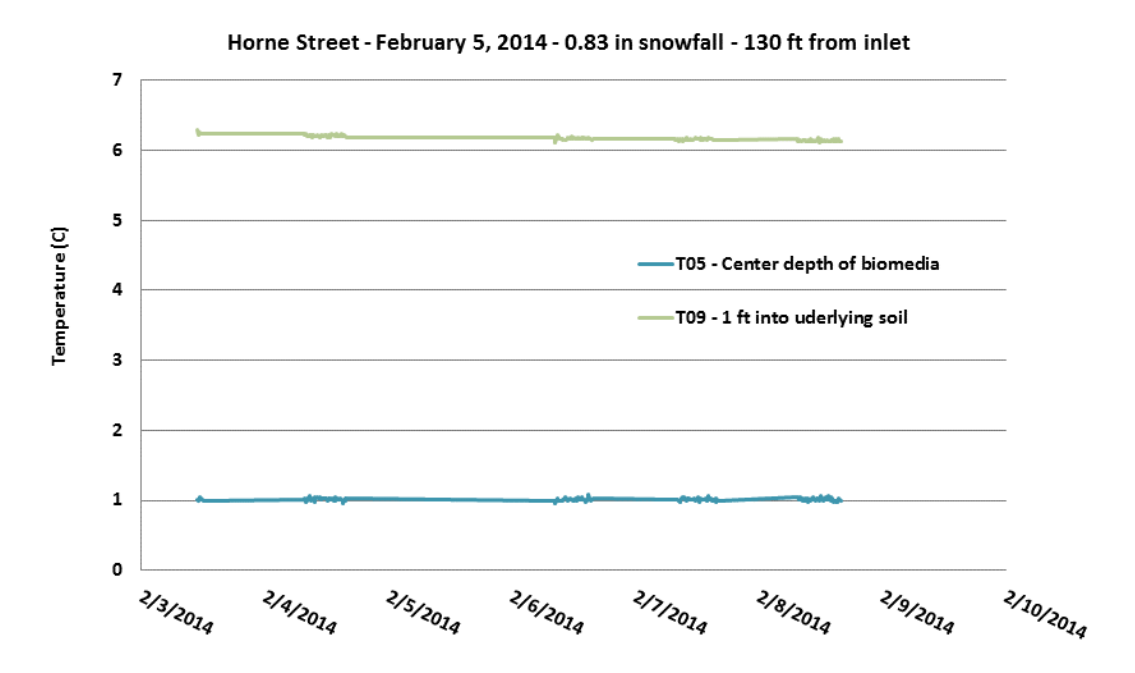


Figure 70: Temperature data for the Horne Street Bioretention system furthest from the inlet for a selected snowfall event.

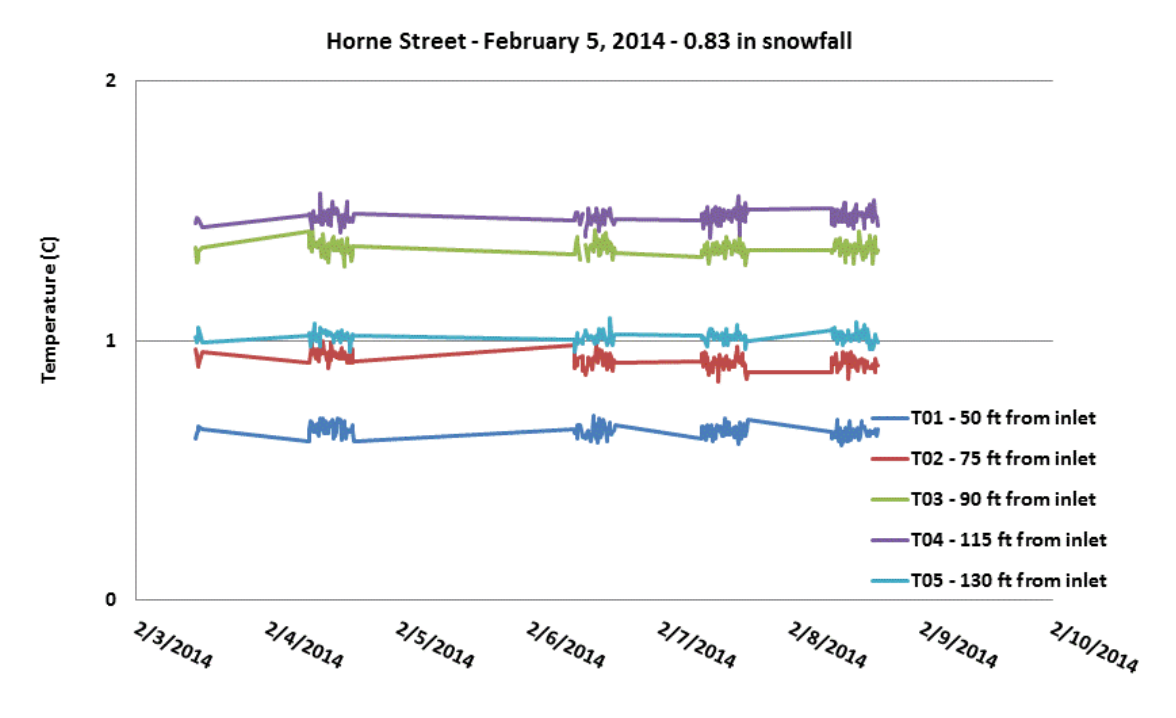


Figure 71: Temperature data for the Horne Street Bioretention system at the center of the BSM across the longitudinal profile of the system for a selected snowfall event.

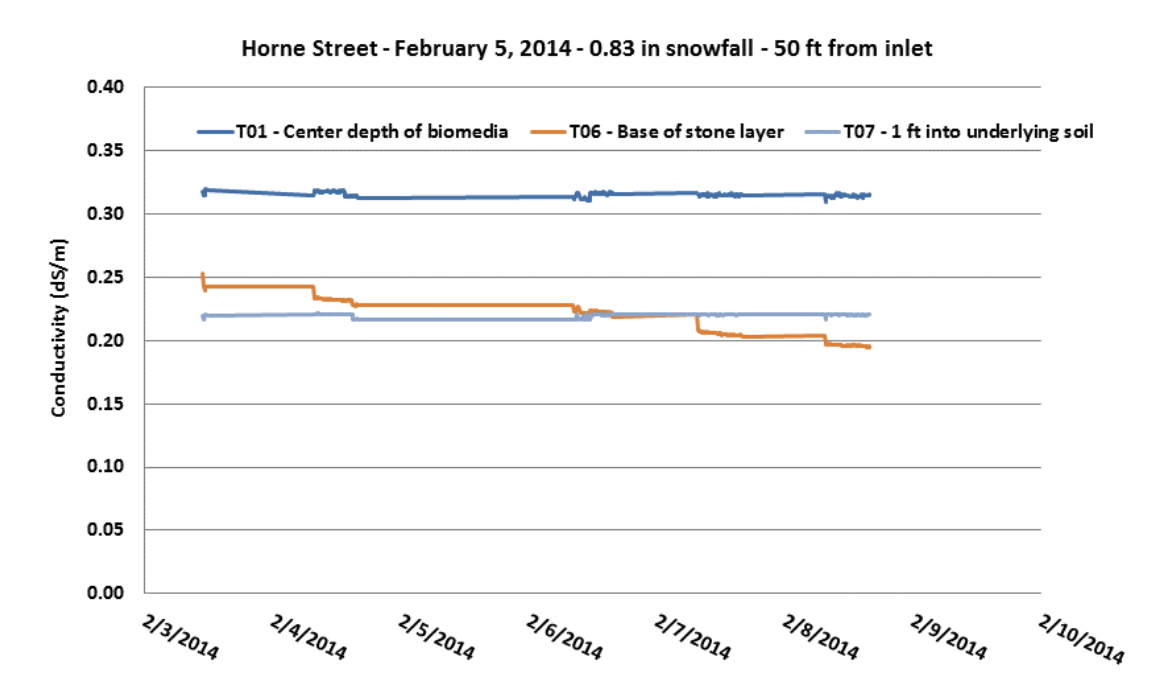


Figure 72: Conductivity data for the Horne Street Bioretention system closest to the inlet for a selected snowfall event.

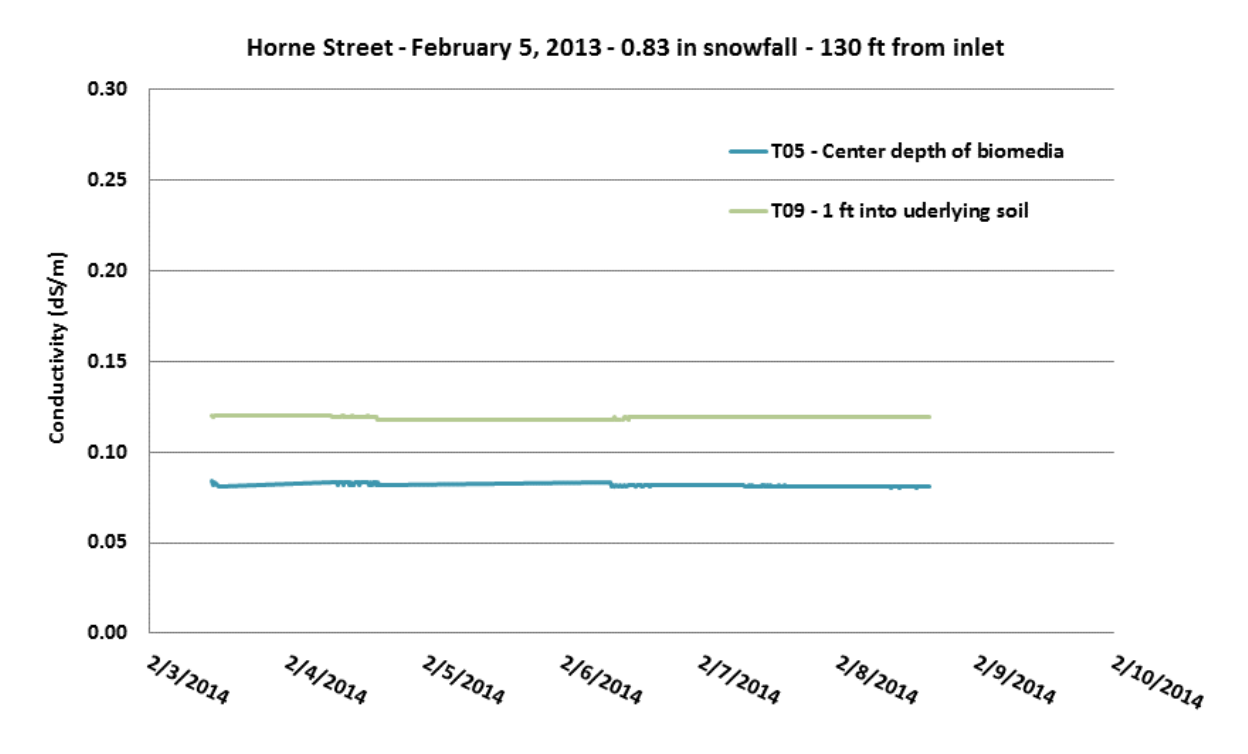


Figure 73: Conductivity data for the Horne Street Bioretention system furthest from the inlet for a selected snowfall event.

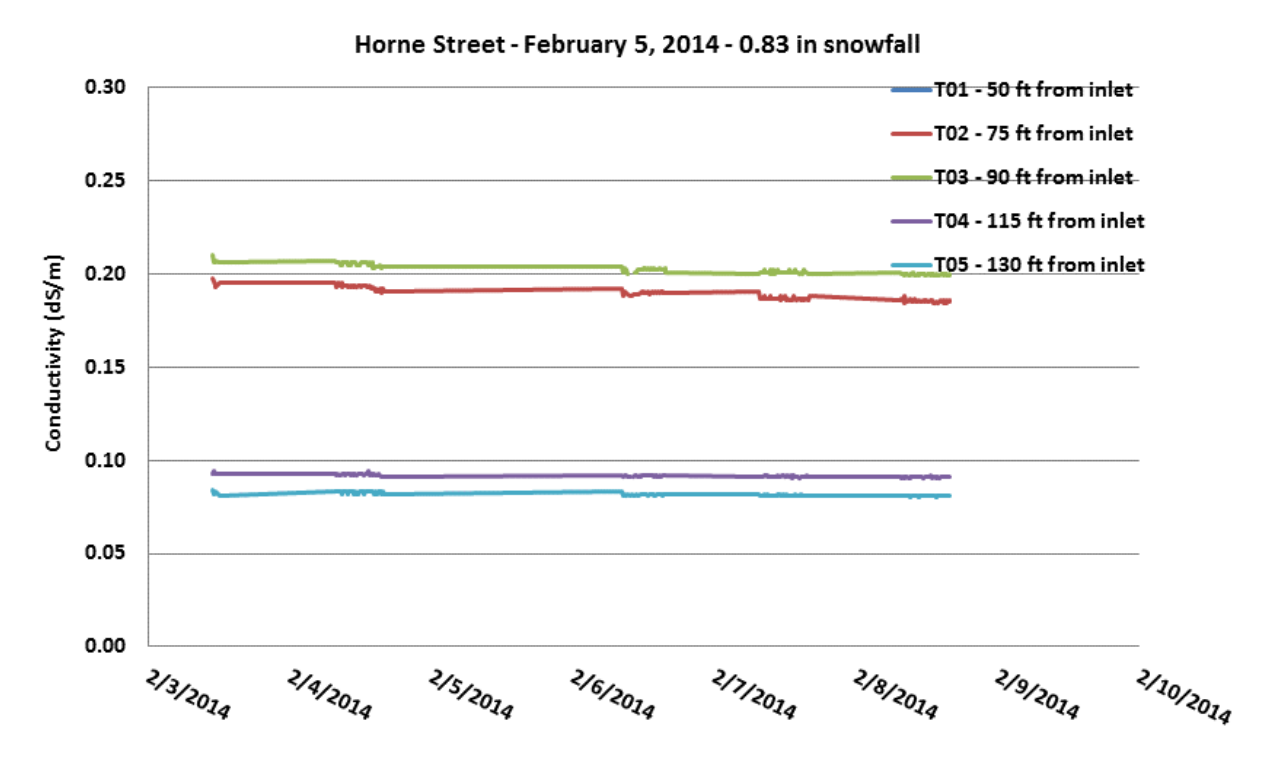


Figure 74: Conductivity data for the Horne Street Bioretention system at the center of the BSM across the longitudinal profile of the system for a selected snowfall event.

The 11-25 February 2014 period is one of rain on melting snow. Precipitation and air temperatures for this period may be seen in Figures 75 and 76. The VMC of the underlying soil does not seem to react to this event possibly because it is at saturation and was at its maximum values for the monitoring period. The VMC of the stone and the biomedia react indicating that infiltration is occurring. The runoff is cold, and the biomedia temperature does not demonstrate much variability. A key element in the bioretention system hydrology for this event is that close to the inlet the biomedia conductivity barely responds, yet the stone does dramatically and the underlying soil more so than the biomedia. This reflects the fact that the low runoff rate of the cold, salty water vertically enters the biomedia closer to the inlet than at 50 feet. When this water then enters the stone layer it then horizontally flows below the system to the outlet while also infiltrating the ground below and on the sides of the excavation. The temperature data bearout this interpretation. During the latter part of this period there is finally sufficient runoff that the conductivity sensor 50 ft from the inlet finally responds to the runoff.

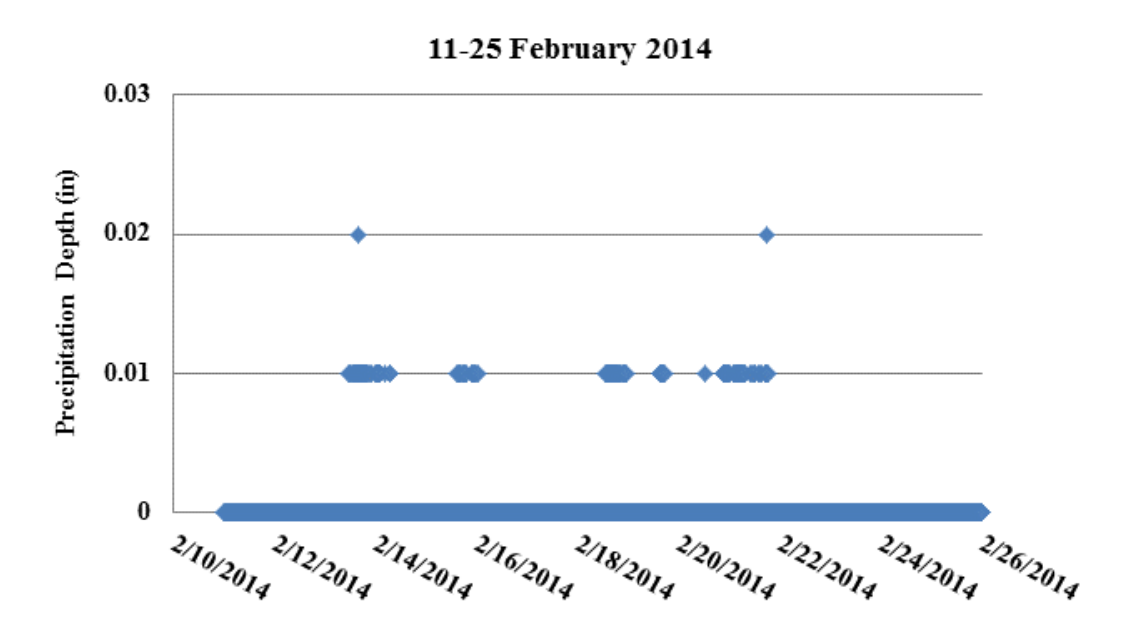


Figure 75: Water equivalent rainfall precipitation for a selected snowfall event.

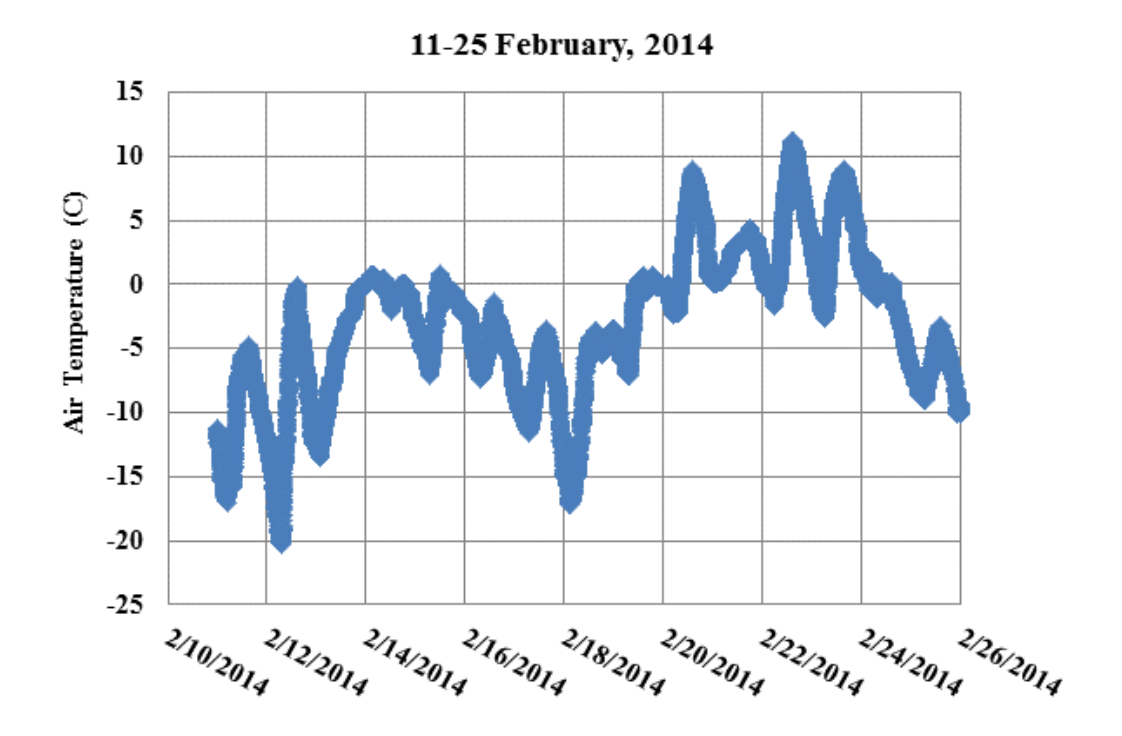


Figure 76: Ambient air temperature data for a selected snowfall event.

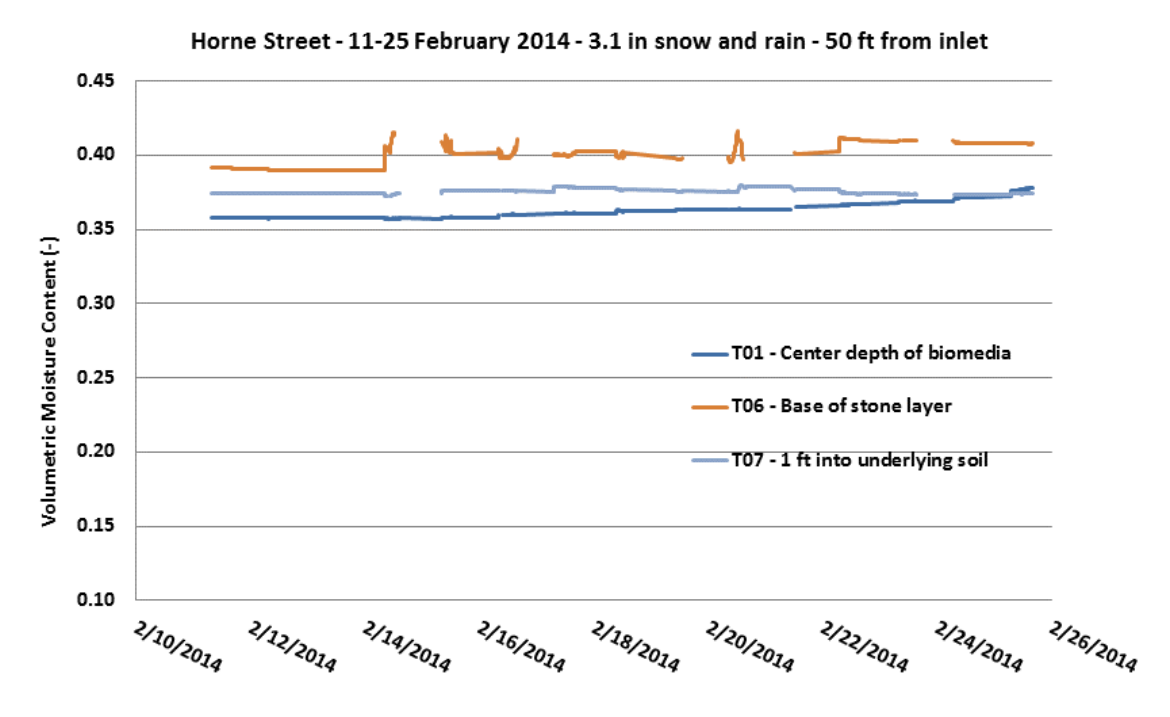


Figure 77: VMC data for the Horne Street Bioretention system Closest the inlet for a selected snowfall event.

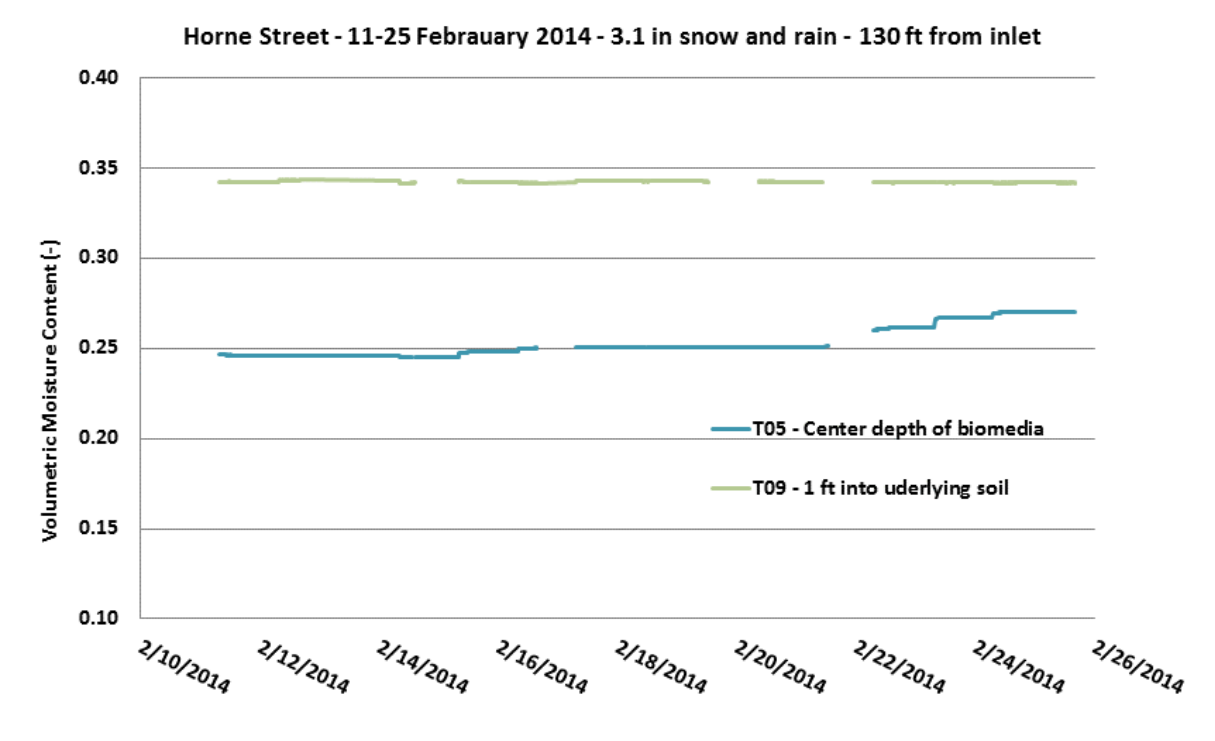


Figure 78: VMC data for the Horne Street Bioretention system furthest from the inlet for a selected snowfall event.

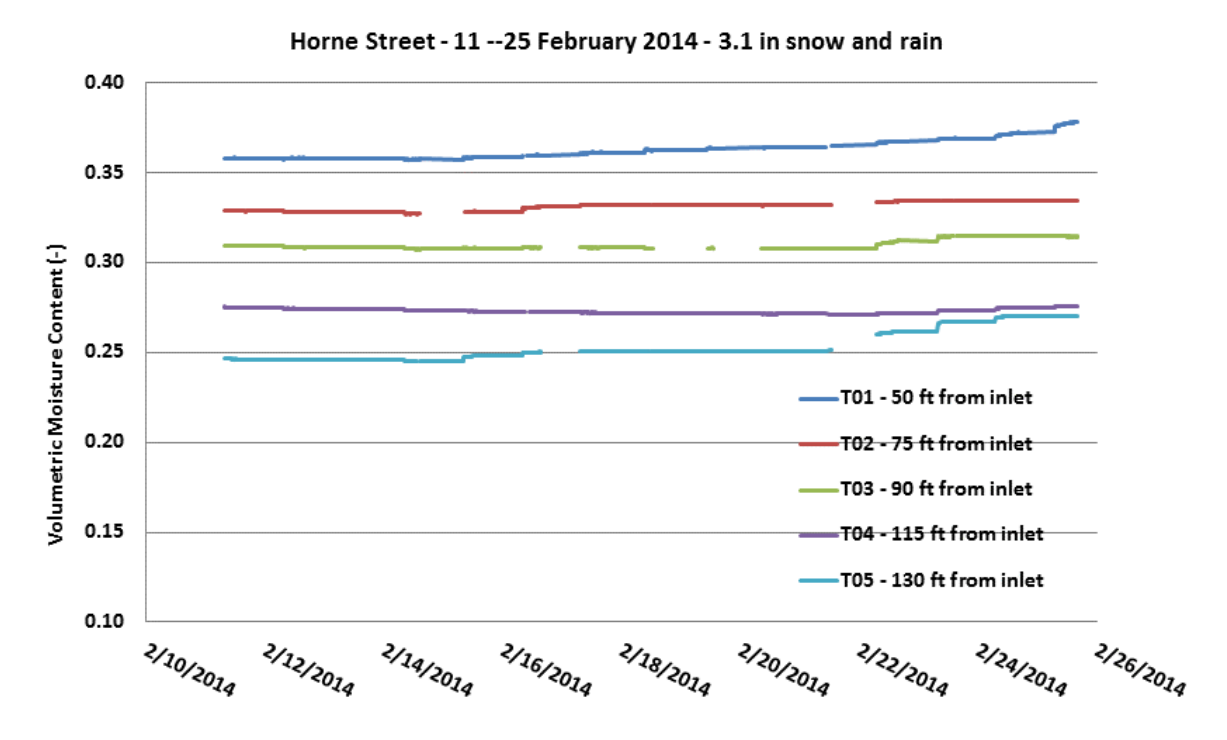


Figure 79: VMC data for the Horne Street Bioretention system at the center of the BSM across the longitudinal profile of the system for a selected snowfall event.

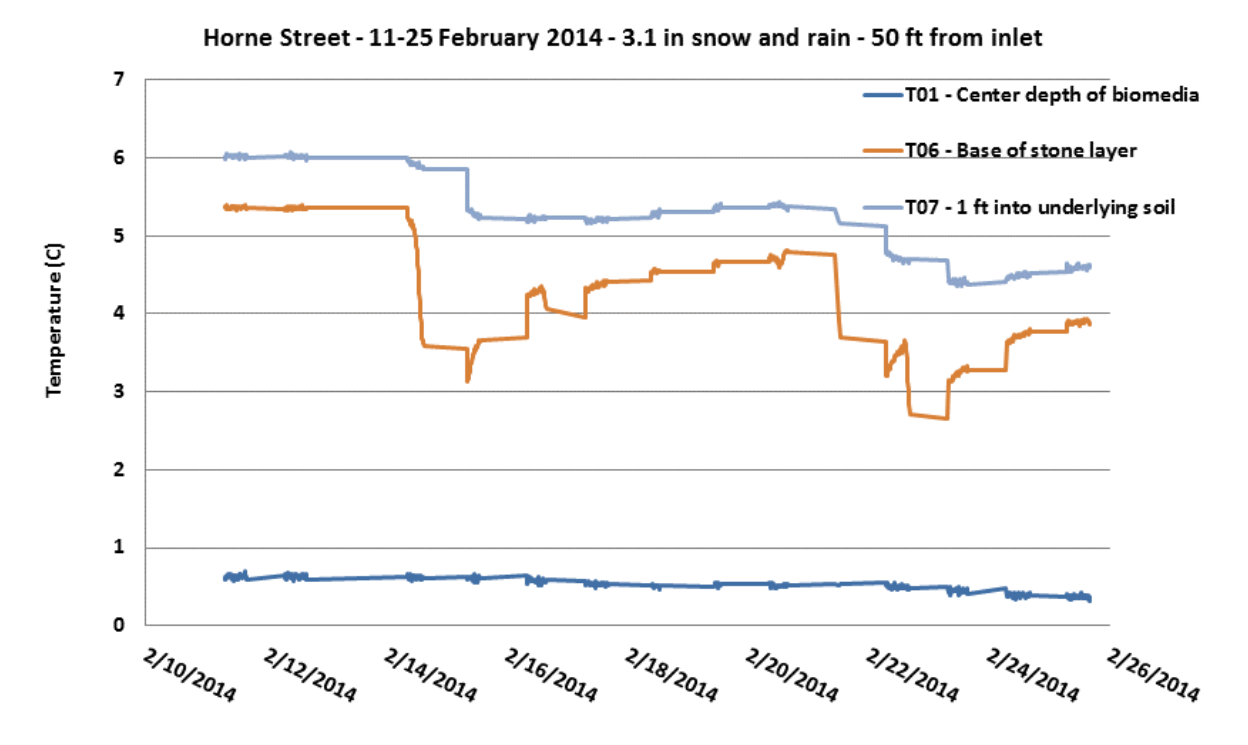


Figure 80: Temperature data for the Horne Street Bioretention system closest to the inlet for a selected snowfall event.

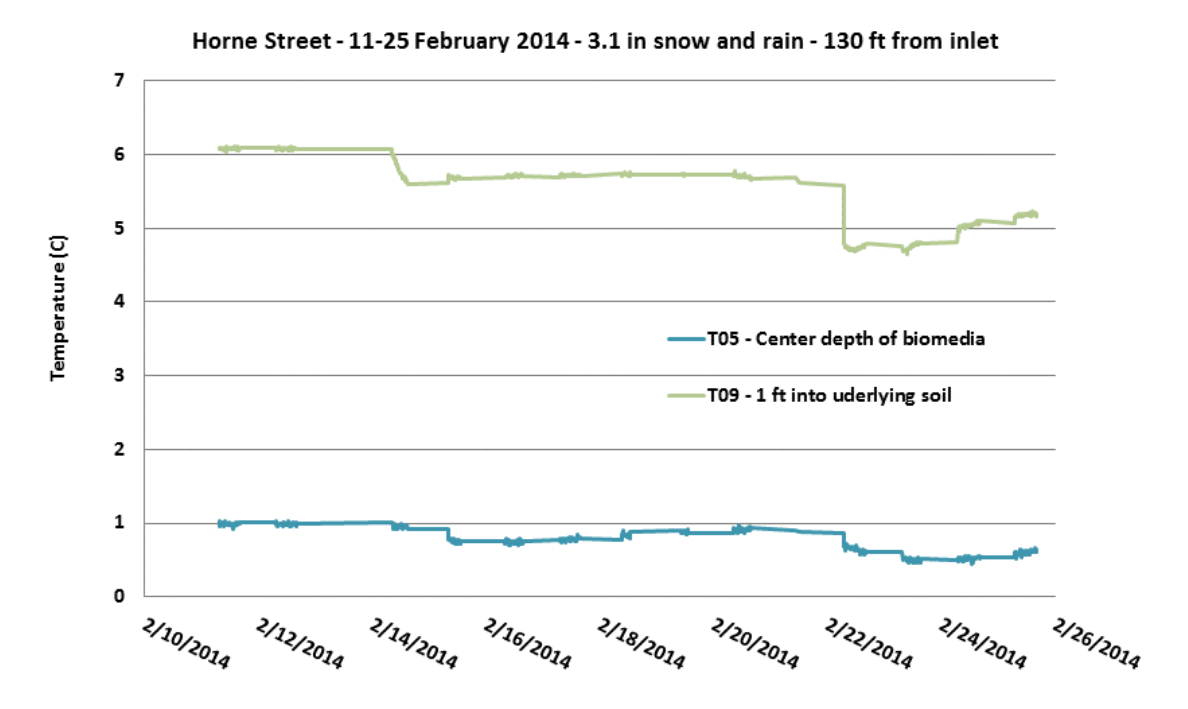


Figure 81: Temperature data for the Horne Street Bioretention system furthest from the inlet for a selected snowfall event.

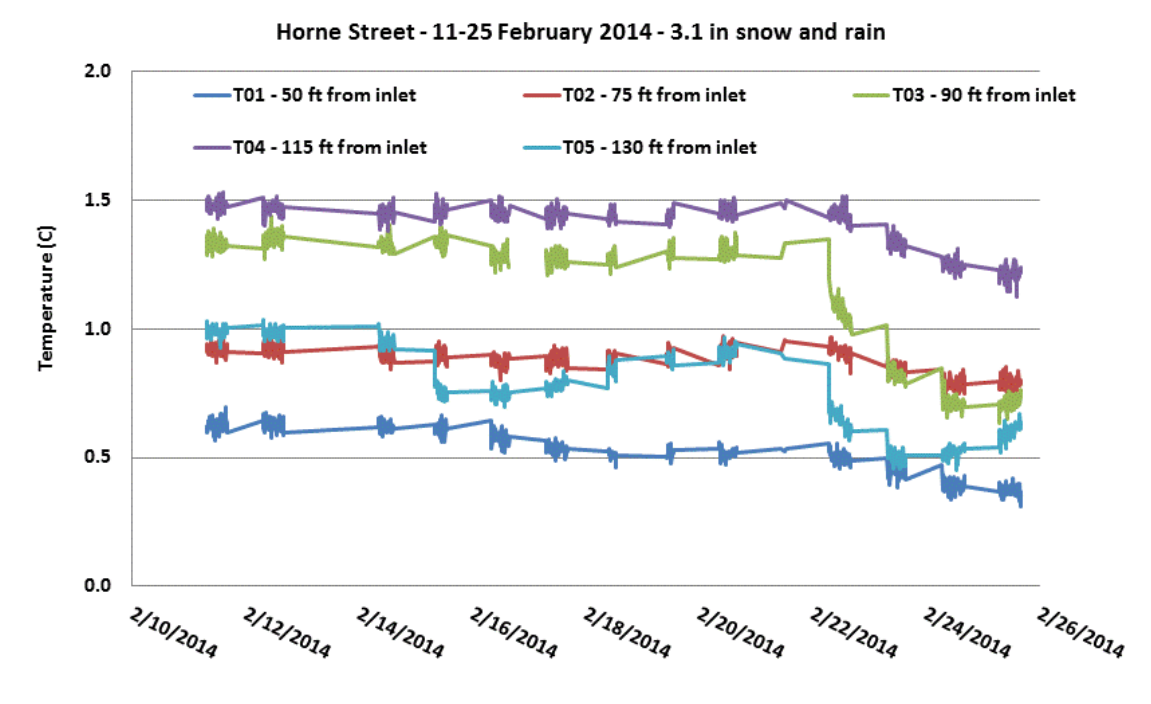


Figure 82: Conductivity data for the Horne Street Bioretention system at the center of the BSM across the longitudinal profile of the system for a selected snowfall event.

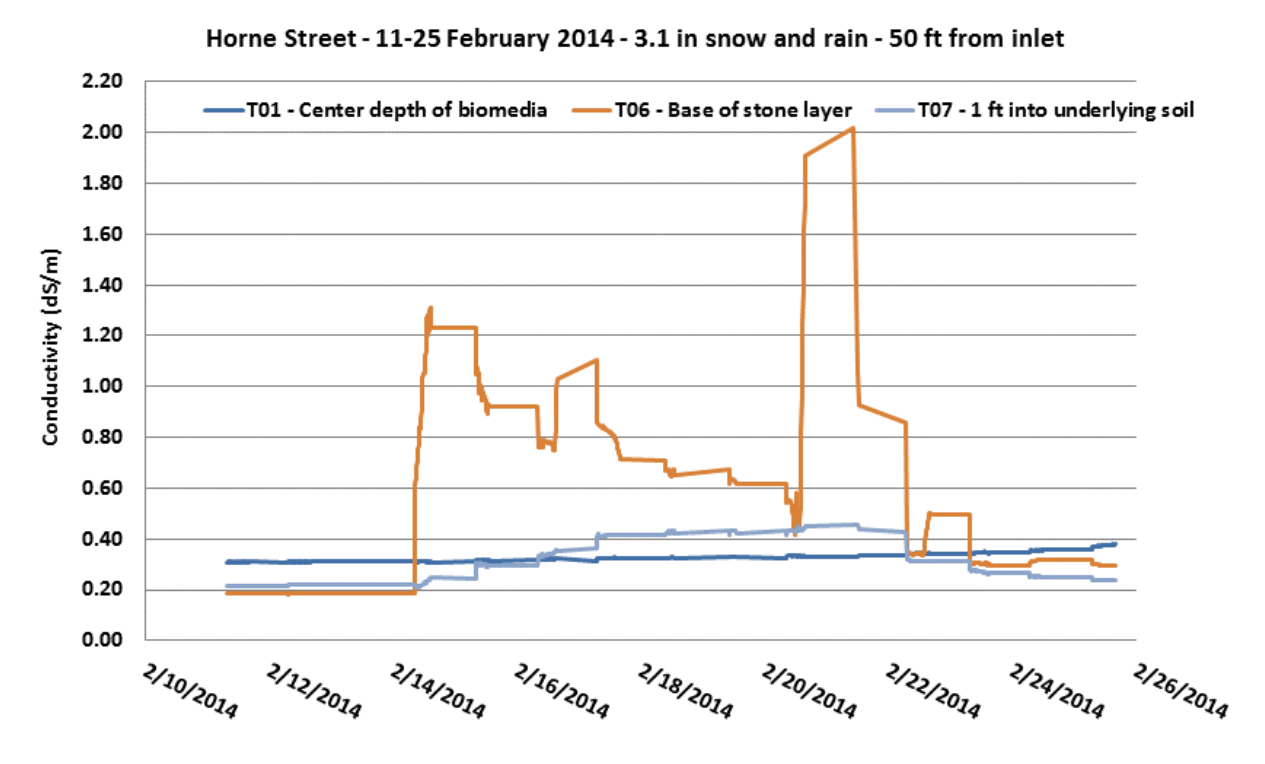


Figure 83: Conductivity data for the Horne Street Bioretention system closest to the inlet for a selected snowfall event.

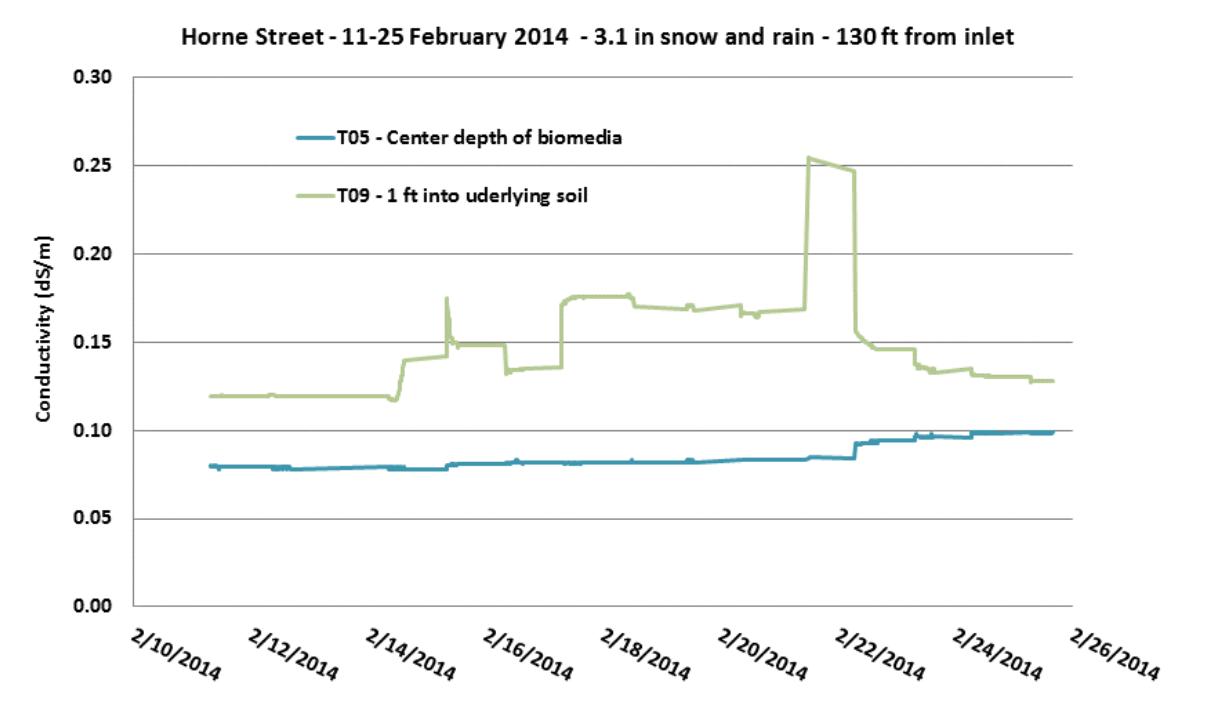


Figure 84: Conductivity data for the Horne Street Bioretention system furthest from the inlet for a selected snowfall event.

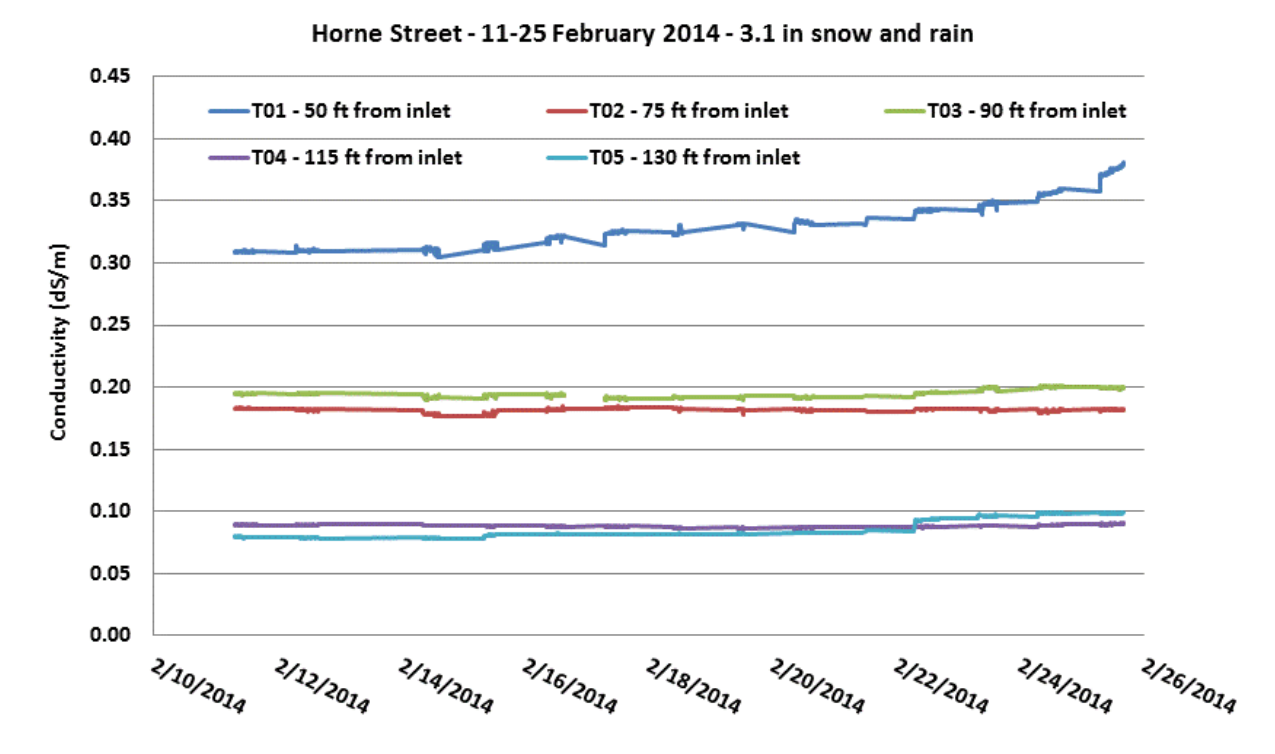


Figure 85: Conductivity data for the Horne Street Bioretention system at the center of the BSM across the longitudinal profile of the system for a selected snowfall event.

Conclusions

Overall, runoff volume reductions are significant and exceed anticipated levels even in areas with low permeability soils. The overall volume reduction results for all TREEPOD events (200) was 79% and 64% for median and average influent volumes, respectively, which is remarkable in that the systems is constructed in a silty-clay soil. The cumulative volume reduction was 77%. Volume reductions in the winter season, associated with melt events exceed non-winter volume reductions. Peak flow and total runoff volume reductions averaged 95% in the winter. This indicates enhanced runoff reduction through lower influent volumes associated with melt events. This is significant as most systems are typically designed for a standard runoff volume or rainfall depth. This research demonstrates enhanced runoff reduction where influent levels are less than design flows. One caution is that with the higher infiltration ratio in the winter is the attendant infiltration of high salt content runoff resulting from winter de-icing.

Throughout the monitoring period for each device unsaturated flow conditions dominated the system hydraulics in the manufactured soil media (biomedia). Even in instances where there was system ponding (TREEPOD) and saturated conditions in the subsurface reservoir course (Horne St Bio) in general the soil media flowed under unsaturated conditions. This indicates that the soil mix is the primary hydraulic control in these systems and according to the empirical data does not exhibit the commonly

assumed design conditions of saturated flow. From a design perspective this would indicated that more dynamic models for Bioretention system design do not accurately depict field conditions, and therefore modeled outflow hydrographs during the design phase most likely do not reflect the real outflow hydrographs. If water quality volume sizing is intended static storage models will more accurately reflect actual hydraulics without additional more sophisticated design approaches. In the same respect most conventional Bioretention models almost exclusively use vertical flow pathways as the primary exfiltration pathway. The volume reduction potential of these installations coupled with the conductivity distributions presented demonstrate that flow pathways are 3 dimensional and depending on native soil conditions could be dominated by exfiltration through system sidewalls.

All the media filter systems studied throughout the project provided thermal and chloride buffering. Temperature buffering occurred in both the summer and winter seasons. Where runoff temperatures were high in the summer the treatment system lowered runoff temperature which carries beneficial implications to temperature impaired receiving waters and cold water fisheries. Conversely where winter runoff temperatures were low, water temperatures in the system subgrade elevated in-situ water temperatures and maintained infiltration pathways. With respect to chloride, where influent concentrations were elevated, the signal was buffered as the water passed from the surface through the system subbase. This attenuation capacity could be seen as a benefit, however when considering long-term function of media filtration systems in chloride impaired watersheds may exacerbate chronic chloride toxicity problems. While not quantified here, the chloride buffering capacity media filtration systems could delay the chloride signal from winter when biotic metabolism is minimal to later months where biotic assimilative capacities increase. This illustrates the complexity of one-size-fits-all solutions. More importantly water quality solutions should be dictated by the prevailing receiving water qualities and toxical sensitivities.

The synthesis and analyses performed for two installed Filter systems; a Tree Box Filter and a bioretention basin provides an organized summary and baseline water balance from an extensive collection of raw data and gives a starting point to begin to look at the data and decide what needs further review and adjustment.

APPENDIX